DOI:10.14753/SE.2020.2400

NOVEL THERAPEUTIC OPTIONS IN DIABETIC KIDNEY DISEASE

PhD Thesis

Dóra Bianka Balogh

Doctoral School of Clinical Medicine
Semmelweis University

Supervisor:	Andrea Fekete, MD, PhD
Official reviewers:	Gábor Kökény, MD, PhD Ágnes Haris, MD, PhD
Head of the Final Examination Committee:	Miklós Kellermayer, MD, DSc
Members of the Final Examination Committee:	Nóra Hosszúfalusi, MD, PhD Tibor Kovács, MD, PhD

Budapest
2020

DOI:10.14753/SE.2020.2400

TABLE OF CONTENTS

DOI:10.14753/SE.2020.2400

DOI:10.14753/SE.2020.2400

DOI:10.14753/SE.2020.2400

ABBREVIATIONS

ACE	angiotensin-converting enzyme
ACR	albumin-to-creatinine ratio
ADA	American Diabetes Association
Ang I	angiotensin I
Ang II	angiotensin II
ARB	angiotensin receptor 1 blocker
α-SMA	alpha-smooth muscle actin
BSA	bovine serum albumin
CANVAS	Canagliflozin Cardiovascular Assessment Study
CKD	chronic kidney disease
CREDENCE	Canagliflozin and Renal Events in Diabetes with Established Nephropathy Clinical Evaluation
CTGF	connective tissue growth factor
CVD	cardiovascular disease
DAPA	dapagliflozin
DAPA-CKD	A Study to Evaluate the Effect of Dapagliflozin on Renal Outcomes and Cardiovascular Mortality in Patients with Chronic Kidney Disease
DECLARE-TIMI 58	Dapagliflozin Effect on Cardiovascular Events-Thrombolysis in Myocardial Infarction 58
DEPICT	Dapagliflozin Evaluation in Patients with Inadequately Controlled Type 1 Diabetes
DKA	diabetic ketoacidosis
DKD	diabetic kidney disease
ECM	extracellular matrix
EMPA-REG OUTCOME	Empagliflozin Cardiovascular Outcome Event Trial in Type 2 Diabetes Mellitus Patients-Removal of Excess Glucose
ELISA	enzyme-linked immunosorbent assay
EPO	erythropoietin

GDM	gestational diabetes mellitus
GFAT1	glutamine-fructose-6-phosphate amidotransferase 1
GFR	glomerular filtration rate
HbA_{1c}	glycated hemoglobin
HBP	hexosamine biosynthetic pathway
HIF-1α	hypoxia-inducible factor 1-alpha
HRP	horseradish peroxidase
IFG	impaired fasting glucose
IGT	impaired glucose tolerance
KIM-1	kidney injury molecule-1
LOS	losartan
MAP	mean arterial pressure
MMP	matrix metalloproteinase
MODY	maturity-onset diabetes of the young
MTT	methyl-thiazoletetrazolium
ncOGT	nucleocytoplasmic *O*-GlcNAc transferase
NGAL	neutrophil gelatinase-associated lipocalin
OGA	*O*-GlcNAcase
O-GlcNAc	*O*-linked N-acetylglucosamine
OGTT	oral glucose tolerance test
PBS	phosphate buffered saline
PDGF	platelet-derived growth factor
SD	standard deviation
SGLT2	sodium-glucose cotransporter 2
sOGT	small *O*-GlcNAc transferase
STZ	streptozotocin
TGF	tubuloglomerular feedback
TGFβ	transforming growth factor beta
TUM	type IV collagen
T1DM	type 1 diabetes
T2DM	type 2 diabetes
RAAS	renin-angiotensin-aldosterone system

DOI:10.14753/SE.2020.2400

rPRO-C3	collagen III formation
UAE	urinary albumin excretion
uC3M	MMP-9-mediated degradation of type III
VEGF-A	vascular endothelial growth factor A
WHO	World Health Organization

DOI:10.14753/SE.2020.2400

1 INTRODUCTION

1.1 Diabetes mellitus

1.1.1 Prevalence

Over the past few decades, diabetes mellitus has become one of the largest epidemics the world has faced, making it an enormous challenge for modern healthcare systems. Between 2000 and 2020, overall prevalence of diabetes in adults snowballed from 151 million to 463 million (Fig. 1). Today, this represents 9.3% of the world's adult population aged 20-79 years. Without urgent multi-sectoral strategies and actions, 578 million (10.2%) people are predicted to live with diabetes by 2030 and this number will rise to 700 million (10.9%) by 2045 (1).

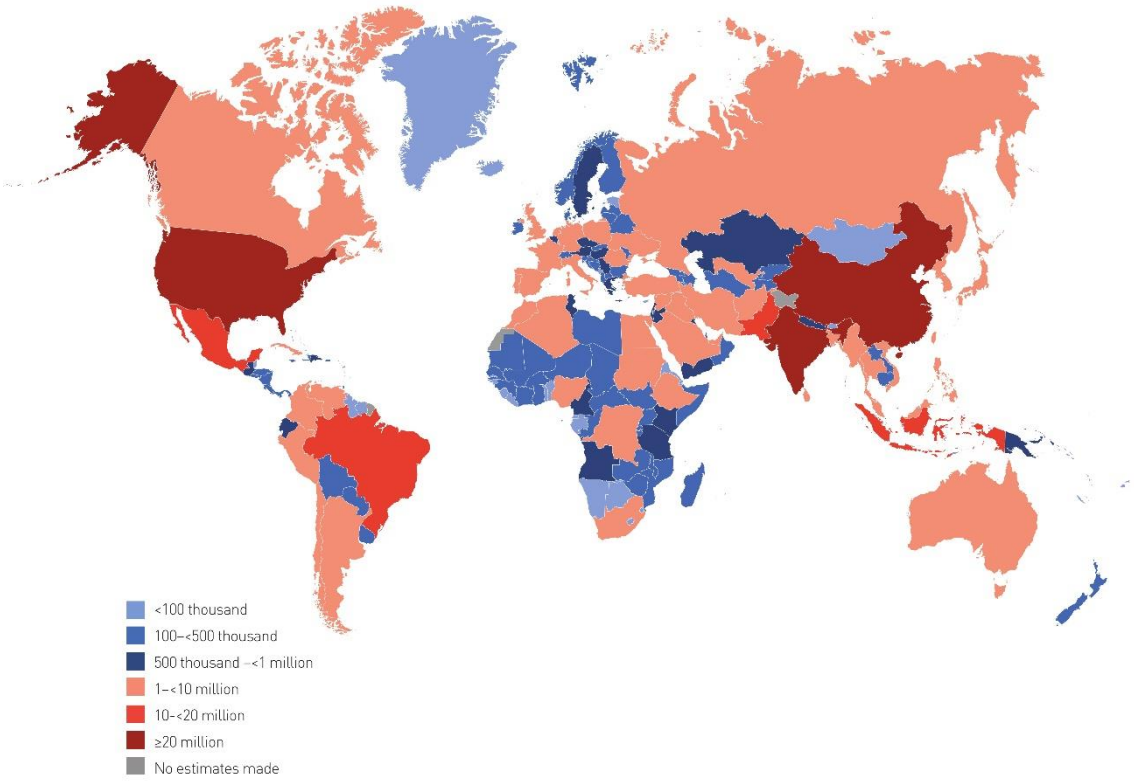

Figure 1 Estimated total number of diabetic adults (20-79 years) in 2019. *(IDF DIABETES ATLAS Ninth edition, 2019)*

Similarly to global trends the prevalence of diabetes has been increasing in Hungary (ca. 7-9%) as well. According to the database analysis of the National Health Insurance Fund 727 000 people are living with diabetes in Hungary (2). Diabetic patients have an increased risk of developing life-threatening health complications resulting in reduced quality of life, increased mortality and higher medical care costs. The global health expenditure on diabetes is estimated to be USD 760.3 billion per year (3).

1.1.2 Classification

Diabetes has a long history reaching back to antiquity. The term "diabetes" (Greek for "passing through" meaning "a large discharge of urine") was first used in the 2nd century, while in the 17th century the term "mellitus" (Latin for "honey") was added describing the extremely sweet taste of urine (4). Diabetes mellitus is a group of metabolic disorders associated with dysregulation of carbohydrate, lipid and protein metabolism. It is characterized by constant hyperglycemia resulting from a relative or absolute deficiency of insulin secretion or peripheral insulin resistance or both. Persistent hyperglycemia causes generalized vascular damage leading to several complications including cardiovascular diseases, neuropathy, retinopathy or kidney disease.

Diabetes can be classified into various groups among which the following categories are the most frequent:

1. Type 1 diabetes (T1DM; caused by autoimmune β-cell destruction, usually leading to absolute insulin deficiency).
2. Type 2 diabetes (T2DM; caused by a progressive loss of β-cell insulin secretion frequently on the background of insulin resistance).
3. Gestational diabetes mellitus (GDM) (diabetes diagnosed in the second or third trimester of pregnancy).
4. Specific types of diabetes due to other causes e.g. monogenic diabetes syndromes (neonatal diabetes, maturity-onset diabetes of the young), diseases of the exocrine pancreas (cystic fibrosis, pancreatitis), drug- or chemical-induced diabetes and infection-related diabetes (5).

T1DM accounts for around 5-10% of diabetes in adults. It is characterized by autoimmune destruction of pancreatic β-cells leading to absolute insulin deficiency. The process is not fully understood, however many mechanisms can lead to the decline in β-cell function (e.g. genetic predisposition and abnormalities, epigenetic processes, auto-immunity, concurrent illnesses, inflammation and environmental factors) (6). The traditional paradigm saying that T1DM occurs only in children or adolescents has been disproven. Despite T1DM developing frequently in childhood, it can be manifested in adults as well (7).

T2DM is the most common type of diabetes, accounting for more than 90% of all cases worldwide. T2DM is a complex chronic disorder primarily associated with insulin resistance in skeletal muscle, liver and adipose tissue and impaired insulin secretion. Environmental (e.g. obesity, unhealthy diet, physical inactivity) and genetic factors (T2DM clusters in families and is heritable) are important determinants of insulin resistance and β-cell dysfunction (8). T2DM mostly occurs in adults, however it has also become a concern in children and adolescents as a result of the increasing prevalence of obesity and metabolic syndrome in this population (9).

GDM develops during pregnancy (generally detected in the second or third trimester) and resolves following delivery. GDM is currently the most common medical complication of pregnancy and its prevalence is increasing (10). In addition, the risk of developing T2DM in later life is substantially higher in women with GDM (11). Intrauterine exposure to diabetes is associated with increased lifetime risk of obesity and T2DM in the offspring as well (12). Detailed discussion of other specific types of diabetes (e.g. monogenic diabetes syndromes, diseases of the exocrine pancreas, endocrine disorders, drug- or chemical-induced diabetes, infections, etc.) exceeds the limits of this thesis.

1.1.3 Diagnosis

The classic symptoms of hyperglycemia are polyuria, polydipsia, blurred vision, hyperphagia and weight loss. Children with T1DM typically present with the hallmark symptoms of polyuria, polydipsia, weight loss and approximately one-third present with

diabetic ketoacidosis (DKA) (13). The majority of patients with T2DM often remain undiagnosed for years, since hyperglycemia develops gradually and is not severe enough at earlier stages to notice the classic symptoms. Increased serum glucose levels are usually noticed during routine laboratory evaluation suggesting the onset of T2DM.

Beside the classic symptoms of hyperglycemia, further blood glucose tests are needed for the diagnosis of diabetes. Fasting plasma glucose, two-hour plasma glucose during a 75 g oral glucose tolerance test (OGTT), glycated hemoglobin (HbA_{1C}) or random plasma glucose test in patients with classic symptoms of hyperglycemia or hyperglycemic crisis can be used for diagnostic testing. According to the current guidelines of the American Diabetes Association (ADA) and World Health Organization (WHO) diagnosis can be established if any of the following criteria is met:

- Fasting plasma glucose ≥ 7.0 mmol/L
- Two-hour plasma glucose ≥ 11.1 mmol/L during a 75 g OGTT
- HbA_{1C} ≥ 6.5%
- Random plasma glucose ≥ 11.1 mmol/L

"Prediabetes" is the term used for individuals whose serum glucose levels do not fulfil the criteria, but are higher than normal. Patients with increased fasting glucose (IFG; 6.1-6.9 mmol/L) and/or impaired glucose tolerance (IGT; fasting plasma glucose < 7.0 mmol/L and two-hour plasma glucose 7.8-11.1 mmol/L) and/or HbA_{1C} 5.7-6.4% have prediabetes indicating a higher risk for the future development of diabetes and cardiovascular disease (CVD) (5, 14).

1.1.4 Complications

Patients with all forms of diabetes are at increased risk of developing serious acute and chronic complications. DKA and severe hypoglycemia are the major life-threatening acute complications of diabetic patients. Poor glycemic control, misdiagnosis, lack of access to insulin or low socioeconomic status result in acute complications leading to permanent neurological consequences or death (6).

In general, the harmful effects of consistent hyperglycemia can be classified as chronic macrovascular complications (coronary artery disease, peripheral arterial disease) and microvascular complications (retinopathy, kidney disease, and neuropathy). Hyperglycemia exacerbates the development of atherosclerosis and heart failure, therefore CVD is the principal cause of death among diabetic patients (15). Diabetic retinopathy may be the most common microvascular complication of diabetes and is the leading cause of blindness in adults. Diabetic kidney disease (DKD) is the main topic of this thesis and will be discussed in detail in the next chapter.

1.2 Diabetic kidney disease

1.2.1 Prevalence

DKD is a major cause of chronic kidney disease (CKD) and end-stage renal disease (ESRD), accounting for approximately 50% of cases in the United States (16) and 30-40% of cases in Hungary (17). It typically develops after 10 years of diabetes in the case of T1DM (ca. 30%), but may already be present at diagnosis of T2DM (ca. 40%) (18, 19). The incidence of DKD has been increasing progressively parallels the dramatic worldwide rise of diabetes in the past decades. The annual healthcare cost of patients with DKD are 49% higher than diabetic patients with no kidney damage (20).

1.2.2 Classification and diagnosis

The clinical diagnosis of DKD is based on the presence of albuminuria and/or reduced estimated glomerular filtration rate GFR (eGFR) in the absence of signs or symptoms of other primary causes of kidney damage (e.g. rapidly decreasing eGFR, abrupt increase in albuminuria, nephrotic syndrome, refractory hypertension or eGFR decline within 2-3 months of initiation of renin-angiotensin system inhibition). However, this paradigm may have changed over the last two decades. In particular, GFR loss has been observed prior to the development of albuminuria (21-23), reduced GFR without albuminuria has been frequently described (24, 25) and albuminuria has been noted to be transient or reversible (26, 27).

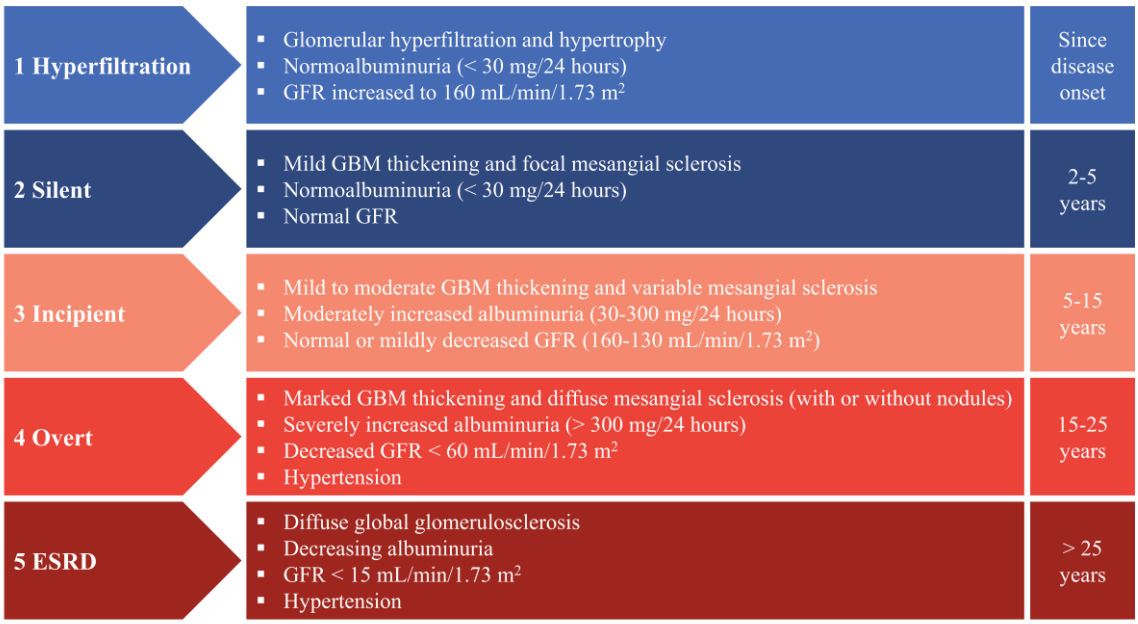

Figure 2 Stages of diabetic kidney disease. The figure illustrates the 5 stages of diabetic kidney disease and the likely renal pathologic and functional alterations in each stage. Based on *Mogensen et al., Diabetes. 1983;32 Suppl 2:64-78* and *Said and Nasr, Kidney International. 2016;90 1:24-26*.
ESRD: end-stage renal disease; GBM: glomerular basement membrane; GFR: glomerular filtration rate.

Stage 1 known as glomerular hyperfiltration is characterized by kidney hypertrophy and normal albumin excretion. An absolute, supraphysiologic elevation in GFR is observed in this early clinical entity (28).

Stage 2 develops silently over many years. Glomerular basement membrane (GBM) thickening without signs of clinical disease is a characteristic early change in diabetes. GBM thickening is a consequence of extracellular matrix (ECM) accumulation, with increased deposition of collagen types IV and VI, laminin and fibronectin (29, 30). A number of patients remain in stage 2 throughout their lives.

Stage 3 is the forerunner of overt DKD. Diagnosis is supported by moderately increased urinary albumin excretion (UAE; 30-300 mg/24 hours) or albumin-to-creatinine ratio (ACR; 30-300 mg/g) confirmed by two independent measurements at least three months apart. A slow, gradual increase of albuminuria is a prominent feature of this very decisive phase of DKD when blood pressure is rising. Increased rate of UAE is higher in patients with elevated blood pressure. Expansion of cellular and matrix components in the

mesangium and mild to moderate GBM thickening can be detected in stage 3 (31). GFR is normal or mildly decreased.

Stage 4 is overt DKD. It is characterized by persistent, severe albuminuria (> 300 mg/24 hours or ACR > 300 mg/g). Renal function declines (GFR < 60 mL/min/1.73 m^2) when associated high blood pressure is left untreated. Segmental mesangiolysis can be observed with progression of diabetes and is associated with development of Kimmelstiel-Wilson nodules (32). These lesions consist of mesangial matrix accumulation with collagen fibrils, small lipid particles and cellular debris.

Stage 5 is ESRD with uremia. It is characterized by decreased UAE due to glomerular loss and < 15 mL/min/1.73 m^2 GFR. Dramatically reduced renal function leads to fluid retention, hypertension, anemia, disturbances of bone and mineral metabolism, dyslipidemia and protein energy malnutrition. Excessive accumulation of ECM proteins in the mesangial space and Kimmelstiel-Wilson lesions finally result in advanced glomerulosclerosis. Interstitial fibrosis and tubular atrophy follow glomerular changes ultimately leading to ESRD requiring dialysis or kidney transplantation (Fig. 2) (33).

1.2.3 Pathogenesis

DKD is a complex and heterogeneous disease with numerous overlapping metabolic and hemodynamic pathways. Hyperglycemia affects most renal cell types; however, some cells are more vulnerable to high glucose concentrations than others. Cells that are unable to regulate glucose uptake are the most sensitive to changes in the diabetic milieu (34). Glucose entry into proximal tubular cells is insulin independent; therefore, these cells are not capable of decreasing glucose transport adequately making them particularly susceptible to high glucose concentrations (35). Hyperglycemia not only affects tubular structures, but also enhances tubular glucose load, exposure and reabsorption. As the tubule grows the amount of reabsorbed glomerular filtrate increases, thus less reaches the macula densa causing GFR increment through the normal physiologic action of the tubuloglomerular feedback (TGF) system (36). Therefore, the proximal tubule may play a role as an initiator and contributor in the early pathogenesis of DKD.

Prolonged hyperglycemia results in production of advanced glycation end products (AGE), activation of the hexosamine and polyol pathway, increased vasoactive renin-angiotensin-aldosterone system (RAAS) activity and hypoxia. All these glucose-induced general mechanisms change renal hemodynamics and promote renal inflammation and fibrosis (37).

1.2.3.1 Renin-angiotensin-aldosterone system

Systemic, circulating RAAS is involved in numerous physiological functions that regulate vasoconstriction, fluid volume regulation, cardiac output and vascular wall integrity. RAAS is a coordinated hormonal cascade that is initiated through renin synthesis in juxtaglomerular cells. Renin enzymatically cleaves liver-derived angiotensinogen into angiotensin I (Ang I). Ang I is further converted to the biologically active peptide angiotensin II (Ang II), a potent vasoconstrictor by pulmonary angiotensin-converting enzyme (ACE). Further investigations proposed that other peptidases (e.g. chymase, cathepsins) could regulate Ang II production as well (38). ACE not only generates Ang II but also degrades the vasodilator bradykinin, thus its activity serves to increase systemic vascular tone (39). ACE2, an enzyme homologue of ACE was identified in the kidney and heart. Their substrate specificities differ; ACE2 hydrolyzes Ang II to form Ang 1-7 400-fold more efficiently than Ang I which generates Ang 1-9 (40-42). These peptides have several opposing actions. Ang II mediates effects via complex intracellular signaling pathways binding to Ang II type 1 receptor (AT1R) and Ang II type 2 receptor (AT2R). Circulating Ang II regulates blood pressure and electrolyte balance via its actions on vascular tone, aldosterone secretion, renal sodium handling, water intake, sympathetic activity and vasopressin release using the AT1R. Ang II stimulation of the AT2R promots vasodilation and growth inhibition, which generally opposes Ang II actions mediated via the AT1R (43).

Data suggest that regulation of renal RAAS is partly independent of systemic circulation. Kidneys express all of the RAAS components necessary for Ang II generation. Renal angiotensinogen is localized in the proximal tubule, where it can interact with renin. Consequently, Ang I is formed and is converted to Ang II in the brush border of proximal

tubular cells (44). In diabetes, high glucose concentration stimulates both angiotensinogen and renin synthesis resulting in Ang II increment (45, 46). Notably, Ang II increases angiotensinogen mRNA expression and this feedback loop establishes a vicious cycle in the kidney. The high Ang II levels and overactivated RAAS lead to elevated blood pressure, mesangial cell contraction with decreased surface area for filtration, renal cell proliferation and hypertrophy, increased production of ECM, induction of growth factors and reactive oxygen species (47, 48). Further, Ang II is a major regulator of Ang II-dependent aldosterone release leading to renal fibrosis (49). Transforming growth factor-β (TGF-β) plays a crucial role in Ang II-dependent renal pathology contributing to epithelial-mesenchymal transition (EMT) (50). Along with TGF-β signaling, Ang II-induced fibrogenesis is also mediated through connective tissue growth factor (CTGF), plasminogen activator inhibitor-1 (PAI-1) and various inflammatory effectors leading to ECM production and renal fibrosis.

1.2.3.2 Protein O-GlcNAcylation

Protein *O*-GlcNAcylation is one of the most common post-translational modifications which was discovered in the early 1980's (51). So far, more than four thousand proteins within the nucleus and cytoplasm have been shown to be modified by *O*-linked N-acetylglucosamine (*O*-GlcNAc) moiety. Unlike other glycosylation forms that consist of sequential chain elongation and complex branching, *O*-GlcNAcylation results in the addition of a single *O*-GlcNAc moiety (52). *O*-GlcNAcylation is the product of nutrient flux through the hexosamine biosynthetic pathway (HBP) to generate uridine diphosphate GlcNAc (UDP-GlcNAc) substrate for *O*-GlcNAcylation. Concentration of UDP-GlcNAc is directly influenced by glucose, amino acids, fatty acids and nucleotides, thus *O*-GlcNAc serves as a nutrient sensor to modulate cellular processes (e.g. signaling, transcription, cytoskeletal functions) in response to nutrient status (53). Under normal physiological conditions, the HBP accounts for 2-5% of glucose utilization. In diabetes, an undesirable effect of hyperglycemia is increased metabolic flux through the HBP leading to several diabetic complications (54). Higher flux via the HBP results in increased UDP-GlcNAc levels causing enhanced *O*-GlcNAcylation, which contributes to

DOI:10.14753/SE.2020.2400

dysregulation of signaling cascades and transcription in cells and tissues of diabetic subjects (55-58).

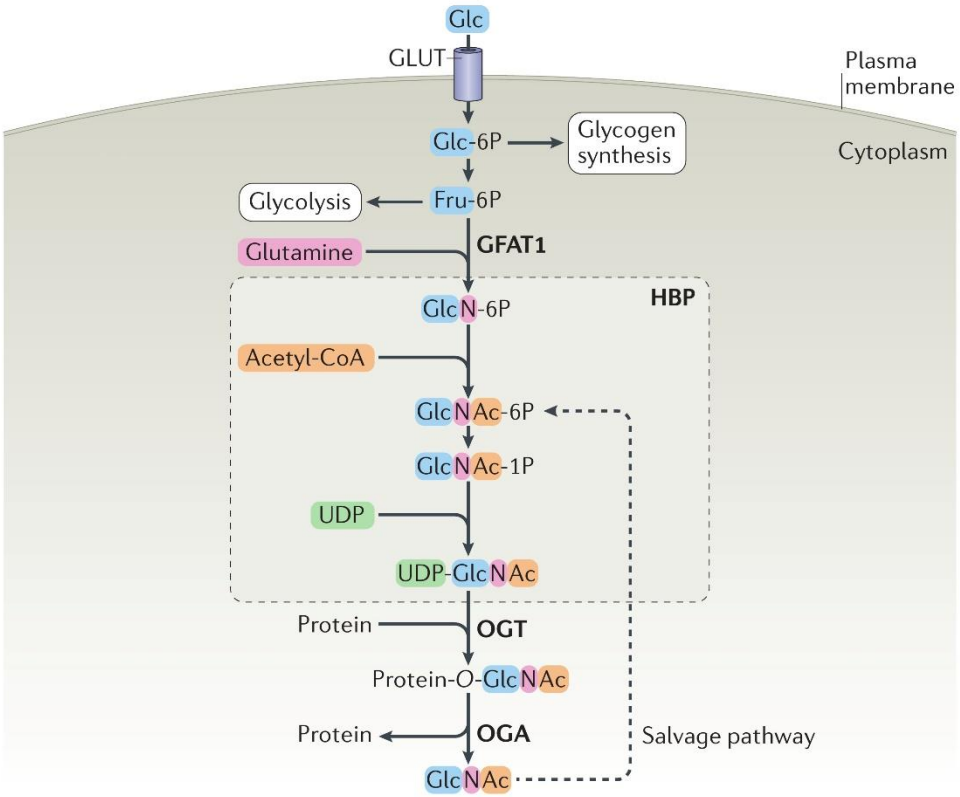

Figure 3 Protein *O*-GlcNAcylation is regulated by nutrient flux via the hexosamine biosynthetic pathway. The majority of glucose is used for glycolysis and glycogen synthesis, while the hexosamine biosynthetic pathway (HBP) accounts for 2-5% of glucose utilization. Glutamine-fructose-6-phosphate amidotransferase 1 (GFAT1) is the rate-limiting enzyme of the HBP, which converts fructose-6-phosphate (Fru-6P) into glucosamine-6-phosphate (GlcN-6P). Subsequent acetylation of GlcN-6P and uridylation of GlcN-1P yields the donor substrate for protein *O*-GlcNAcylation, uridine diphosphate GlcNAc (UDP-GlcNAc). *O*-GlcNAc transferase (OGT) and *O*-GlcNAcase (OGA) catalyse the addition and removal of *O*-GlcNAc, respectively. Free GlcNAc can be recycled via the GlcNAc salvage pathway converting GlcNAc into GlcNAc-6P that can be utilized by the HBP. Modified image of *Yang X, Qian K; Nat Rev Mol Cell Biol. 2017;18(7):452-465.*

O-GlcNAcylation is controlled by a pair of intracellular enzymes. *O*-GlcNAc transferase (OGT) catalyses the addition of a GlcNAc moiety from the donor substrate UDP-GlcNAc to the hydroxyl groups of target proteins at serine and/or threonine residues, while *O*-GlcNAcase (OGA) is responsible for removing β-D-N-acetylglucosamine residues from previously modified proteins. OGT is highly conserved but has three known splice

variants defined as nucleocytoplasmic (ncOGT; 110 kDa), mitochondrial (mOGT; 103 kDa), and short OGT (sOGT; 78 kDa), all of which vary in abundance between tissues. The three isoforms differ only in the number of N-terminal tetratricopeptide repeat (TPR) motifs which affects their substrate recognition (59). Evolutionarily conserved OGA has two major splice variants: the long (OGA-L; 130 kDa) and short (OGA-S; 75 kDa) isoforms. OGA-L is localized in the cytosol and nucleus, whereas OGA-S resides primarily in lipid droplets (Fig. 3) (60).

A growing body of evidence demonstrates the importance of *O*-GlcNAcylation in insulin resistance and glucose toxicity, which are the fundamental pathological processes of diabetes. Literary data indicate that glutamine-fructose-6-phosphate amidotransferase 1 (GFAT1), the rate-limiting enzyme of the HBP is expressed in most tissues involved in the development of diabetic complications (61). Increased GFAT activity appears to be associated with insulin resistance, postprandial hyperglycemia and oxidative stress in T2DM (62). In diabetes, enhanced *O*-GlcNAcylation contributes to the development of complications in several ways. Insulin-responsive glucose uptake is affected by *O*-GlcNAcylation in skeletal muscle and adipose tissue (63). Furthermore, *O*-GlcNAcylation contributes to insulin resistance in adipocytes (64). In addition, deterioration of insulin secretion and pancreatic β-cell death is in part a consequence of diabetes-related increased protein *O*-GlcNAcylation (65, 66).

O-GlcNAcylation has a major role in the regulation of renal fibrosis. *O*-GlcNAcylation plays an essential role in high glucose-induced upregulation of PAI-1 and TGF-β expression contributing to the development of renal fibrosis (67-69). Further, hyperglycemia-induced *O*-GlcNAcylation mediates fibrosis in mesangial cells (70). A study suggests that increased *O*-GlcNAcylation contributing to the development of renal injury and inflammation (71). All these data clearly support that disruption of *O*-GlcNAc homeostasis in diabetes, which has been implicated in the pathogenesis of diabetes and subsequent DKD.

1.2.3.3 Hypoxia

Renal oxygenation is based on a balance between O_2 supply and consumption. A complex interplay between renal blood flow, GFR, O_2 consumption and arteriovenous O_2 shunting maintain renal O_2 tension at constant levels (72). The kidneys are less than 1% of total body weight but use 10% of total O_2 consumption. O_2 is mostly utilized to fuel Na^+/K^+-ATPase in proximal tubular cells, which regulates sodium reabsorption and other transport processes (e.g. solutes, glucose, amino acids). The kidney carries out its complex transport functions in a relatively narrow range of O_2 tension; therefore, it is highly vulnerable to hypoxic injury (73).

Numerous studies have highlighted the pivotal contribution of hypoxia to DKD (74). As early as 1994, Körner *et al.* reported that O_2 consumption of proximal tubules isolated from STZ-diabetic rats is greater than that of control animals (75). These findings have been confirmed by various models and methods throughout the years. Palm *et al.* used Clark-type microelectrodes to show that renal tissue O_2 tension is decreased in diabetic rats (76). Blood oxygenation level-dependent (BOLD) MRI demonstrated that hypoxia is present in the outer medulla as well (77). Renal hypoxia is a consequence of increased blood flow resulting in elevated GFR. In turn, this increases sodium and glucose reabsorption via sodium-glucose cotransporters (SGLT), which leads to enhanced Na^+/K^+-ATPase activity resulting in elevated O_2 consumption. Further, a diabetes-related rapid decline in peritubular capillary density causes inadequate oxygen delivery to tubular cells making them susceptible to hypoxic injury. Collectively, all these processes lead to decreased tissue O_2 tension.

Cells harbor many mechanisms with which they withstand hypoxic challenges; low O_2 tension leads to activation of various genes facilitating adaptation (e.g. erythropoiesis, angiogenesis, iron and glucose metabolism) and survival. Although several transcription factors are participated in the control of hypoxia, hypoxia-inducible factor (HIF) system is the master regulator of this cellular response (78). HIF is a heterodimeric basic helix-loop-helix complex consisting of an α-subunit (HIF-1α, HIF-2α, HIF-3α) and a β-subunit (HIF-1β). In normoxic conditions, HIF-1α is hydroxylated by prolyl 4-hydroxylases

DOI:10.14753/SE.2020.2400

(PHD) and targeted for proteosomal degradation by the von Hippel-Lindau-E3 ubiquitin ligase complex. On the other hand, PHD is inactive and HIF-α degradation is inhibited during hypoxia, thus HIF signaling is activated. HIF-α translocates from the cytoplasm to the nucleus, where it dimerizes with HIF-1β. The HIF complex then binds to hypoxia responsive elements in the promoter sequences of numerous genes involved in maintaining cellular and tissue O_2 homeostasis e.g. erythropoietin (EPO), vascular endothelial growth factor (VEGF) and glucose transporter-1 (GLUT1) (Fig. 4).

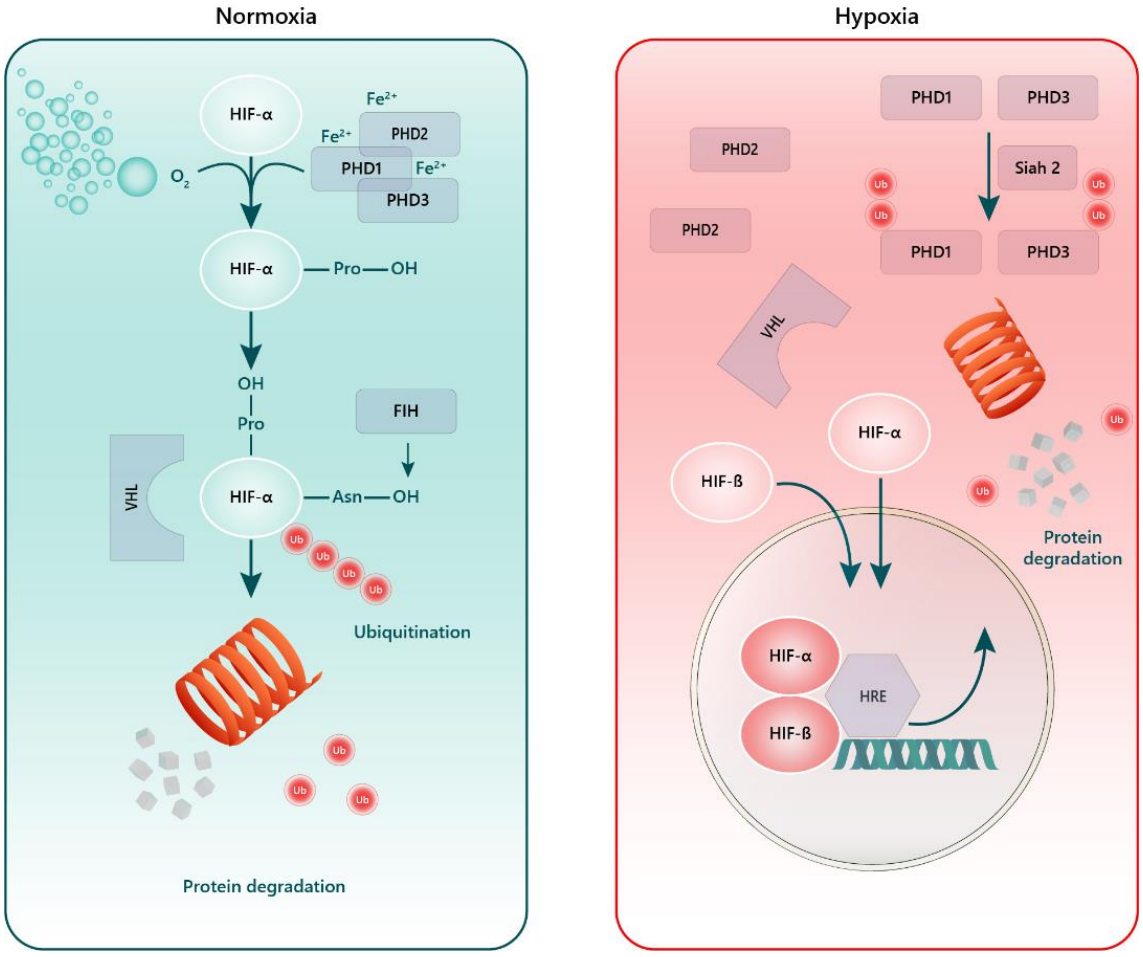

Figure 4 Oxygen regulates HIF-α protein expression. HIF is a heterodimeric transcription factor complex that is composed of an oxygen regulated HIF-1α subunit and a constitutively expressed HIF-1β subunit. HIF-1 activity depends on the degradation of HIF-1α subunit. HIF: hypoxia-inducible factor, FIH: Factor-inhibiting hypoxia-inducible factor, HRE: hypoxia responsive elements, PHD: prolyl 4-hydroxylases, VHL: von Hippel-Lindau-E3

Several studies support the tubular ‘chronic hypoxia hypothesis’ as a dominant pathogenic pathway in DKD, which not only promotes its progression but also initiates (79-81). Hypoxia triggers fibrotic response in tubulointerstitial cells and enhances myofibroblast differentiation. In response to low O_2 tension collagen I production is increased, while matrix-metallopeptidase (MMP) 2 is decreased leading to ECM accumulation (82). Hypoxia also induces TGF-β expression, moreover they can act synergistically in the regulation of VEGF and EPO (83, 84). Activation of HIF plays an important role in tubulointerstitial fibrosis via direct transcriptional regulation of PAI-1, TGF-β and CTGF (85). Tubular hypoxia contributes to the development of tubular atrophy and interstitial fibrosis in a vicious circle promoting DKD progression. Targeting these processes can offer novel opportunities for therapeutic intervention.

1.2.3 Treatment of diabetic kidney disease

Optimization of glucose and blood pressure control to reduce the risk or to slow the progression of DKD are the primary standards of medical care. ADA recommends that targets for glycemic control should be considered with respect to age, comorbidities and life expectancy of patients. According to ADA and Kidney Disease Improving Global Outcomes (KDIGO) guidelines the target HbA_{1C} is about 7.0%. For hypertension management, blood pressure levels of 140/90 mmHg are generally recommended, however, blood pressure targets at 130/80 mmHg may be considered for patients based on anticipated individual benefits and risks. For DKD patients, dietary protein intake should be approximately 0.8 g/bwkg/day and restriction of dietary sodium intake may be useful as well. Avoiding alcohol and tobacco is highly recommended since smoking has already been identified as an independent risk factor of DKD.

ACE inhibitors or ARBs are the preferred first-line medication regimen for blood pressure treatment in diabetic patients with hypertension and moderately increased UAE (86-88). If UAE is moderately increased ACE inhibitor or ARB therapy has been demonstrated to reduce cardiovascular events (89). However, combination of ACE inhibitors and ARBs increase the risk of adverse events (hyperkalemia and/or acute kidney injury) and offers no benefits on DKD. Therefore, the combination should be avoided (90, 91). Aldosterone

antagonists (also known as mineralocorticoid receptor antagonists) combined with ACE inhibitors or ARBs are an area of great interest. Aldosterone antagonists are effective for treatment of resistant hypertension, have been shown to reduce albuminuria in short-term studies of DKD and may have additional cardiovascular benefits. Contrarily, dual therapy may results in increased hyperkalemic episodes (92, 93).

1.3 Role of the kidney in glucose metabolism

Renal involvement in glucose metabolism was first described in the 1930s. The kidney bears a crucial role in the regulation of glucose homeostasis in three different ways: (I) glucose utilization for its energy needs; (II) glucose release through gluconeogenesis; (III) tubular glucose reabsorption from glomerular filtrate. Although each of these can be altered in diabetes, the focus of this thesis is summarizing the mechanism of glucose reabsorption targeted in the management of diabetes.

1.3.1 Renal glucose reabsorption is mediated by SGLT2 and SGLT1

The kidney of a normoglycemic person filters ~180 g glucose per day. Almost all filtered glucose (ca. 99%) is reabsorbed and urine is essentially glucose free. Experiments on isolated rabbit proximal convoluted tubules in the early 1980s proved the presence of two different glucose transporters along the apical surface (94). Wright *et al.* demonstrated the existence of two proximal tubular Na^+/glucose cotransporters by molecular cloning: SGLT2 and SGLT1 as the primary mechanisms of glucose reabsorption in the kidney (95). Later, it was confirmed that low-affinity high-capacity SGLT2 protein is localized in the early proximal tubule (S1 and S2 segments), while high-affinity low-capacity SGLT1 is expressed in the late proximal tubule (S3 segment) in rodents using validated antibodies and knockout mice (96, 97). Recent studies showed the same expression pattern in the human kidney (98).

Tubular glucose reabsorption requires a driving force through the apical to the basolateral membrane. Na^+ and glucose are co-transported from the tubular lumen to the intracellular space through SGLTs by a Na^+ dependent electrochemical gradient. Intracellular glucose is reabsorbed via GLUT1 or GLUT2, while sodium is reclaimed by Na^+/K^+-ATPase on the basolateral membrane, thus releasing them into the bloodstream. The majority of luminal glucose (ca. 97%) is reabsorbed in the early proximal tubule through SGLT2. The transport of Na^+ and glucose occurs in a 1:1 ratio. SGLT1 reclaims the remaining 3% luminal glucose in the late proximal tubule with a Na^+:glucose coupling ratio of 2:1 (Fig. 5). All of the above was demonstrated by renal clearance and micropuncture studies in euglycemic *Sglt1-/-* and *Sglt1/Sglt2* double knockout mice (99).

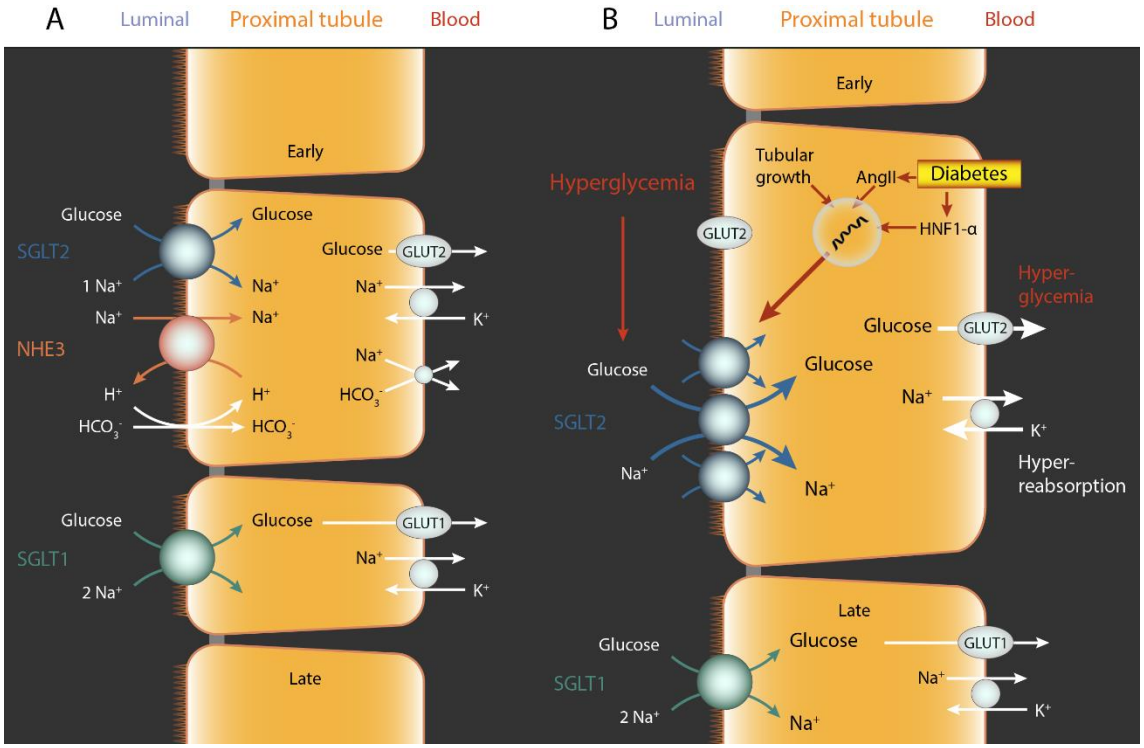

Figure 5 Renal glucose reabsorption is mediated by SGLT2 and SGLT1. (A) SGLT2 reabsorbs ~97% and SGLT1 reabsorbs ~3% of filtered glucose in the proximal tubules. (B) Diabetes increases the expression of SGLT2. This may be due to increased angiotensin II (Ang II) levels, hepatocyte nuclear factor HNF-1α and/or tubular growth. Hyperglycemia and increased SGLT2 expression enhance glucose and Na^+ reabsorption in the proximal tubule. Glucose exits via basolateral GLUT2 to the blood stream. The relevance of luminal translocation of GLUT2 in diabetes remains to be determined. The elevation in filtered glucose and SGLT2 expression enhance the glucosuric effect of SGLT2 inhibitors in diabetes. Based on *Vallon V.; Annu. Rev. Med. 2015;66:255-70.*

Renal glucose filtration and the tubular glucose reabsorption are enhanced to around 600 g per day in T1DM and T2DM. If GFR is normal, the renal transport maximum of glucose is reached when blood glucose levels exceed 11.1 mmol/L leading to a linear increase in glucosuria (100, 101). This process acts as a renal safety valve preventing extreme hyperglycemia. The elevated renal transport capacity of glucose is a consequence of tubular growth (102) or primary upregulation of SGLT2 or SGLT1 in diabetes (103, 104). Diabetes-induced enhanced glucose reabsorption contributes to prolonged hyperglycemia, therefore it can be thought to be maladaptive. The tubular reabsorption capacity of glucose is reducing to the residual capacity of SGLT1 (~80 g/day) in response to SGLT2 inhibition. That is to say, SGLT2 inhibition causes the renal safety valve to open at a lower threshold resulting in normoglycemic and moderately hyperglycemic range of glucose homeostasis (Fig. 6).

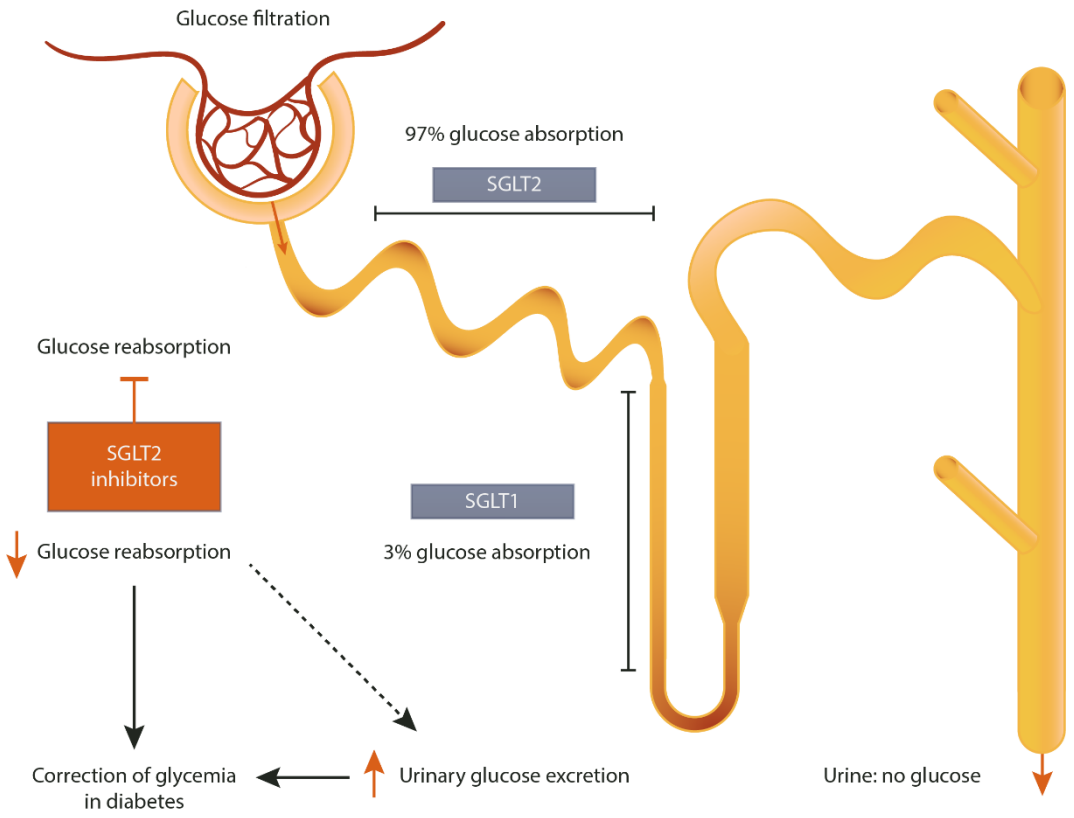

Figure 6 Glucose reabsorption in the kidneys. The kidney of a normoglycemic person filters ~180 g glucose per day. Almost all filtered glucose (ca. 99%) is reabsorbed and urine is essentially glucose free. The majority of luminal glucose (ca. 97%) is reabsorbed in the early proximal tubule through Na^+/glucose cotransporter 2 (SGLT2). Renal glucose filtration and the tubular glucose reabsorption are enhanced in diabetes. SGLT2i induce sustained glucosuria associated with good blood glucose lowering effect in type 2 diabetes.

SGLTs belong to the *SLC5* gene family including six isoforms of the SGLT gene. SGLT1 and SGLT2 are the best characterized cotransporters. SGLT1 is expressed mainly in the brush border membrane of the intestines and the kidney mediating glucose and/or galactose absorption. SGLT2 is localized in the proximal tubules and facilitates glucose reabsorption from the glomerular filtrate. SGLT3 as a renal glucose sensor and/or transporter has only recently been discovered. SGLT4-6 have also been identified but their function and structure is unknown yet (105).

Glucose-galactose malabsorption is an autosomal recessive disorder and is a consequence of a genetic mutation in SGLT1 leading to severe diarrhea (106). Individuals with mutations in SGLT2 gene are diagnosed as having familiar renal glucosuria. Patients with familiar renal glucosuria have reduced tubular glucose reabsorption resulting in persistent glucose excretion of 60-150 g/1.73 m^2 per day without hyperglycemia. Most patients do not develop significant clinical complications over time, however the disorder can be associated with polyuria, polydipsia, polyphagia and recurrent urinary tract infections (107). These observations supported the potential role of SGLT2 inhibitors (SGLT2i) as safe glucose lowering drugs. SGLT2i act by inhibiting glucose reabsorption in renal proximal tubules, thereby lowering plasma glucose levels in an insulin-independent manner.

1.4 Novel antidiabetic drugs: SGLT2 inhibitors

The history of SGLT inhibitor development began with phlorizin, a natural flavonoid and dietary constituent contained in various fruit trees. It was first isolated from the bark of an apple tree in 1835 by French chemists (108). Phlorizin is a potent glucosuric agent and played a key role in uncovering the function of renal glucose reabsorption and the discovery of SGLTs. Phlorizin turned out to be a non-selective inhibitor of both SGLT2 and SGLT1. Since blocking SGLT1 leads to glucose-galactose malabsorption associated with diarrhea, phlorizin was not considered a suitable drug candidate. Further, it has poor metabolic stability due to rapid hydrolysis by β-glucosidase resulting in low oral bioavailability, short plasma half lives and toxic effects of the aglycon phloretin. To minimize the gastrointestinal side effects, the chemical structure of phlorizin was

modified in the late 1990s. The *O*-glucoside analog T-1095 showed promising glucose lowering effects in several diabetes models, however its development was discontinued in phase II (109). Several *O*-glucoside SGLT2 inhibitors were developed, but all "first generation" compounds were rejected due to the metabolic lability of the *O*-glucoside bond resulting in insufficient plasma half life. This problem was solved by C-glucoside-based "second generation" SGLT2i providing greater resistance to β-glucosidase, hence greater oral bioavailability. This discovery has led to the development of longer-acting and more selective SGLT2i.

Dapagliflozin (DAPA) was the frontrunner of C-glucoside-based SGLT2i development. The *in vitro* SGLT inhibitory potential (EC_{50}) of DAPA is 1.1 nM for human SGLT2, equaling 1200-fold selectivity for SGLT2 over SGLT1 compared with phlorizin's 10-fold selectivity. This proved that DAPA is a metabolically robust and selective SGLT2 inhibitor (110). Forxiga™ (DAPA) was the first agent approved by the European Medicines Agency (EMA) for the treatment of T2DM in April 2012, followed by the Food and Drug Administration (FDA) in the United States shortly after. DAPA was followed by canagliflozin and empagliflozin; all three have been approved in the United States and in the European Union. Ipragliflozin, tofogliflozin and luseogliflozin have been approved in Japan. This new class of oral drugs is generally well tolerated and all of them induce sustained glucosuria associated with good blood glucose lowering effect in T2DM. Due to SGLT2i's unique insulin-independent mode of action, their efficacy does not decrease with progressive β-cell dysfunction and/or insulin resistance. Further, SGLT2i can be prescribed as add-on therapy to other antidiabetic agents.

Metabolic control in diabetes requires lifelong treatment, thus drug safety is of paramount importance. Human trial reports on the safety and efficacy of SGLT2i have not revealed major adverse side effects. Despite of this, genital and urinary tract and mycotic infections are the most common salutary effects of SGLT2i; however, these were generally mild to moderate in intensity. In addition, FDA issued a Drug Safety Communication warning in 2015 that SGLT2i treatment may lead to euglycemic DKA. Cases have been reported in both T1DM and T2DM diabetic patients. Euglycemic DKA is a consequence of lower insulin levels, hyperglucagonemia and volume depletion leading to lipolysis and

ketogenesis. Of note, the FDA identified potential triggering factors of DKA e.g. intercurrent illness, reduced food and fluid intake, reduced insulin doses and history of alcohol intake. Despite of this, the Empagliflozin Cardiovascular Outcome Event Trial in Type 2 Diabetes Mellitus Patients-Removal of Excess Glucose (EMPA-REG OUTCOME) study did not find any difference in rates of ketoacidosis in T2DM patients treated with empagliflozin *vs.* placebo. Nevertheless, further studies are needed to define the clinical relevance and the mechanisms involved.

1.4.1 Pleiotropic effects of SGLT2 inhibitors

The proof of cardiovascular safety for new glucose-lowering therapies has been required by FDA since 2008. Empagliflozin, canagliflozin, and dapagliflozin have been evaluated for cardiovascular safety in large-scale multicenter clinical trials: EMPA-REG OUTCOME, Canagliflozin Cardiovascular Assessment Study (CANVAS) and Dapagliflozin Effect on Cardiovascular Events-Thrombolysis in Myocardial Infarction 58 (DECLARE-TIMI 58), respectively (111-113). Each of these trials showed low incidence of heart failure and mitigated loss of kidney function in patients with T2DM and cardiovascular disease. These data indicate that renoprotection may be a class effect of SGLT2i. The objective of these trials was to investigate the cardiovascular safety of SGLT2i, hence subjects at high cardiovascular risk were primary enrolled and only relatively few patients with established CKD were included. Improved renal outcomes in these trials suggested that SGLT2i might also improve renal outcomes for patients with established DKD. The Canagliflozin and Renal Events in Diabetes with Established Nephropathy Clinical Evaluation (CREDENCE) trial recently proved that SGLT2i slow the progression of DKD. Patients with T2DM and albuminuric CKD (ratio of albumin [mg] to creatinine [g], >300 to 5000 and eGFR 30-90 mL/min/1.73 m^2) who were already receiving RAAS blockers were enrolled in the CREDENCE study. The progression to ESRD, a doubling of the creatinine level or death from renal failure were 34% lower in the SGLT2i treatment group *vs.* placebo at a median follow-up of 2.6 years (114). Another ongoing clinical trial, A Study to Evaluate the Effect of Dapagliflozin on Renal Outcomes and Cardiovascular Mortality in Patients With Chronic Kidney Disease (DAPA-CKD) is evaluating the effect of DAPA on renal outcomes and cardiovascular mortality in patients

with chronic kidney disease (eGFR 25-75 mL/min/1.73m^2). Comparison studies suggest that SGLT2i are more renoprotective than other antidiabetics (e.g. GLP analogues) with similar glucose lowering effect (115). These results were substantiated by another study in which reduced albuminuria was independent of changes in HbA_{1c}, blood pressure or body weight in DAPA-treated T2DM patients (116). Thus, renoprotection may arise not only beacuse of lower glucose levels, but due to other mechanisms of SGLT2i, such as inhibition of TGF, anti-inflammatory or anti-fibrotic effects. These renoprotective outcomes are encouraging and indicate that SGLT2i offer a promising therapeutic option in the future management of patients with T2DM.

1.4.2 SGLT2 inhibitors for the treatment of type 1 diabetes

DAPA is the first SGLT2i approved in the European Union as an adjunct to insulin in T1DM adults with a body mass index (BMI) of ≥ 27 kg/m^2, when insulin alone does not provide adequate glycemic control despite optimal insulin therapy. The therapeutic efficacy of DAPA as an adjunct to insulin in adult patients with insufficiently controlled T1DM was assessed in 24-week, phase III studies, Dapagliflozin Evaluation in Patients with Inadequately Controlled Type 1 Diabetes (DEPICT)-1 and in DEPICT-2. The results of DEPICT-1 showed a significant reduction in HbA_{1c}, body weight, total insulin dose and glycemic variability with no increase in the risk of hypoglycemia or DKA (117). Improved HbA_{1c}, mean glucose levels, glycemic variability and time in glycemic target range with no increase in hypoglycemia *vs.* placebo were demonstrated in DEPICT-2. Although there were several events of DKA in patients receiving DAPA (118). Overall, the DEPICT trials provide short-term evidence for using DAPA as adjunct therapy to adjustable insulin to improve glycemic control in T1DM patients. Therefore, the aim of my PhD work was to investigate the potential protective properties of DAPA as a promising therapeutic option of DKD in a rat model of T1DM.

DOI:10.14753/SE.2020.2400

2 OBJECTIVES

The objective of our study was to identify new therapeutic options in the management of DKD. Based on the current literary data indicating that SGLT2i are renoprotective beyond their blood glucose lowering properties, the aim of our experiments was to investigate the potential antifibrotic effects of DAPA in DKD with special focus on protein *O*-GlcNAcylation and tubular hypoxia. We also wanted to compare the renoprotective effects of SGLT2i with the current gold-standard clinical therapy with RAAS inhibitors.

Specific aims:

1. To determine the antifibrotic and renoprotective effects of various RAASi in monotherapy in experimental model of T1DM

2. To investigate the safety and efficacy of DAPA and DAPA combined with ARB losartan in T1DM

3. To analyze the protective effects of DAPA in DKD

4. To evaluate the possible antifibrotic role of DAPA both *in vivo* and *in vitro*

5. To determine the effects of DAPA and DAPA combined with losartan on protein *O*-GlcNAcylation and hypoxia in human proximal tubular cells

DOI:10.14753/SE.2020.2400

3 METHODS

Study approval

All experiments were conducted in accordance with guidelines of the Committee on the Care and Use of Laboratory Animals of the Semmelweis University Budapest, Hungary (PEI/001/1731-9-2015).

Materials

All chemicals and reagents were purchased from Sigma-Aldrich (St. Luis, MO, USA) and all standard plastic laboratory equipment was purchased from Sarstedt (Numbrecht, Germany) unless stated otherwise.

3.1 Animals and experimental design

Experiments were performed on eight-week old male Wistar rats (*Rattus norvegicus*) purchased from Toxi-Coop Ltd. (Budapest, Hungary). Rats were housed in plastic cages under a 12-hour light/dark cycle at constant temperature (24±2 °C) with *ad libitum* access to standard rodent chow and tap water.

Diabetes was chemically induced with a single intraperitoneal injection of 65 mg/bwkg streptozotocin (STZ) dissolved in 0.1 M citrate buffer (pH 4.5). Blood glucose levels were measured with a Dcont Ideal device (77 Elektronika, Budapest, Hungary) three times from tail vein. Rats with a peripheral blood glucose value above 15 mmol/L 72 hours after the STZ injection were enrolled in the study. Two different experimental protocols were used.

Protocol I

After five weeks of diabetes rats were randomized into five groups (n=7-8/group) and were treated daily by oral gavage for 2 weeks as follows:

1. isotonic saline as vehicle (D)
2. enalapril dissolved in isotonic saline (D + ENA; 40 mg/bwkg/day)
3. losartan dissolved in isotonic saline (D + LOS; 20 mg/bwkg/day)
4. spironolactone dissolved in isotonic saline (D + SPI; 50 mg/bwkg/day)
5. eplerenone dissolved in isotonic saline (D + EPL; 50 mg/bwkg/day).

Doses were adopted from our previous studies in line with literary data where effective blockade of ACE, AT1R or aldosterone activity was achieved without changes in systemic blood pressure (119-121). Non-diabetic, age-matched controls (n=7-8/group) received equivalent volumes of citrate buffer without STZ once, and the same amount of saline by oral gavage daily at the same time as the diabetic animals throughout the 2-week treatment period (Fig. 7).

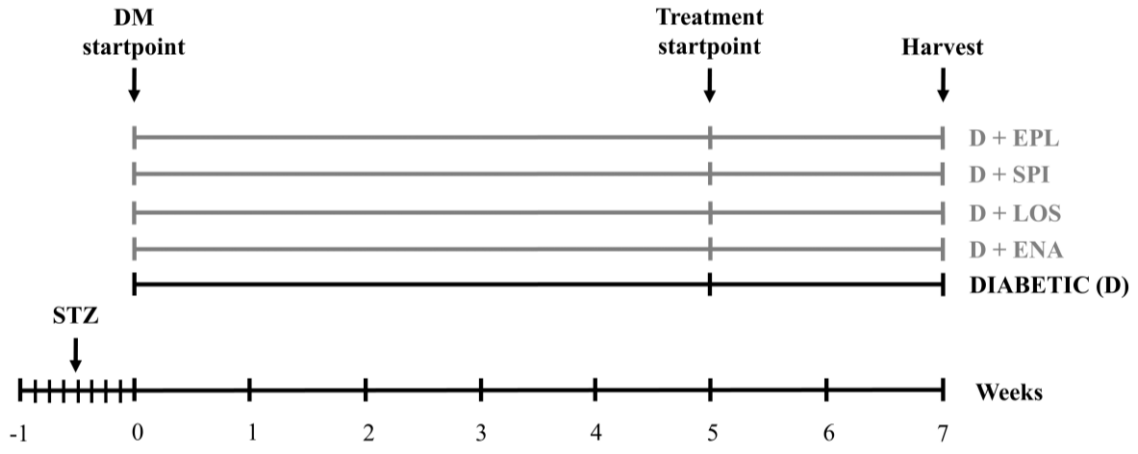

Figure 7 Experimental design of Protocol I. After five weeks of diabetes rats were randomized into five groups (n=7-8/group) and were treated daily by oral gavage for 2 weeks with isotonic saline as vehicle or D+ENA: D+enalapril, D+LOS: D+losartan, D+SPI: D+spironolactone, D+EPL: D+eplerenon. DM: diabetes mellitus, STZ: streptozotocin

Protocol II

Rats were randomly divided into three groups immediately after the onset of diabetes (n=6 in D and n=7 in treatment groups) and were treated *per os* as follows:

1. isotonic saline as vehicle (D)
2. DAPA dissolved in isotonic saline (D + DAPA; 1 mg/bwkg/day for six weeks)
3. DAPA + losartan dissolved in isotonic saline (D + DAPA + LOS; 1 mg/bwkg/day DAPA for six weeks + 20 mg/bwkg/day losartan in the last three weeks of the protocol)

Age-matched controls (n=6) received the equivalent volume of citrate buffer without STZ once, and the same amount of saline by oral gavage daily at the same time as the diabetic animals during the 6-week study period. Rats were weighed daily; blood glucose levels were measured weekly. Blood pressure, serum and urinary parameters were determined twice throughout the study period (Fig. 8).

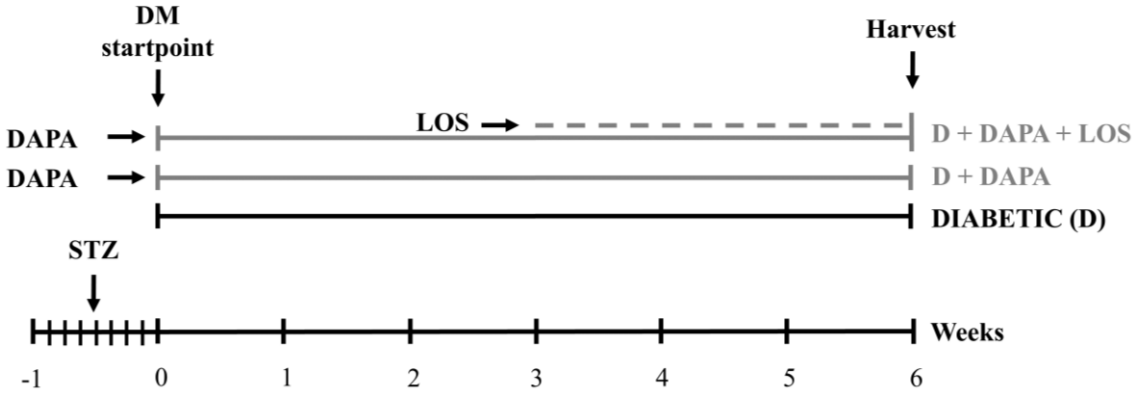

Figure 8 Experimental design of Protocol II. Rats were randomly divided into three groups immediately after the onset of diabetes (n=6 in D and n=7 in treatment groups) and were treated *per os* as follows: isotonic saline as vehicle (diabetic) or dapagliflozin (D+DAPA) or dapagliflozin + losartan (D + DAPA + LOS; DAPA for six weeks + losartan in the last three weeks of the protocol). STZ: streptozotocin

In both protocols, rats were placed into metabolic cages to collect urine for a 24-hour period before euthanasia. At the end of the experiments rats were anesthetized by a mixture of 75 mg/bwkg ketamine (Richter Gedeon, Budapest, Hungary) and 10 mg/bwkg xylazine (Medicus Partner, Biatorbagy, Hungary) after which terminal blood was drawn from the abdominal aorta to sacrifice the animals. Blood, urine and kidney samples were collected and stored for further investigations.

3.2 Measurement of arterial blood pressure

Systolic and diastolic pressures were measured on tail vein using a CODA Standard monitor system (EMKA Technologies, Paris, France) which uses clinically validated proprietary volume pressure recording. Mean arterial pressure (MAP) was calculated.

3.3 Metabolic and renal parameters

Serum and urinary parameters were photometrically determined with commercially available kits on a Hitachi 912 photometric chemistry analyzer (Roche Hitachi, Basel, Switzerland). Creatinine clearance, albumin excretion and glucosuria were determined from 24-hour collected urine. Urinary kidney injury molecule-1 (KIM-1) and neutrophil gelatinase-associated lipocalin (NGAL) levels were measured using rat specific enzyme-linked immunosorbent assays (ELISA) (R&D Systems, Minneapolis, MI, USA).

3.4 Cell cultures and experimental design

Human proximal tubular epithelial cell line (HK-2; LGC Standards, ATCC Cat#CRL-2190, American Type Culture Collection, Manassas, VA, USA) was grown in DMEM (5.5 mM or 25 mM D-glucose) supplemented with 10% FBS, 1% L-glutamine, 1% antibiotic, antimycotic solution containing 10,000 IU/mL penicillin, 10 mg/mL streptomycin and 25 mg/mL Amphotericin B (Thermo Fisher Scientific, Waltham, MA, USA). Cells were incubated at 37 °C in a humidified atmosphere of 5% CO_2 and 95% air. Then, cells were plated either in 6-well plates (5×10^5 cells/well) or in 24-well plates

(1.2×10^5 cells/well) and there was a growth arrest period of 24 hours in serum-free medium before treatment in all experiments. Three sets of experiments were performed.

Hyperglycemia model

The effect of high glucose was tested on HK-2 proximal tubular cells cultured in DMEM containing 5.5 mM glucose and treated with high glucose (HG; final cc. 35 mM) or high mannitol (final cc. 35 mM) for 24 hours. HG cells were treated with 10 μM DAPA (HG + DAPA; Santa Cruz Biotechnology Inc., Heidelberg, Germany) or 10 μM DAPA combined with 10 μM LOS (HG + DAPA + LOS) for 24 hours. Cells in 5.5 mM glucose conditions served as controls and mannitol treated cells were used for testing hyperosmolarity *per se*.

Hypoxia model

Hypoxia was induced in bold line stage top CO_2/O_2 incubator (Okolab, Ottaviano, Italy) by keeping the cells in 1% O_2 for 2 hours. HK-2 cells cultured in medium containing 25 mM glucose were treated as follows: 10 μM DAPA (H + DAPA) or 10 μM DAPA combined with 10 μM LOS (H + DAPA + LOS) for 24 hours before harvest. Cells were harvested at the end of hypoxia. Cells cultured under normoxic conditions served as controls.

Cell viability and proliferation assay

Prior to the experiments, the non-toxic dosage of DAPA and LOS was confirmed by methyl-thiazoletetrazolium assay (MTT) (Roche Diagnostics, Mannheim, Germany). Cell viability was determined by MTT assay according to the manufacturer's instructions.

Cell viability was also assessed by trypan blue exclusion. Cells were detached with trypsin-EDTA and re-suspended in medium diluted 1:1 with trypan blue solution. Live cells from triplicate wells were counted in a Bürker chamber.

3.5 Conventional renal histology

Periodic acid-Schiff staining

Renal cortex was separated under light microscope and fixed in 4% buffered formalin, embedded in paraffin and 5 μm thick sections were cut. Images were taken with a Zeiss AxioImager A1 light microscope (Zeiss, Jena, Germany). To evaluate mesangial matrix expansion sections were stained with periodic acid-Schiff (PAS). Twenty fields of x400 magnification containing glomeruli were randomly selected per animal, excluding incomplete glomeruli along the sample edge. The ratio of mesangial area (number of pixels containing purple mesangial matrix deposition) per glomerular tuft area (total number of pixels in the glomerulus) was measured in each glomerulus.

Masson's trichrome staining

To evaluate tubulointerstitial fibrosis sections were stained with Masson's trichrome. Ten fields of x200 magnification were randomly selected from cortical and cortico-medullary regions respectively per animal. The ratio of Masson-stanied fibrotic area (pixels containing stained interstitial fibrotic tissue) per total area (total number of pixels in the area) was measured in each field.

Picrosirius red staining

To evaluate collagen accumulation sections were stained with Picrosirius red. Ten fields of x200 magnification were randomly selected from cortical and cortico-medullary regions per animal. The ratio of Picrosirius red-stanied interstitial area per total area was measured in each field area to obtain the percentage of collagen deposition.

Areas were measured with Panoramic Viewer software version 1.15.2 (3DHISTECH, Budapest, Hungary). Analysis was performed in a double blinded fashion with computer-assisted morphometry using Adobe Photoshop CS6 (Adobe Inc., San José, CA, USA) and Image J (US National Institute of Health, Bethesda, MD, USA) softwares.

3.6 Immunohistochemistry

All reagents for and fibronectin immunohistochemistry were obtained from Hisztopatologia (Pecs, Hungary) respectively. Slides were deparaffinized in xylene, rehydrated in graded ethanol series and washed in dH_2O. Heat-induced epitope retrieval was performed by boiling the paraffin-embedded tissue sections in citrate buffer (pH=6). Slides were peroxidase blocked and nonspecific attachments were inhibited with protein solution. Sections were incubated against fibronectin (ab2413; Abcam, Cambridge, MA, USA) antibody followed by peroxidase labelled anti-rabbit antibody. Fibronectin was visualized with HISTOLS-Resistant AEC Chromogen/Substrate System counterstained with hematoxylin and eosin and mounted with permanent mounting medium. Evaluation of fibronectin staining was performed similarly to PAS stained samples.

3.7 Immunocytochemistry

HK-2 cells were cultured in tissue culture chambers and various treatments or hypoxia were applied. After repeated washing cells were fixed in 4% paraformaldehyde, washed again with phosphate buffered saline (PBS) and permeabilized with Triton X-100. After blocking with 5% bovine serum albumin (BSA) cells were incubated with the same *O*-GlcNAc and HIF-1α antibodies used for western blotting for overnight at 4 °C. After repeated washing cells were incubated with specific secondary antibodies: Alexa Fluor 488 goat anti-mouse (A-11001; Invitrogen™, Carlsbad, CA, USA) and Alexa Fluor 488 chicken anti-rabbit (A-21441; Invitrogen™) respectively for 1 hour at room temperature. Samples were washed with PBS and nuclei were counterstained with Hoechst 33342 (4082S; Cell Signaling Technology Inc., Danvers, MA, USA). Cells were mounted with ProLong Glass Antifade Mountant then a glass coverslip was added (P36982, Invitrogen™). Appropriate controls were performed, omitting the primary antibody to assure specificity and to avoid autofluorescence. Cells were imaged using an inverted microscope (Ti2; Nikon, Tokyo, Japan) equipped with a 20x objective (CFI Plan Apochromat Lambda, N.A. 0.75). For the semi-quantitative evaluation of fluorescence 10 visual fields/treatment were analyzed with ImageJ software (US National Institute of Health) (122).

3.8 Measurement of biomarkers of ECM formation and degradation

The biomarkers rPRO-C3 (measuring collagen type III formation), uC3M (measuring collagen type III degradation by MMP-9), and TUM (measuring tumstatin, a collagen type IV fragment degraded by MMP-9) were measured in rat urine samples using competitive ELISA developed by Nordic Bioscience (Herlev, Denmark). Biomarker levels were normalized to urinary creatinine levels measured using the QuantiChrom™ Creatinine Assay kit (BioAssay Systems, USA). The assays were carried out at Nordic Bioscience laboratories following previously described protocols (123). Briefly, a streptavidin-coated 96-well ELISA plate were coated with biotinylated peptide for 30 min. Plates were washed and incubated with standard peptide or sample together with HRP-conjugated monoclonal antibody and incubated for overnight at 4°C (uC3M, rPRO-C3) or 1 hour at room temperature (TUM). Plates were washed and incubated with 3,3′,5,5-tetramethylbenzidine (4380H, Kem-En-Tec, Taastrup, Denmark) for 15 min at room temperature in the dark. To stop the reaction, 1% sulfuric acid solution was added, and plates were analysed with the ELISA reader at 450 nm with 650 nm as reference (VersaMax, Molecular Devices, CA, USA).

3.9 Quantitative RT-PCR

Total RNA was extracted using the Total RNA Mini Kit (Geneaid Biotech Ltd, New Taipei City, Taiwan). The quality and quantity of isolated RNA was measured on a NanoDrop ND-1000 spectrophotometer (Baylor College of Medicine, Houston, TX, USA). 500 ng RNA was reverse-transcribed using Maxima™ First Strand cDNA Synthesis Kit for RT-qPCR (Thermo Fisher Scientific, Waltham, MA, USA) to generate first-strand cDNA. *Tgfb1, Ctgf, Pdgfb, Fn1, Havcr1, Lcn2, Rn18S, TGFB1, CTGF, PDGFB, HIF1A, GAPDH* and *RN18S* mRNA expressions were determined in duplicates using LightCycler 480 SYBR Green I Master enzyme mix (Roche Diagnostics, Indianapolis, IN, USA) and specific primers listed in Table 1. Primer sequences were designed using Lasergene PrimerSelect software version 7.1.0 (DNASTAR, Madison, WI, USA) based on nucleotide sequences from the nucleotide database of National Center for Biotechnology Information. Results were analyzed by the LightCycler® 480 software

version 1.5.0.39 (Roche Diagnostics, Indianapolis, IN, USA). Target gene expressions were normalized against *Rn18S* or *RN18S* mRNA or *GAPDH* housekeeping genes.

Table 1 Sequences of primer pairs for quantitative RT-PCR.

Gene	NCBI reference	Primer Pairs	Product length (bp)
Tgfb1	NM_021578.2	Forward: 5' GCACCGGAGAGCCCTGGATACC 3' Reverse: 5' CCCGGGTTGTGTTGGTTGTAGAGG 3'	222
Ctgf	NM_022266.2	Forward: 5' TCCACCCGGGTTACCAATGACAATAC 3' Reverse: 5' CTTAGCCCGGTAGGTCTTCACACTGG 3'	195
Pdgfb	NM_031524.1	Forward: 5' TCGATCGCACCAATGCCAACTTCC 3' Reverse: 5' CACGGGCCGAGGGGTCACTACTGT 3'	236
Fn1	NM_019143.2	Forward: 5' GGGCCGGGGCAGATGGAAATG 3' Reverse: 5' CCCAATGCCACGGCCCTAACAGTA 3'	142
Havcr1	NM_173149.2	Forward: 5' CGCAGAGAAACCCGACTAAG 3' Reverse: 5' CAAAGCTCAGAGAGCCCATC 3'	194
Lcn2	NM_130741.1	Forward: 5' CAAGTGGCCGACACTGACTA 3' Reverse: 5' GGTGGGAACAGAGAAAACGA 3'	194
Rn18s	NR_046237.1	Forward: 5' GCGGTCGGCGTCCCCCAACTTCTT 3' Reverse: 5' GCGCGTGCAGCCCCGGACATCTA 3'	105
RN18S	NR_003286.4	Forward: 5' GGCGGCGACGACCCATTC 3' Reverse: 5' TGGATGTGGTAGCCGTTTCTCAGG 3'	136
HIF1A	NG_029606.1	Forward: 5' CATAAAGTCTGCAACATGGAAGGT 3' Reverse: 5' ATTTGATGGGTGAGGAATGGGTT3'	148
EPO	NM_000799.4	Forward: 5' - GAGCCCAGAAGGAAGCCATC - 3' Reverse: 5' - GTCAGCAGTGATTGTTCGGA - 3'	71
VEGFA	NM_001025366.3	Forward: 5' - GCAAGACAAGAAAATCCCTGTG - 3' Reverse: 5' - TGAGAGATCTGGTTCCCGAA - 3'	220
TGFB1	NM_000660.7	Forward: 5' CGAGGCGCCCGGGTTATGC 3' Reverse: 5' GCGTGCGGCAGCTGTACATTGACT 3'	174
CTGF	NM_001901.3	Forward: 5' CTCCACCCGGGTTACCAATGACAA 3' Reverse: 5' CAGCATCGGCCGTCGCTACATACT 3'	228
PDGFB	NM_002608.4	Forward: 5' GCGCCGGGAGATCTCGAACACCT 3' Reverse: 5' AGATGGGGCCGAGTTGGACCTGAA 3'	163
GAPDH	NM_001289745.3	Forward: 5' AGCAATGCCTCCTGCACCACCAA 3' Reverse: 5' GCGGCCATCACGCCACAGTTT 3'	159

3.10 Western blot

All reagents and equipment for Western blot were obtained from Bio-Rad Laboratories Inc. (Hercules, CA, USA) unless stated otherwise. Total protein was extracted from kidney cortex and HK-2 cells. Samples were homogenized in lysis buffer (1 M Tris, 0.5 M EGTA, 1% Triton X-100, 0.25 M NaF, 0.5 M phenylmethylsulfonyl fluoride, 0.5 M sodium orthovanadate, 5 mg mL^{-1} leupeptin, and 1.7 mg mL^{-1} aprotinin, pH 7.4) by Fastprep RP120 homogenisator (Thermo Fisher Scientific). Lysates were centrifuged at 13 000 rpm at 4°C for 10 min. Protein concentration of the supernatants was measured in 96-well microplates with a *DC*™ Protein Assay kit at 650 nm by a SPECTROstar Nano microplate reader (BMG Labtech, Ortenberg, Germany). Protein samples were mixed with 4x Laemmli sample buffer (1:3) and heated at 95 °C for 5 minutes or 37 °C for 30 minutes.

Samples were electrophoretically resolved on polyacrylamide gradient gels (4-20%) and transferred to nitrocellulose membranes with fast and high-efficiency semi-dry Trans-Blot Turbo™ Transfer System. The protein transfer was verified by 1% Ponceau S staining. After blocking, membranes were immunoblotted with specific primary antibodies. After repeated washing, the blots were incubated with the appropriate horseradish peroxidase (HRP)-conjugated secondary antibodies. Luminata™ Forte Western HRP Substrate (Millipore Corporation, Billerica, MA, USA) was used for chemiluminescent detection of blots. Details of antibodies are listed in Table 2 and Table 3.

Densitometric analysis of bands was performed by Quantity One Analysis software (Bio-Rad Laboratories Inc.). After background subtraction, integrated optical densities of bands of interest were factored for Ponceau S staining to correct for variations in total protein loading. Each blot was normalized to an internal control so that bands on separate blots could be compared.

Table 2 List of primary antibodies used for Western blots.

Target protein	Manufacturer	Catalog number	Source	Dilution buffer	Dilution
α-SMA	Sigma Aldrich St. Luis, MO, USA	A2547	mouse monoclonal	1% wt/vol non-fat milk, 1xTBS 0.4% wt/vol Tween 20	1:500
CTGF	Santa Cruz Biotechnology Heidelberg, Germany	SC-14939	goat polyclonal	5% wt/vol non-fat milk, 1xTBS 0.1% wt/vol Tween 20	1:500
EPO	Santa Cruz Biotechnology Heidelberg, Germany	SC-5290	mouse monoclonal	5% wt/vol non-fat milk, 1xTBS 0.1% wt/vol Tween 20	1:500
HIF-1α	Abcam, Cambridge, MA, USA	ab2185	rabbit polyclonal	5% wt/vol BSA, 1xTBS 0.1% wt/vol Tween 20	1:1000
OGA	Proteintech Europe, Manchester, UK	14711-1-AP	rabbit polyclonal	5% wt/vol non-fat milk, 1xTBS 0.1% wt/vol Tween 20	1:1000
***O*-GlcNAc**	Sigma Aldrich St. Luis, MO, USA	07764	rabbit polyclonal	1% wt/vol BSA, 1xTBS 0.05% wt/vol Tween 20	1:1000
OGT	Sigma Aldrich St. Luis, MO, USA	O6264	rabbit polyclonal	1% wt/vol non-fat milk, 1xTBS 0.4% wt/vol Tween 20	1:1000
PDGF	Santa Cruz Biotechnology Heidelberg, Germany	SC-7878	rabbit polyclonal	5% wt/vol non-fat milk, 1xTBS 0.1% wt/vol Tween 20	1:500
VEGF-A	Abcam, Cambridge, MA, USA	ab46154	rabbit polyclonal	5% wt/vol BSA, 1x TBS 0.1% wt/vol Tween 20	1:1000

Table 3 List of secondary antibodies used for Western blots.

Target protein	Manufacturer	Catalog number	Source	Dilution buffer	Dilution
Goat IgG	Santa Cruz Biotechnology Heidelberg, Germany	2020	donkey	1x TBS 0.05% wt/vol Tween 20	1:3000
Mouse IgG	Cell Signaling Technology Inc. Danvers, MA, USA	7076	goat		
Rabbit IgG	Cell Signaling Technology Inc. Danvers, MA, USA	7074	goat		

3.11 Statistical analysis

Data are expressed as means±standard deviations (SD) or means±95% confidence intervals. Statistical analysis was performed using Prism software (version 7.0; GraphPad Software Inc., San Diego, CA, USA). Multiple comparisons and interactions were evaluated by one-way ANOVA followed by Holm-Sidak *post hoc* test. For non-parametrical data, the Kruskal-Wallis ANOVA on ranks followed by with Dunn correction was used. *P* values of <0.05 were considered significant.

DOI:10.14753/SE.2020.2400

4 RESULTS

4.1 Effect of RAASi on metabolic parameters and renal function

4.1.1 MAP remained unaltered in control, diabetic and RAASi-treated groups

Our aim was to investigate the effect of RAAS blockade regardless of their antihypertensive properties. Doses were adopted from our previous studies in line with literary data. The protocol was successfully applied, since MAP remained unchanged in all groups confirming that the examined effects of RAASi are independent of their antihypertensive properties (Table 4).

Table 4 Mean arterial pressure of control, diabetic and RAASi treated diabetic rats. Mean arterial pressure (MAP) values of control, diabetic (D) and RAASi-treated (D+ENA: D+enalapril, D+LOS: D+losartan, D+SPI: D+spironolactone, D+EPL: D+eplerenon) diabetic rats. Values indicate means±SDs and data were analyzed by oneway ANOVA with Holm-Sidak multiple comparisons test (n=7-8 rats/group).

	Control	Diabetic (D)	D + ENA	D + LOS	D + SPI	D + EPL
MAP (mmHg)	74.7±3.83	73.9±4.48	62.9±2.72	73.8±7.13	77.4±8.16	77.3±6.73

DOI:10.14753/SE.2020.2400

4.1.2 RAASi are not affect metabolic parameters

Metabolic parameters were evaluated after seven weeks of diabetes. Rats had significant weight loss, elevated blood glucose, fructosamine and lipid levels confirming the development of T1DM. RAASi did not alter any of these parameters. Enalapril and aldosterone antagonists improved cholesterol levels. Liver enzymes remained unaltered in all groups (Table 5).

Table 5 Metabolic parameters of control, diabetic and RAASi treated diabetic rats. Values indicate means±SDs and data were analyzed by one-way ANOVA with Holm-Sidak multiple comparisons test (n=7-8 rats/groups). *p<0.05 *vs.* Control, **p<0.01 *vs.* Control, §p<0.05 *vs.* Diabetic. GOT: serum glutamate-oxaloacetate transaminase. GPT: serum glutamate-pyruvate transaminase, D+ENA: D+enalapril, D+LOS: D+losartan, D+SPI: D+spironolactone, D+EPL: D+eplerenon

Metabolic Parameters	Control	Diabetic (D)	D + ENA	D + LOS	D + SPI	D + EPL
Body weight (g)	418±23.4	276±28.9*	291±13.3*	258±24.8*	245±35.1*	288±20.9*
Glucose (mmol/L)	12.7±1.15	47.3±7.80*	35.3±3.23*	43.8±4.79*	42.6±2.55*	34.8±3.57
Fructosamine (μmol/L)	153±8.28	243±16.3**	250±5.09**	256±17.6**	239±11.5**	239±16.5**
Cholesterol (mmol/L)	1.90±0.05	2.28±0.06*	1.82±0.10§	2.06±0.08	1.72±0.11§	1.82±0.14§
Triglycerides (mmol/L)	0.57±0.07	1.90±0.50*	0.99±0.43	1.31±0.37	1.13±0.12	0.88±0.09
GOT (U/L)	168±8.20	221±27.0	186±21.6	158±31.6	160±14.7	156±12.2
GPT (U/L)	53.9±1.53	74.5±9.18	76.2±10.7	88.9±14.7	74.3±7.41	70.9±6.74

DOI:10.14753/SE.2020.2400

4.1.3 RAASi and renal function

Development of DKD was confirmed by the decline of renal function. Creatinine clearance decreased, while serum creatinine, blood urea nitrogen (BUN) and UAE elevated in diabetic rats. ENA, SPI and EPL improved creatinine clearance. BUN and albumin excretion were significantly reduced by all treatments (Fig. 9).

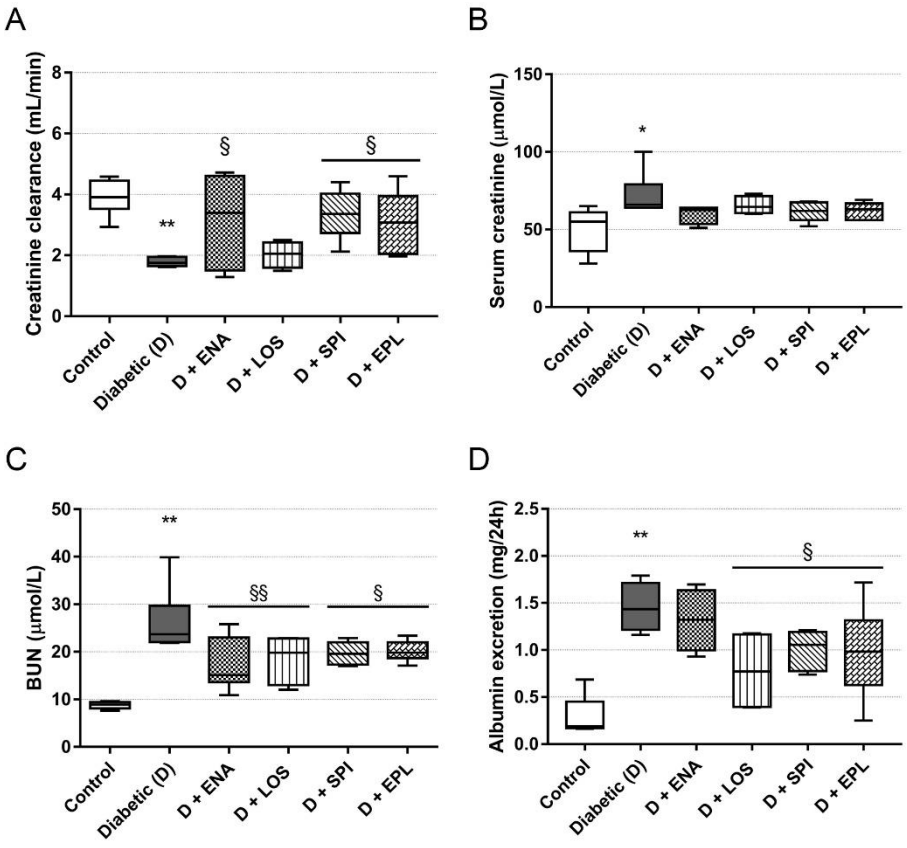

Figure 9 Renal function is improved by RAASi. (A) Creatinine clearance, (B) serum creatinine, (C) blood urea nitrogen (BUN) and (D) albumin excretion of control, diabetic (D) and RAASi treated (D+ENA: D+enalapril, D+LOS: D+losartan, D+SPI: D+spironolactone, D+EPL: D+eplerenon) diabetic rats. Values are presented as means±95% confidence intervals and data were analyzed by one-way ANOVA with Holm-Sidak multiple comparisons test or by Kruskal-Wallis test with Dunn correction (n=7-8 rats/group). *p<0.05 *vs.* Control, **p<0.01 *vs.* Control, §p<0.05 *vs.* Diabetic, §§p<0.01 *vs.* Diabetic

DOI:10.14753/SE.2020.2400

4.1.4 Tubulointerstitial fibrosis and RAASi

Renal interstitial fibrosis is a common pathological feature of progressive kidney diseases. Tubulointerstitial fibrosis was assessed on Masson's trichrome-stained sections. The quantity of fibrotic connective tissue increased in diabetic rats. All of the RAASi decreased tubulointerstitial fibrosis (Fig. 10).

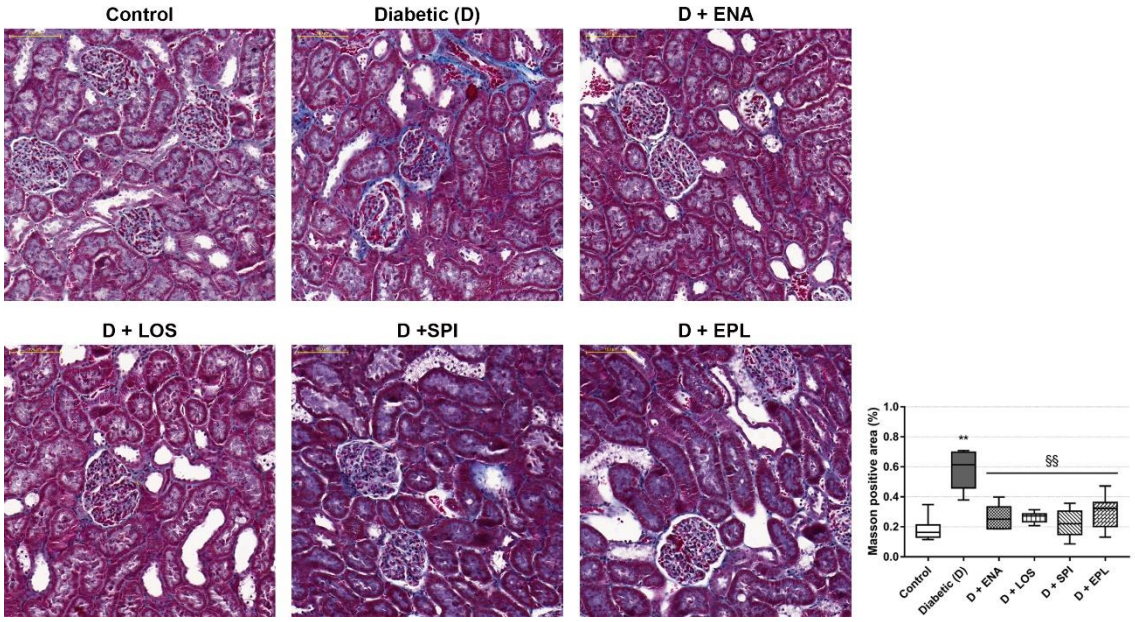

Figure 10 RAASi reduce tubulointerstitial fibrosis. Representative Masson′s trichrome-stained kidney sections of control, diabetic (D) and RAASi treated (D+ENA: D+enalapril, D+LOS: D+losartan, D+SPI: D+spironolactone, D+EPL: D+eplerenon) diabetic rats. Original magnification, x200. Scale bar, 100 µm. Quantitative evaluation of renal tubulointerstitial fibrosis by Masson-positive and glomerulus-free *vs.* total areas in the kidney cortex. Values are presented as means±95% confidence intervals and data were analyzed by one-way ANOVA with Holm-Sidak multiple comparisons test (n=7-8 rats/group). **p<0.01 *vs.* Control, §§p<0.01 *vs.* Diabetic

4.2 DAPA prevents metabolic decline in diabetic rats

As expected, DAPA markedly improved all the metabolic parameters that was elevated due to diabetes. Blood glucose levels were decreased in the first week, reaching a decline of 41% by the second week. By the end of the experiment, blood glucose levels were 47% lower in DAPA *vs.* diabetic group, which is in line with literary data. In parallel, urinary glucose excretion was enhanced in DAPA-treated groups. Hemoglobin levels were lower in diabetic rats but were restored by DAPA to control levels (Table 6). Our results confirm the efficacy of DAPA in T1DM experimental rat model. Combination therapy with LOS did not result in a synergistic effect.

Table 6 Six weeks of DAPA treatment ameliorates T1DM-induced metabolic changes. Metabolic parameters of control, diabetic (D), dapagliflozin (D+DAPA) or DAPA+losartan (D+DAPA+LOS) treated diabetic rats at the end of the 6 week experimental period. Values indicate means±SDs and data were analyzed by one-way ANOVA with Holm-Sidak multiple comparisons test (n=6 in control and diabetic and n=7 in treatment groups). *p<0.05 *vs.* Control, **p<0.01 *vs.* Control, §p<0.05 *vs.* Diabetic, §§p<0.01 *vs.* Diabetic. UN: undetermined, MAP: mean arterial pressure, LDL-C: low-density lipoprotein cholesterol, GOT: serum glutamate-oxaloacetate transaminase, GPT: serum glutamate-pyruvate transaminase

Metabolic Parameters	Control	Diabetic (D)	D + DAPA	D + DAPA + LOS
Body weight (g)	434±37.9	256±26.7**	333±39.2**§§	312±37.8**§§
Non-fasting blood glucose (mmol/L)	6.52±0.57	33.0±1.12**	17.7±5.63**§§	18.1±6.16**§§
Fructosamine (μmol/L)	142±4.12	274±13.6**	206±34.2**§§	217±27.8**§§
Cholesterol (mmol/L)	1.98±0.14	2.69±0.41**	1.96±0.36§§	2.26±0.34§
Triglycerides (mmol/L)	1.39±0.58	2.84±1.26**	1.08±0.58§§	0.91±0.20§§
LDL-C (mmol/L)	0.44±0.15	0.84±0.12**	0.51±0.14§§	0.77±0.13**
GOT (U/L)	127±17.5	347±170**	191±25.4§	214±88.6§
GPT (U/L)	42.8±7.54	166±82.2**	84.6±16.3§§	65.2±10.8§§
Hemoglobin (g/L)	155±16.0	88.3±9.50**	149±9.45§§	153±8.08§§
Glucosuria (mmol/L)	UN	346±47.1**	479±91.8**§	401±105**

4.3 Diabetes-induced SGLT2 and GLUT2 increment are mitigated by DAPA

Protein levels of SGLT2 and GLUT2 were upregulated in diabetic kidneys. This was not unexpected in light of multiple studies showing increased renal SGLT2 expression in various diabetic rodent models. DAPA treatment minimized protein levels of both glucose transporters to control levels (Fig. 11A-B).

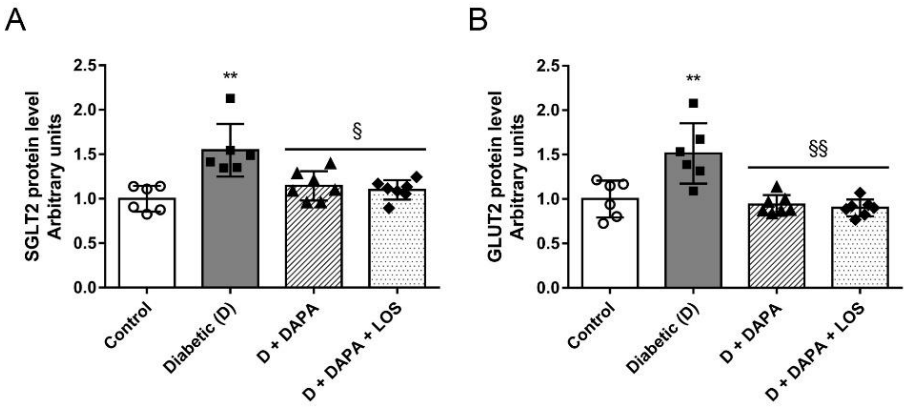

Figure 11 Diabetes-induced SGLT2 and GLUT2 increment are mitigated by DAPA. (A) Sodium-glucose cotransporter 2 and (B) glucose transporter 2 protein levels of control, diabetic (D), dapagliflozin (D+DAPA) and DAPA+losartan (D+DAPA+LOS) treated diabetic rats. Bars indicate means±SDs and data were analyzed by one-way ANOVA with Holm-Sidak multiple comparisons test or by Kruskal-Wallis test with Dunn correction (n=6 in control and diabetic and n=7 in treatment groups). **p<0.01 *vs.* Control, §p<0.05 *vs.* Diabetic, §§p<0.01 *vs.* Diabetic

4.4 DAPA slows the loss of renal function

4.4.1 Renal retention parameters are improved by DAPA

First, we investigated classic renal retention parameters. Development of DKD was confirmed by the decline of renal function after six weeks of diabetes. Creatinine clearance decreased, while serum creatinine, BUN and albumin excretion elevated in diabetic rats. DAPA markedly improved creatinine clearance, serum creatinine, BUN and albumin excretion (Fig. 12A-D).

DOI:10.14753/SE.2020.2400

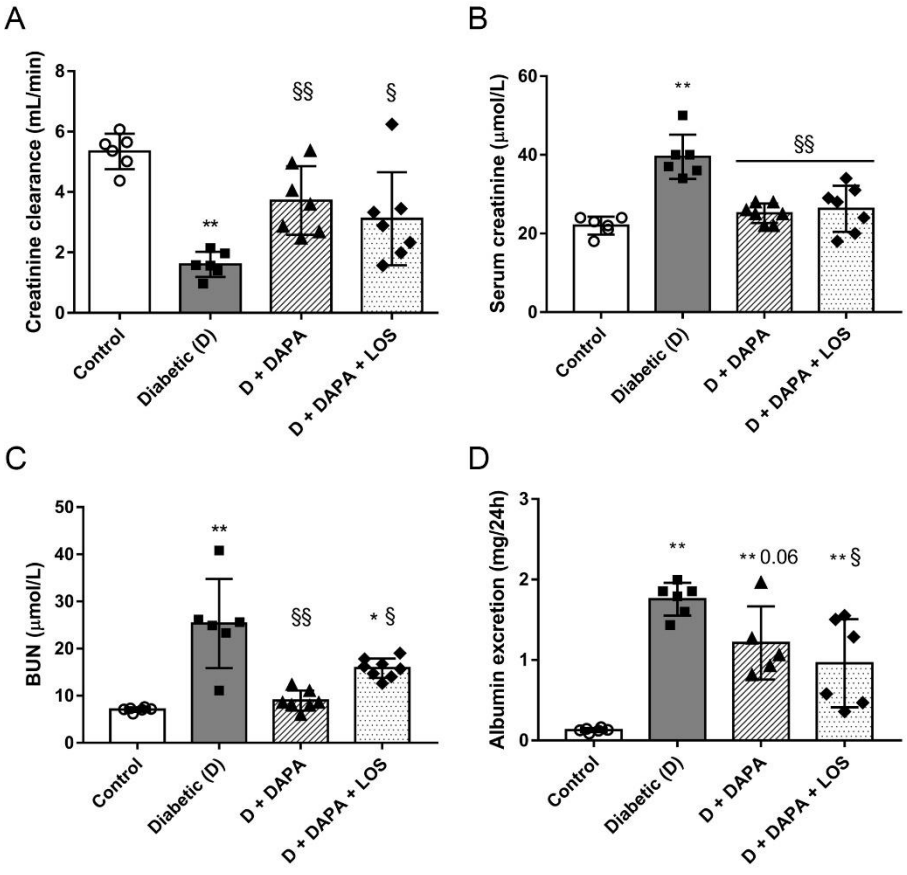

Figure 12 DAPA treatment slows the decline of renal function. (A) Creatinine clearance, (B) serum creatinine, (C) blood urea nitrogen (BUN) and (D) albumin excretion of control, diabetic (D), dapagliflozin (D+DAPA) and DAPA+losartan (D+DAPA+LOS) treated diabetic rats. Bars indicate means±SDs and data were analyzed by one-way ANOVA with Holm-Sidak multiple comparisons test (n=6 in control and diabetic and n=7 in treatment groups). *p<0.05 *vs.* Control, **p<0.01 *vs.* Control, §p<0.05 *vs.* Diabetic, §§p<0.01 *vs.* Diabetic

4.4.2 DAPA minimizes the early and sensitive biomarkers of tubular damage

Recently, the interest of clinicians has focused on KIM-1 and NGAL (also known as lipocalin-2) as very early and highly sensitive biomarkers of renal tubular damage (124, 125). Urinary excretion of KIM-1 and NGAL were elevated in the diabetic group *vs.* controls, while DAPA decreased their levels by more than 50% indicating milder tubular damage (Fig. 13A-B). In parallel, *Havcr1* (KIM-1) and *Lcn2* (NGAL) mRNA expressions were increased in the diabetic kidney as well (Fig. 13C-D). Furthermore, creatinine clearance correlated with urinary KIM-1 (R^2=0.202. p=0.0252) and urinary NGAL (R^2=0.546. p=0.0001), respectively (Fig. 13E-F).

DOI:10.14753/SE.2020.2400

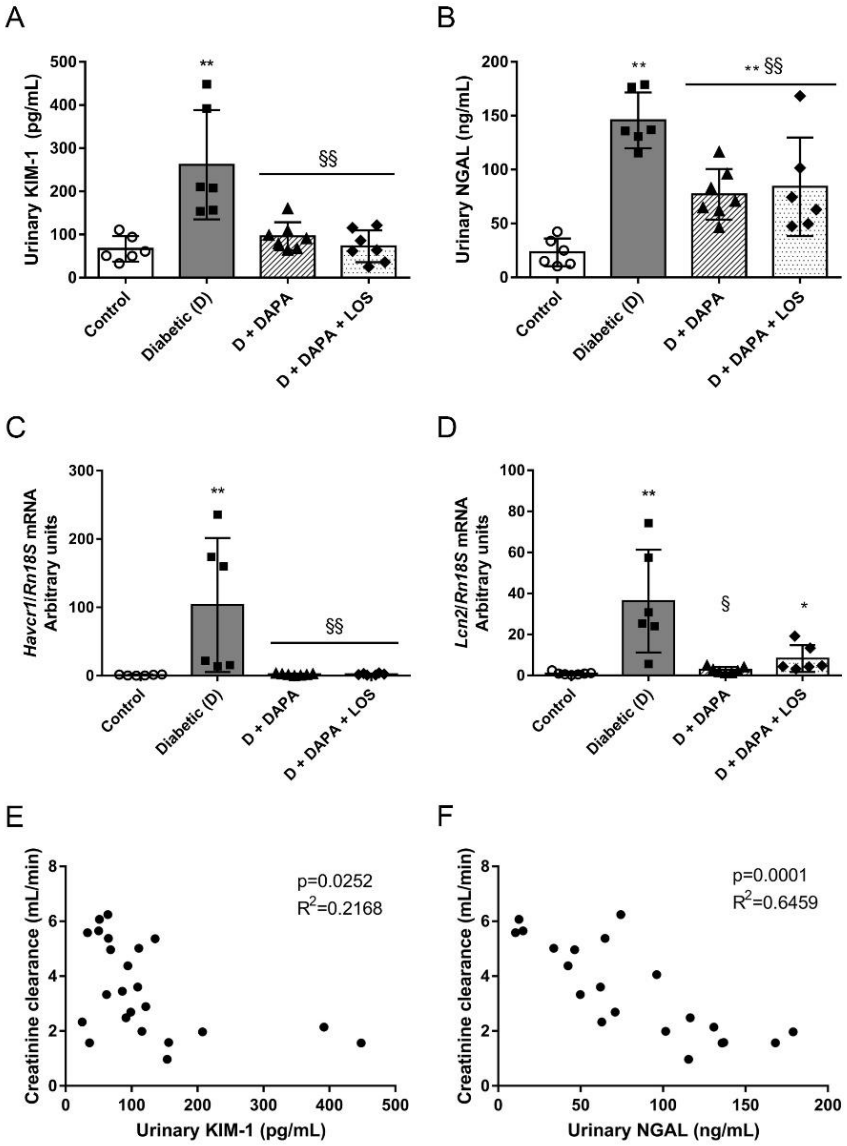

Figure 13 Early and sensitive biomarkers of tubular damage is decreased by DAPA. (A) Urinary levels of kidney injury molecule-1 (KIM-1), (B) urinary levels of neutrophil gelatinase-associated lipocalin (NGAL), (C) renal *Havcr1* mRNA expression and (D) renal *Lcn2* mRNA expression of control, diabetic (D), dapagliflozin (D+DAPA) and DAPA+losartan (D+DAPA+LOS) treated diabetic rats. (E,F) Scatter plot illustrating the correlation between creatinine clearance and KIM-1 or NGAL, resp. Bars indicate means±SDs and data were analyzed by one-way ANOVA with Holm-Sidak multiple comparisons test (n=6 in control and diabetic and n=7 in treatment groups). *p<0.05 *vs.* Control, **p<0.01 *vs.* Control, §p<0.05 *vs.* Diabetic, §§p<0.01 *vs.* Diabetic

DOI:10.14753/SE.2020.2400

4.4.3 DAPA ameliorates mesangial matrix expansion in the diabetic kidney

Kidney sections were stained with PAS and mesangial fractional volume values (Vv) were defined by the ratio of mesangial area/glomerular tuft area. Histological changes were consistent with functional deterioration. Evaluation of PAS-stained sections revealed massive hypertrophy, mesangial matrix expansion and basal membrane thickening in the glomeruli of diabetic rat kidneys. DAPA minimized mesangial matrix expansion and ameliorated structural damage as reflected by smaller PAS positive glomerular areas (Fig. 14).

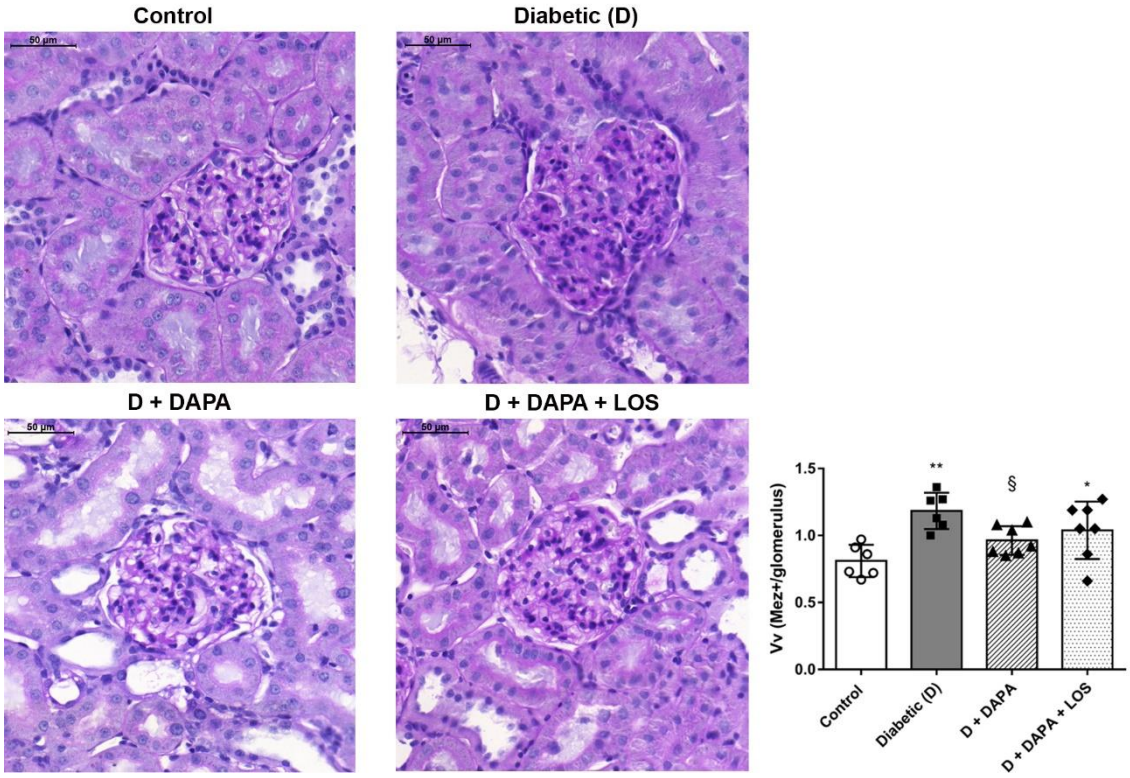

Figure 14 Mesangial matrix expansion was ameliorated in the diabetic kidney by DAPA. PAS-stained kidney sections of control, diabetic (D), dapagliflozin (D+DAPA) and DAPA+losartan (D+DAPA+LOS) treated diabetic rats. Mesangial area was determined by assessment of PAS-positive and nucleus-free areas in the mesangium. Original magnification, x400. Scale bar, 50 µm. Mesangial fractional volume values (Vv) were defined by the ratio of PAS-stained mesangial area/glomerular tuft area. Bars indicate means±SDs and data were analyzed by one-way ANOVA with Holm-Sidak multiple comparisons test (n=6 in control and diabetic and n=7 in treatment groups). *p<0.05 *vs.* Control, **p<0.01 *vs.* Control, §p<0.05 *vs.* Diabetic

Additional LOS treatment did not result in a synergistic effect in any of the investigated parameters.

DOI:10.14753/SE.2020.2400

4.5 Renal fibrogenesis is alleviated by DAPA

4.5.1 Novel urinary fibrosis markers were diminished by DAPA

Our collaborator partner, Nordic Bioscience develops novel urinary biomarkers of ECM remodeling, which are promising in early diagnosis and prognosis of renal fibrosis and might replace the invasive renal biopsy. In our experiment, collagen III formation (rPRO-C3), MMP-9-mediated degradation of type III collagen (uC3M) and type IV collagen (TUM) were elevated in diabetic rats. DAPA treatment decreased rPRO-C3 and TUM levels, while uC3M remained unchanged (Fig. 15A-C).

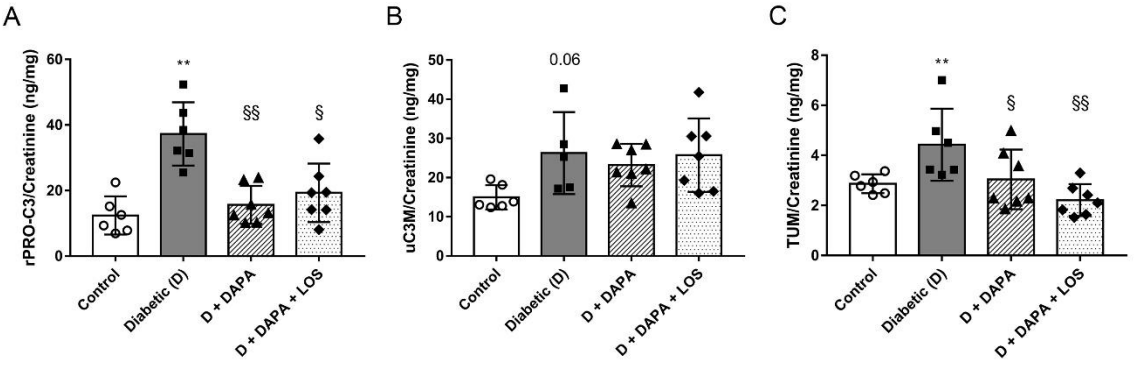

Figure 15 Novel urinary biomarkers of ECM remodeling are decreased in the DAPA-treated diabetic rats. (A-C) Urinary levels of N-terminal pro-peptide of type III collagen (rPRO-C3), collagen type III degradation fragment (uC3M) and collagen type IV degradation fragment tumstatin (TUM) of control, diabetic (D), dapagliflozin (D+DAPA) and DAPA+losartan (D+DAPA+LOS) treated diabetic rats. Bars indicate means±SDs and data were analyzed by one-way ANOVA with Holm-Sidak multiple comparisons test (n=6 in control and diabetic and n=7 in treatment groups). **p<0.01 *vs.* Control, §p<0.05 *vs.* Diabetic, §§p<0.01 *vs.* Diabetic

4.5.2 DAPA mitigates profibrotic growth factor levels

Profibrotic growth factors have a major role in the development of fibrosis in various organs including the kidneys. Here we investigated the renal mRNA expressions of *Tgfb1*, *Pdgfb* and *Ctgf*, which were upregulated in diabetic rats. DAPA decreased *Pdgfb* and *Ctgf* to control levels, while surprisingly it had no effect on *Tgfb1* expression (Fig. 16A-C).

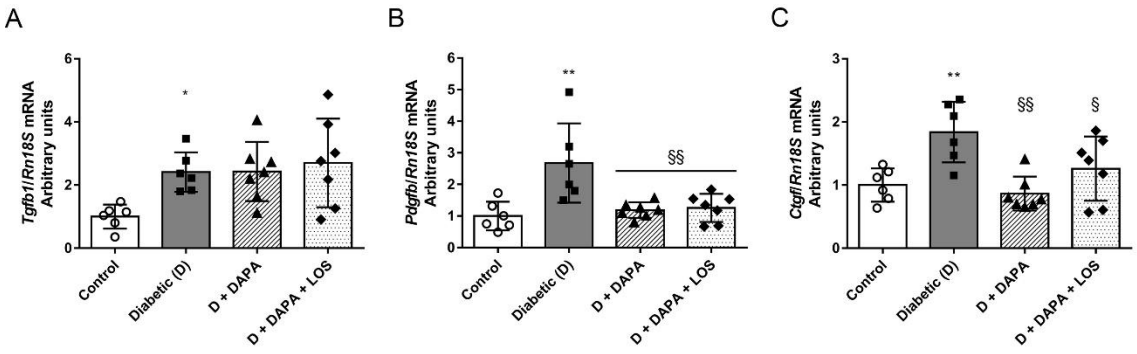

Figure 16 Profibrotic growth factor mRNA expressions were diminished by DAPA. (A) Transforming growth factor beta 1 (*Tgfb1*), (B) platelet derived growth factor subunit B (*Pdgfb*) and (C) connective tissue growth factor (*Ctgf*) of control, diabetic (D), dapagliflozin (D+DAPA) and DAPA+losartan (D+DAPA+LOS) treated diabetic rats. mRNA expressions were normalized to housekeeping *Rn18S* mRNA expression. Bars indicate means±SDs and data were analyzed by one-way ANOVA with Holm-Sidak multiple comparisons test (n=6 in control and diabetic and n=7 in treatment groups). *p<0.05 *vs.* Control, **p<0.01 *vs.* Control, §p<0.05 *vs.* Diabetic, §§p<0.01 *vs.* Diabetic

DOI:10.14753/SE.2020.2400

4.5.3 Myofibroblast activation and tubulointerstitial fibrosis was decreased by DAPA

The activated myofibroblast is the primary matrix secreting cell type. Alpha-smooth muscle actin (α-SMA), the best marker of the myofibroblast was investigated. Diabetes-induced α-SMA increment was minimized by DAPA (Fig. 17A). The extent of diabetes-induced tubulointerstitial fibrosis was evaluated on Masson's trichrome-stained sections. Extensive tubulointerstitial fibrosis and dilated tubules were observed in diabetic kidneys. DAPA reduced the amount of renal fibrotic tissue (Fig. 17B-C).

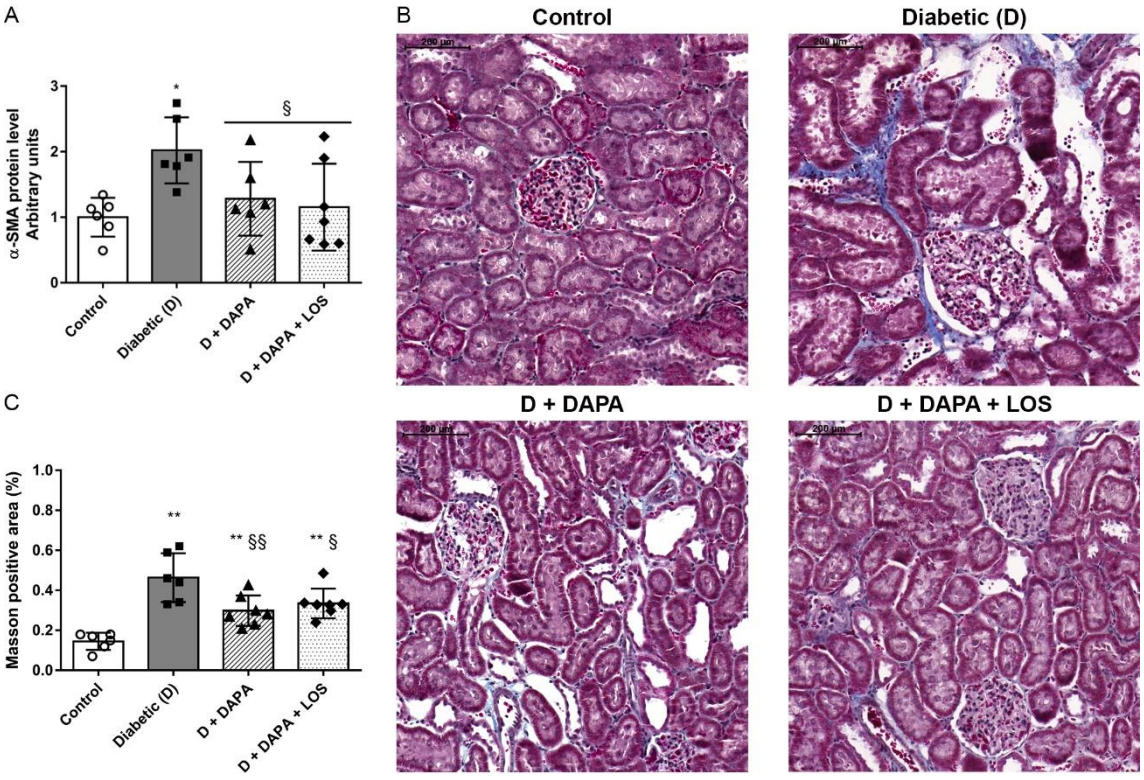

Figure 17 DAPA reduces tubulointerstitial fibrosis. (A) Alpha-smooth muscle actin (α-SMA) protein levels. Proteins were normalized to total protein Ponceau S staining as loading control. (B) Representative Masson′s trichrome-stained kidney sections of control, diabetic (D), dapagliflozin (D+DAPA) and DAPA+losartan (D+DAPA+LOS) treated diabetic rats. Original magnification, x200. Scale bar, 200 μm. (C) Quantitative evaluation of renal tubulointerstitial fibrosis by Masson-positive and glomerulus-free *vs.* total areas in the kidney cortex. Bars indicate means±SDs and data were analyzed by one-way ANOVA with Holm-Sidak multiple comparisons test (n=6 in control and diabetic and n=7 in treatment groups). *p<0.05 *vs.* Control, **p<0.01 *vs.* Control, §p<0.05 *vs.* Diabetic, §§p<0.01 *vs.* Diabetic

The combination with LOS had no synergistic effect in any of the investigated parameters.

DOI:10.14753/SE.2020.2400

4.5.4 Correlation between tubulointerstitial fibrosis and urinary markers of ECM remodeling

Correlation analysis was performed to strengthen the relevance of novel urinary markers of ECM remodeling in early diagnosis and prognosis of renal fibrosis. Positive correlation was found between tubulointerstitial fibrosis (evaluated on Masson's trichrome-stained sections) and rPRO-C3 (R^2=0.4459, p=0.0003), uC3M (R^2=0.1922, p=0.0364) and TUM (R^2=0.2285, p=0.0182), respectively (Fig. 18A-C). Our experimental results support the use of these biomarkers in the diagnosis of renal fibrosis.

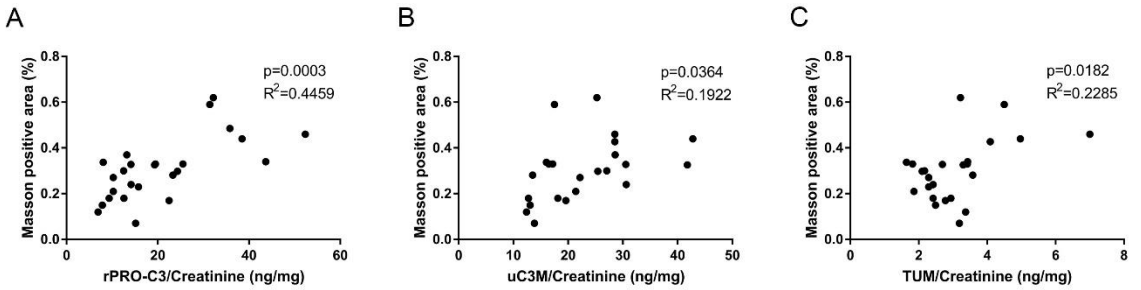

Figure 18 Tubulointerstitial fibrosis correlates with urinary markers of ECM remodeling. Scatter plots illustrating the correlation between Masson's trichrome evaluation and N-terminal pro-peptide of type III collagen (rPRO-C3) and collagen type III degradation fragment (uC3M) and collagen type IV degradation fragment tumstatin (TUM).

DOI:10.14753/SE.2020.2400

4.5.5 DAPA prevents renal collagen accumulation

Collagens are the most common matrix components in renal fibrosis. Picrosirius Red staining was performed to assess accumulation of collagen components. Weak collagen staining was detected in glomeruli and around blood vessels in control kidneys. Extensive fibrotic tissue accumulation was observed in diabetic kidneys as shown by collagen deposition in the interstitium. Diabetes-induced collagen deposition was lower in the DAPA group compared to the diabetic group, while DAPA+LOS treatment had no additional effect (Fig. 19).

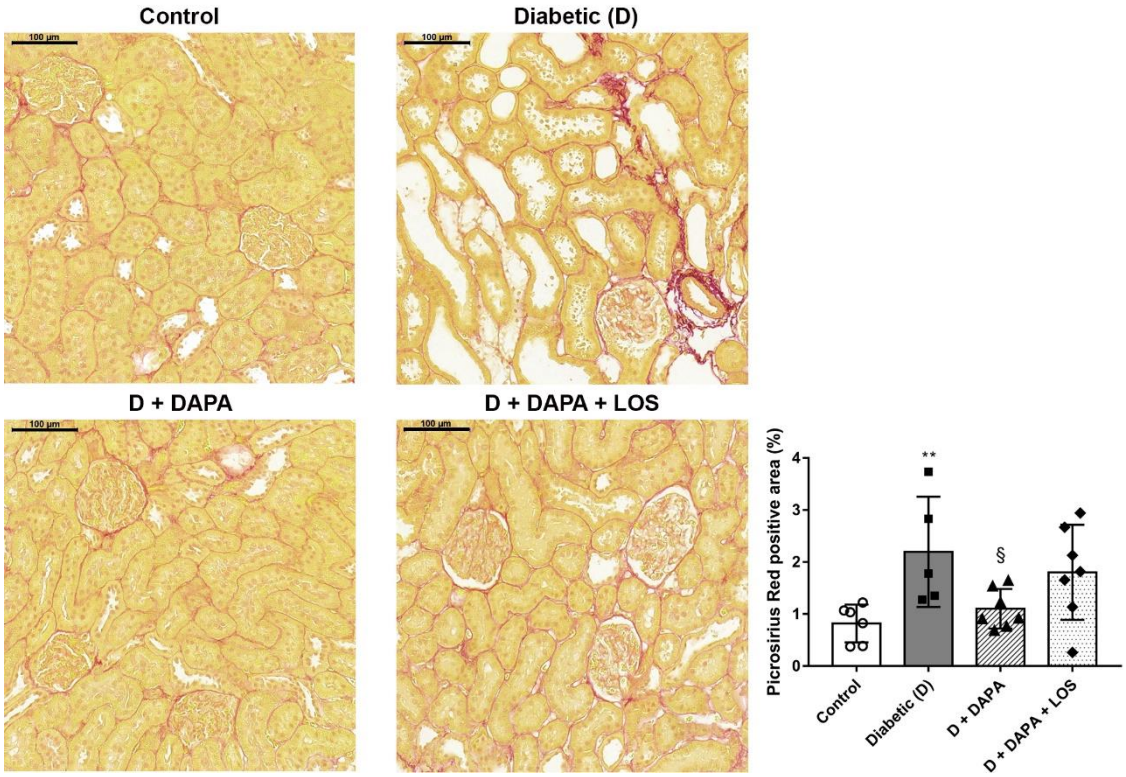

Figure 19 Diabetes-induced collagen deposition are ameliorated by DAPA. Representative Sirius red-stained kidney sections of control, diabetic (D), dapagliflozin (D+DAPA) and DAPA+losartan (D+DAPA+LOS) treated diabetic rats. The ratio of Picrosirius red-stanied interstitial area per total area was measured to obtain the percentage of collagen deposition. Original magnification, x200. Scale bar, 100 µm. Bars indicate means±SDs and data were analyzed by one-way ANOVA with Holm-Sidak multiple comparisons test (n=6 in control and diabetic and n=7 in treatment groups). **p<0.01 *vs.* Control, §p<0.05 *vs.* Diabetic, §§p<0.01 *vs.* Diabetic

DOI:10.14753/SE.2020.2400

4.5.6 Diabetes-induced fibronectin accumulation is ameliorated by DAPA

In renal fibrosis, deposition of the adhesive glycoprotein, fibronectin precedes the production of fibrillar collagens. Considerable fibronectin-positive staining was detected in the glomeruli and to a lesser extent in the tubulointerstitium of diabetic kidneys which was attenuated by both treatments (Fig. 3B,D). In parallel with histology, renal fibronectin mRNA expression increased in diabetes *vs.* controls and was decreased by 50% in DAPA-treated rats (Fig. 20).

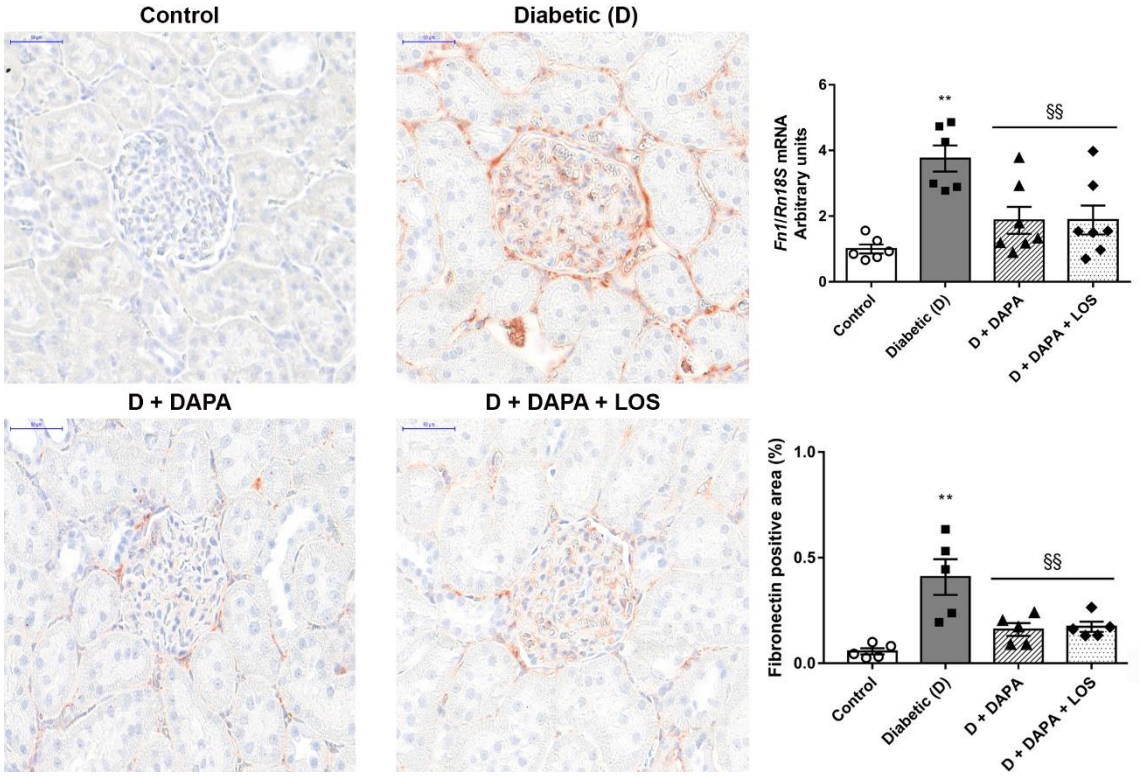

Figure 20 DAPA reduces fibronectin deposition and mRNA expression. Representative fibronectin stained kidney sections of control, diabetic (D), dapagliflozin (D+DAPA) and DAPA+losartan (D+DAPA+LOS) treated diabetic rats. The ratio of mesangial area per glomerular tuft area was measured to obtain the percentage area of fibronectin accumulation. Original magnification, x400. Scale bar, 50 µm. Renal mRNA expression of fibronectin 1 *(Fn1)* was normalized to *Rn18S* mRNA expression. Bars indicate means±SDs and data were analyzed by one-way ANOVA with Holm-Sidak multiple comparisons test (n=6 in control and diabetic and n=7 in treatment groups). **p<0.01 *vs.* Control, §§p<0.01 *vs.* Diabetic

DAPA+LOS combination has no additional effect on the decrement of fibronectin accumulation.

DOI:10.14753/SE.2020.2400

4.6 Hyperglycemia-induced *O*-GlcNAcylation is prevented by DAPA in HK-2 cells

Since SGLT2i act on proximal tubular cells, the direct effects of DAPA on *O*-GlcNAcylation were investigated in HK-2 proximal tubular cells cultured in hyperglycemic conditions. Both Western-blot and immunocytochemistry measurements revealed that protein *O*-GlcNAcylation is induced after 24 hours of high glucose (HG) treatment. DAPA prevented HG-induced protein *O*-GlcNAcylation. The changes were not detected in mannitol-treated cells confirming that the observed phenomenon is a consequence of hyperglycemia and not hyperosmolarity (Fig. 21A-C).

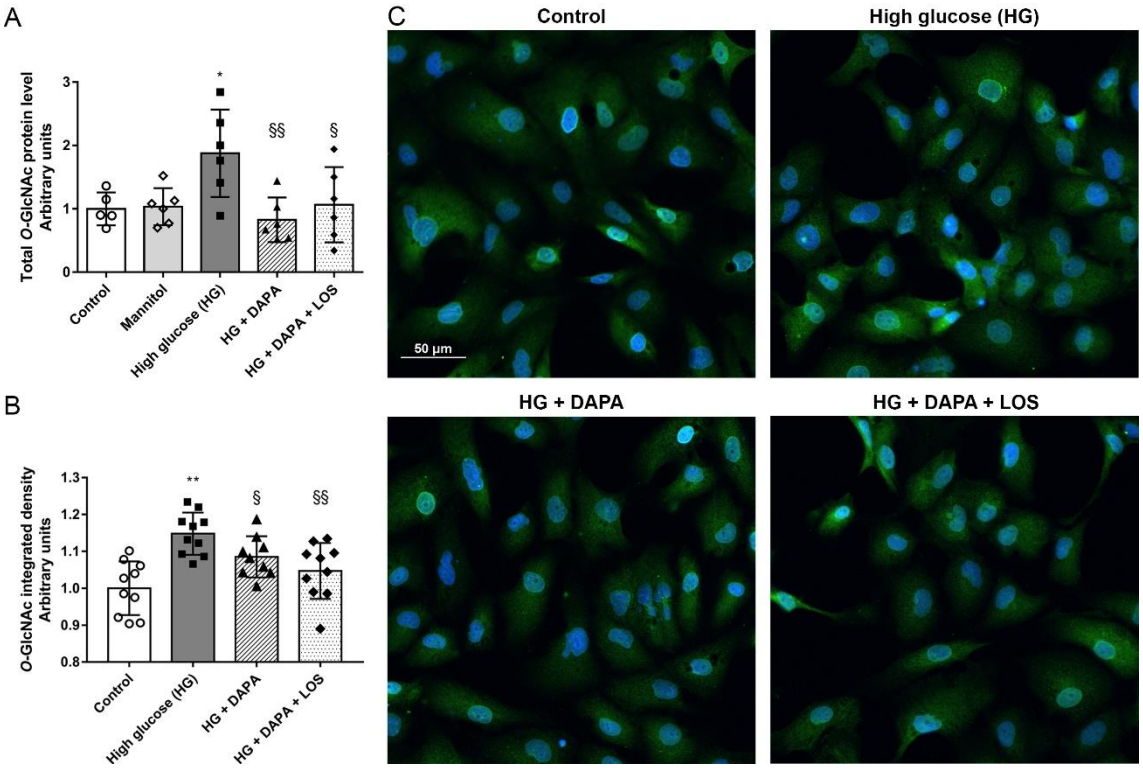

Figure 21 DAPA reduces hyperglycemia-induced protein *O*-GlcNAcylation in human proximal tubular cells (HK-2). Proximal tubular cells were incubated with normal glucose (5.5 mM), high mannitol (35 mM) or high glucose (35 mM) for 24 hours. (A) Total protein levels of *O*-GlcNAcylation and of control, mannitol, high glucose (HG), dapagliflozin (HG+DAPA) and DAPA+losartan (HG+DAPA+LOS) treated high glucose HK-2 cells. Proteins were normalized to total protein Ponceau S staining as loading control. (B) *O*-GlcNAc integrated density. (C) Representative immunocytochemistry staining and integrated density of *O*-GlcNAc (green *O*-GlcNAc; blue nucleus; 20x objective; scale bar, 50 µm). Bars indicate means±SDs and data were analyzed by one-way ANOVA with Holm-Sidak multiple comparisons test or Kruskal-Wallis with Dunn comparison test (n=5-6/group and n=10 visual fields/group). *p<0.05 *vs*. Control, **p<0.01 *vs*. Control, §p<0.05 *vs*. High glucose, §§p<0.01 *vs*. High glucose

In parallel, levels of ncOGT and sOGT, the enzymes responsible for adding *O*-GlcNAc moiety were higher after 24 hours of HG treatment (Fig. 22A-B). DAPA prevented HG-induced ncOGT and sOGT upregulation in proximal tubular cells. OGA-L, which is responsible for removing *O*-GlcNAc residues remained unchanged in all of the groups (Fig. 22C). Changes were not detected in mannitol-treated cells confirming that the observed phenomenon is a consequence of hyperglycemia and not of hyperosmolarity.

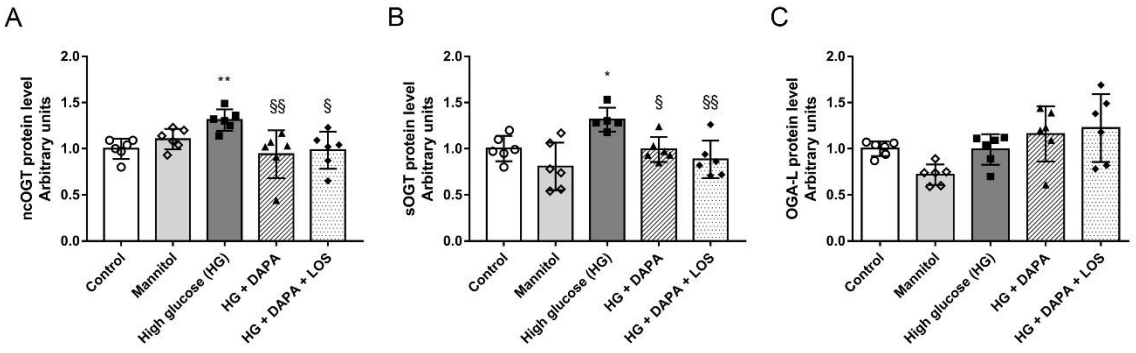

Figure 22 Hyperglycemia-induced OGT elevation is prevented by DAPA treatment. (A-C) Protein levels of nucleocytoplasmic *O*-GlcNAc transferase (ncOGT), small *O*-GlcNAc transferase (sOGT) and *O*-GlcNAcase (OGA-L) of control, mannitol, high glucose (HG), dapagliflozin (HG+DAPA) and DAPA+losartan (HG+DAPA+LOS) treated high glucose HK-2 cells. Proteins were normalized to total protein Ponceau S staining as loading control. Bars indicate means±SDs and data were analyzed by one-way ANOVA with Holm-Sidak multiple comparisons test or Kruskal-Wallis with Dunn comparison test (n=5-6/group). *p<0.05 *vs*. Control, **p<0.01 *vs*. Control, §p<0.05 *vs*. High glucose, §§p<0.01 *vs*. High glucose

DOI:10.14753/SE.2020.2400

4.7 High glucose-induced profibrotic growth factor increment is diminished by DAPA in proximal tubular cells

We showed that diabetes-induced renal profibrotic growth factor increment was mitigated by DAPA; therefore, we investigated the effect of DAPA on *TGFB1*, *PDFGB* and *CTGF* in HK-2 proximal tubular cells cultured in hyperglycemic conditions. All growth factors were increased in HG conditions. DAPA significantly decreased the level of *CTGF*, while the level of *TGFB1* and *PDGFB* remained unaltered. However, similarly to *in vivo* experiments a slight decrement was observed in *PDGF*. LOS treatment had no synergistic effect *in vitro* either (Fig. 23A-C).

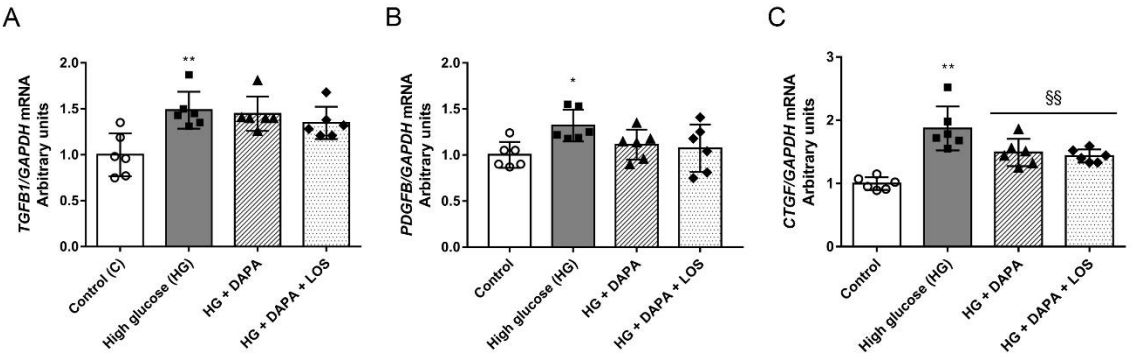

Figure 23 DAPA reduces hyperglycemia-induced *CTGF* expression in human proximal tubular cells (HK-2). (A-C) mRNA expression of transforming growth factor β (*TGFB1),* platelet-derived growth factor *(PDGFB)* and connective tissue growth factor (*CTGF)* which were normalized to *GAPDH* mRNA expression. Bars indicate means±SDs and data were analyzed by one-way ANOVA with Holm-Sidak multiple comparisons test or Kruskal-Wallis with Dunn comparison test (n=5-6/group). *p<0.05 *vs*. Control, **p<0.01 *vs*. Control, §§p<0.01 *vs*. High glucose

4.8 DAPA moderates tubular response to hypoxia

4.8.1 Hypoxia-induced HIF-1α elevation is suspended by DAPA

To investigate the effect of DAPA independently of its glucose-lowering action HK-2 cells cultured in DMEM containing 25 mM glucose were placed into a hypoxic chamber (1% O_2 for 2h). Hypoxic injury was investigated using three different methods (qRT-PCR, Western blot, immunofluorescence analysis). In response to hypoxia, enhanced HIF-1α mRNA expression and protein level (by Western blot and immunocytochemistry as well) were observed. DAPA suspended HIF-1α elevation in both experiments indicating milder hypoxic injury. Moreover, DAPA treatment prevented HIF-1α translocation to the nucleus, thereby confirming abolished HIF-1α activation (Fig. 24A-B; Fig. 25A-C).

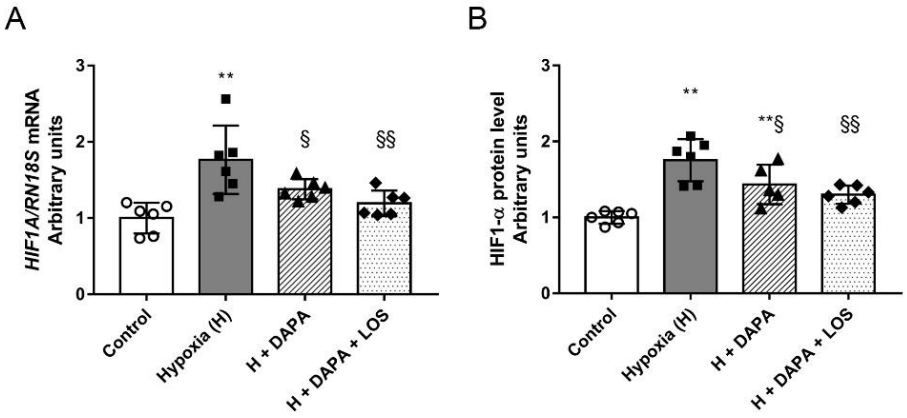

Figure 24 DAPA treatment minimizes tubular HIF-1α elevation. (A) HIF-1α mRNA expressions and (B) HIF-1α protein levels of control, hypoxia (H), dapagliflozin (H+DAPA) and DAPA+losartan (H+DAPA+LOS) treated hypoxic HK-2 cells. *HIF1A* was normalized to *RN18S* mRNA expression. Proteins were normalized to total protein Ponceau S staining as loading control. Proximal tubular cells were treated with DAPA or DAPA+LOS for 22 hours before 2 hours hypoxia (1% O_2). Bars indicate means±SDs and data were analyzed by one-way ANOVA with Holm-Sidak multiple comparisons test or Kruskal-Wallis with Dunn comparison test (n=5-6/group). **p<0.01 *vs.* Control, §p<0.05 *vs.* Hypoxia, §§p<0.01 *vs.* Hypoxia

DOI:10.14753/SE.2020.2400

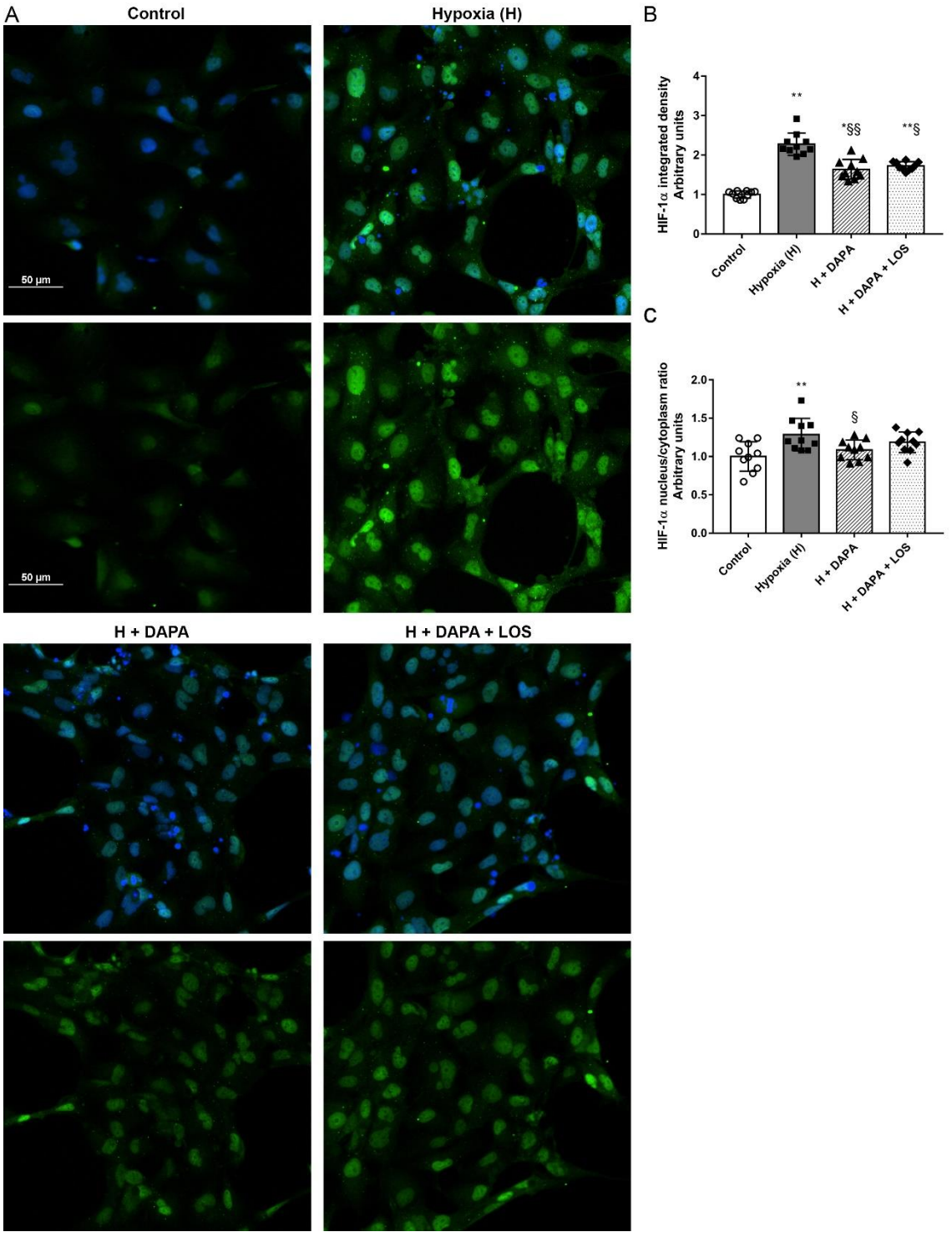

Figure 25 DAPA prevents HIF-1α translocation to the nucleus. (A) Hypoxia-inducible factor-1-alpha (HIF-1α) immunocytochemistry (green HIF-1α; blue nucleus; 20x objective; scale bar, 50 µm). (B) HIF-1α integrated density and (C) HIF-1α nucleus/cytosol ratio, protein levels of control, hypoxia (H), dapagliflozin (H+DAPA) and DAPA+losartan (H+DAPA+LOS) treated hypoxic HK-2 cells. Bars indicate means±SDs and data were analyzed by one-way ANOVA with Holm-Sidak multiple comparisons test or Kruskal-Wallis with Dunn comparison test (n=10 visual fields/group). **p<0.01 *vs.* Control, §p<0.05 *vs.* Hypoxia, §§p<0.01 *vs.* Hypoxia

4.8.1 Downstream elements of HIF pathway are moderated by DAPA

Hematopoietic growth factor EPO is produced by the kidneys and regulates the production of red blood cells, thereby it is one of the key determinants of physiological oxygen homeostasis. VEGF, an angiogenic factor is produced by glomerular and tubular epithelia and it may help to restore vascular supply to cells, thereby reducing hypoxia (126). The HIF system is the central transcriptional mediator of these processes, therefore downstream elements EPO and VEGF-A were investigated. Both EPO and VEGF-A mRNA expressions and protein levels were enhanced in response to hypoxic insult and DAPA prevented the induction of EPO (Fig. 26A-D).

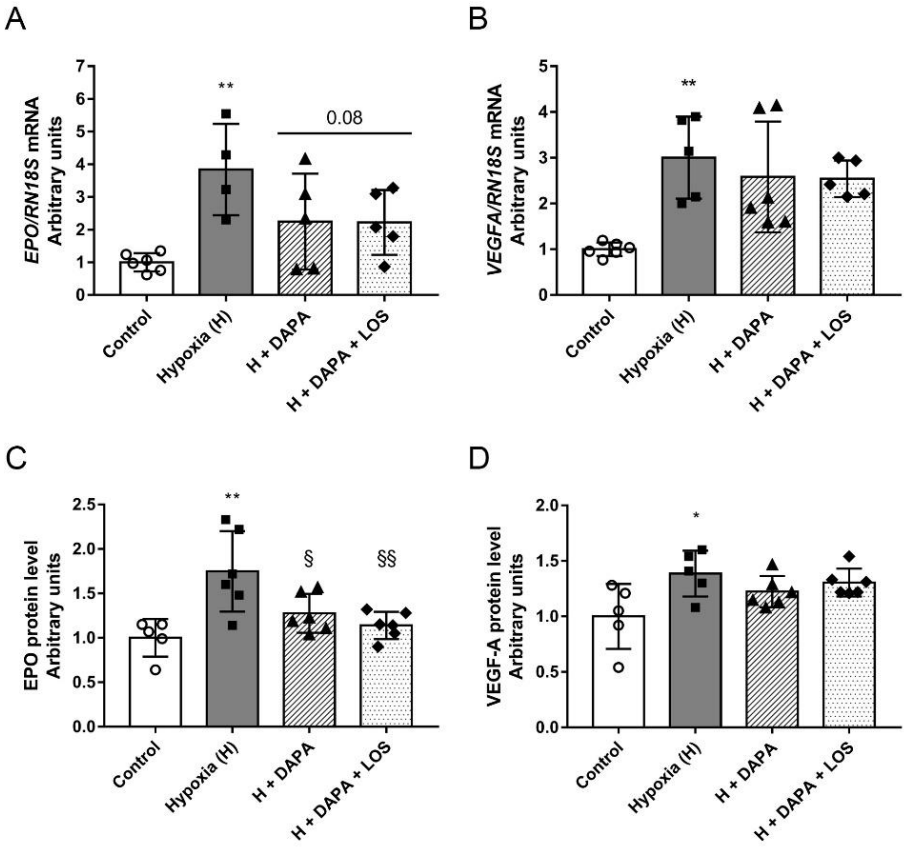

Figure 26 DAPA moderates the downstream element EPO of HIF pathway. (A) Erythropoietin (EPO) and (B) vascular endothelial growth factor A (VEGF-A) mRNA expressions of control, hypoxia (H), dapagliflozin (H+DAPA) and DAPA+losartan (H+DAPA+LOS) treated hypoxic HK-2 cells. *EPO* and *VEGFA* was normalized to *RN18S* mRNA expression. (C) EPO and (D) VEGF-A protein levels. Proteins were normalized to total protein Ponceau S staining as loading control. Bars indicate means±SDs and data were analyzed by one-way ANOVA with Holm-Sidak multiple comparisons test (n=5-6/group). *p<0.05 *vs.* Control, **p<0.01 *vs.* Control, §p<0.05 *vs.* Hypoxia, §§p<0.01 *vs.* Hypoxia

DOI:10.14753/SE.2020.2400

4.8.2 DAPA alters profibrotic growth factor expression in response to hypoxia

Hypoxia triggers fibrotic response, thus TGF-β, PDGF and CTGF were investigated. *TGFB1*, *PDGFB* and *CTGF* mRNA expressions increased in hypoxic tubular cells. DAPA prevented the induction of *TGFB1* and *PDGFB*, however had no effect on *CTGF* (Fig. 27A-C).

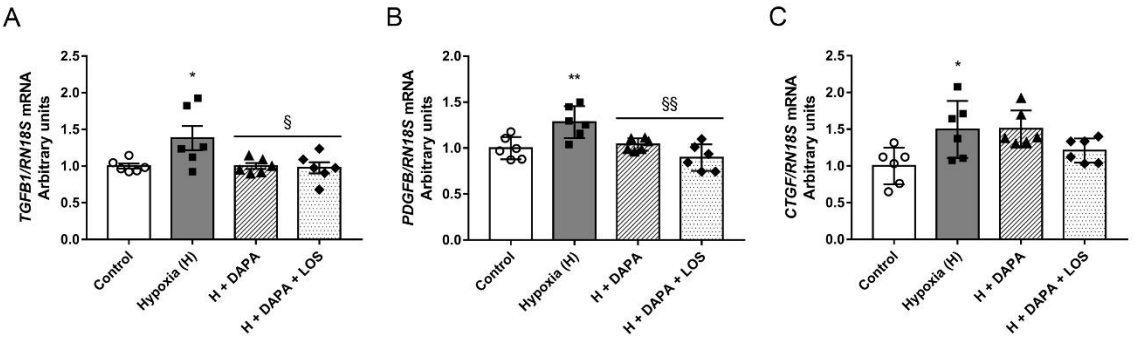

Figure 27 Hypoxia-induced profibrotic growth factor mRNA expressions were diminished by DAPA. (A) Transforming growth factor beta 1 (*TGFF1*), (B) platelet derived growth factor subunit B (*PDGFB*) and (C) connective tissue growth factor (*CTGF*) of control, hypoxia (H), dapagliflozin (H+DAPA) and DAPA+losartan (H+DAPA+LOS) treated hypoxic HK-2 cells. *TGFB1*, *PDGFB* and *CTGF* was normalized to *RN18S* mRNA expression. Bars indicate means±SDs and data were analyzed by one-way ANOVA with Holm-Sidak multiple comparisons test (n=5-6/group). *p<0.05 *vs.* Control, **p<0.01 *vs.* Control, §p<0.05 *vs.* Hypoxia, §§p<0.01 *vs.* Hypoxia

DOI:10.14753/SE.2020.2400

5 DISCUSSION

Diabetes is a serious global health issue that has reached alarming levels; today, nearly half billion adults are living with diabetes worldwide. If current trends continue, ~700 million people are predicted to have diabetes by 2045 (3). DKD, a microvascular complication develops in approximately 30-40% of diabetic patients and is the leading cause of ESRD. The escalating prevalence of DKD parallels the dramatic worldwide rise of diabetes; therefore, novel therapies and early intervention directly targeting the diabetic kidney are of paramount importance.

The management of DKD mainly aims to regulate metabolic and hemodynamic abnormalities. Current guidelines recommend ACEi or ARBs as the first-line therapy for hypertensive patients with diabetes, especially when renal involvement is present. ACEi and ARBs improve renal outcomes in patients with CKD causing improved blood pressure control and decreased proteinuria. Aldosterone antagonists are still mainly used as diuretics in the treatment of hypertension. Increased aldosterone levels were reported in CKD patients treated with ACEi or ARBs, called the "aldosterone escape phenomenon" (127, 128). This supports the use of aldosterone antagonists in addition to ACEi or ARBs, which further reduces albuminuria in DKD; however, at the risk of worsening hyperkalemia.

Impaired renal function and pathophysiological changes including glomerulosclerosis, progressive mesangial expansion, tubulointerstitial fibrosis and endothelial injury are the result of hypertension, hyperglycemia, activated RAAS and various other factors. Furthermore, aldosterone alone also promotes proteinuria and renal fibrosis (129). Therefore, identification of therapeutics controlling the pathological fibrogenic response would be beneficial for DKD treatment. Thus, the aim of our first experiment was to evaluate the monotherapeutic effect of different RAASi in diabetes-induced renal fibrosis. The antifibrotic potential of different RAASi has already been shown in various animal models (130-132). To test whether the antifibrotic properties of RAASi are associated with or restricted to their antihypertensive effect, we used lower treatment

doses avoiding blood pressure changes. In this study, neither diabetes nor RAASi affected blood pressure confirming the non-depressor doses used in our protocol.

In line with our previous studies, loss of renal function and severe structural damage were observed in diabetic rats (119). All RAASi improved classic retention parameters. According to our results, RAASi in monotherapy are effective in ameliorating diabetes-induced tubulointerstitial fibrosis. From the first part of our experiments one can conclude that in this T1DM rat model RAASi successfully minimize renal functional decline and reduce fibrosis independently of their antihypertensive properties. These results might support the indication of RAASi as renoprotective agents, but human clinical trials are needed to confirm this suggestion and to evaluate of the risk/benefit ratio, especially of aldosterone antagonists. Futhermore one can hypothesize that antifibrotic effect of RAASi might be used as therapeutic option in kidney fibrosis originated from other diseases.

Glycemic control and RAAS inhibition have long been the mainstream therapy in patients with DKD. RAAS inhibition with ACEi and ARBs reduces albuminuria, but cannot fully prevent renal failure. Beyond these recommendations, clinicians have little else to offer DKD patients; hence, there is a great demand for novel therapies.

SGLT2i are the newest breakthrough antidiabetics showing potent renoprotective effect recently proven in large clinical multicenter trials. From the EMPA-REG OUTCOME trial (112) to the CANVAS Program (133) and later to the DECLARE-TIMI 58 trial (134) SGLT2i have shown a significant and reproducible attenuation of the rate of GFR decline and a reduction in the risk of progression to ESRD. These findings were confirmed in the CREDENCE trial which is the only study reported so far designed specifically to assess the effects of canagliflozin on renal outcomes (114). The renoprotective effects of SGLT2i were consistent across studies indicating that renoprotection seems to be a class effect of SGLT2i. However, this observation has not been confirmed in T1DM yet and the molecular background is not fully understood. Therefore, the primary goal of our second experiment was to investigate the renoprotective effect of DAPA in a STZ-induced T1DM rat model. On the second hand, we aimed to determine the possible

synergistic effect of DAPA combined with ARB LOS. DKD is traditionally presumed to predominantly affect the glomeruli, but proximal tubules play a role as an initiator and contributor in the early pathogenesis of DKD (135). The focus of our study was on the proximal tubule, where chronic hyperglycemia elevates tubular glucose load, increased exposure and reabsorption lead to structural and functional changes.

Decline in renal function and severe structural damage were observed in diabetic rats similarly to our previous experiments confirming the reproducibility of the STZ-model. Here we showed that DAPA treatment prevented the progression of renal functional and structural damage. Beside the classic renal retention parameters, early and highly sensitive biomarkers of renal tubular damage were investigated (124, 125). KIM-1 and NGAL are expressed at very low levels in the normal human and rodent tubules, but they are upregulated in response to structural renal injury. Urinary elevation of KIM-1 and NGAL in T1DM patients was demonstrated in a cross-sectional study indicating tubular damage at an early stage (136). A recent study showed that renal KIM-1 and NGAL were decreased in DAPA-treated T2DM rats (137). In our T1DM model, DAPA reduced both urinary and renal KIM-1 and NGAL by 50% proving milder tubular damage. The preventive effect of DAPA was substantiated by a robust improvement of all retention parameters and novel biomarkers.

Renal fibrosis is the common final pathway of nearly all chronic and progressive nephropathies. Chronic injury such as diabetes leads to fibrotic matrix deposition disrupting kidney architecture, reducing blood supply and ultimately disturbing renal function. In the diabetic milieu, connective tissue accumulation leads to tubulointerstitial fibrosis which is characterized by dysregulation of ECM remodeling and matrix protein deposition secreted by activated myofibroblasts (138). TGF-β is the primary driver of fibrosis resulting in myofibroblast activation, excessive ECM production and inhibition of ECM degradation (139). PDGF and CTGF also play a key role of EMT and ECM production (140, 141). A more recent study showed that DAPA attenuated renal tubulointerstitial fibrosis in a mouse model of T1DM (142). Recently in a DKD network model combined with plasma measurements of fourty-four T2DM patients Heerspink *et al.* reported that canagliflozin reverses the molecular processes involved in diabetes-

induced ECM turnover and fibrosis (143). We demonstrated that DAPA successfully regulates the diabetes-induced fibrotic response and suppresses the level of profibrotic growth factors *Ctgf* and *Pdgfb*. Concurrently myofibroblast marker α-SMA and accumulation of ECM components, collagens and fibronectin were less increased in DAPA-treated diabetic kidneys as well. Here we provide novel data of the antifibrotic properties of DAPA strengthening the previous experimental and clinical observations.

At the moment kidney biopsy is the diagnostic method of renal fibrosis, which is an invasive process with possible complications (144); therefore, research is ongoing to discover specific non-invasive urinary or serum markers. Formation and degradation of ECM components leads to specific Protein Fingerprint^{TM} peptides: fragments derived from the collagen pro-peptides describe active collagen formation, while neo-epitope fragments of collagen mediated by MMP cleavage reflect collagen degradation. These peptides coming from the remodeling kidney are released into urine and can be measured by newly developed immunoassays (145). We showed in two different studies that the level of Protein Fingerprint^{TM} peptides, rPRO-C3 (collagen type III formation), uC3M (collagen type III degradation) and TUM (collagen type IV degradation) were increased in the urine of T1DM rats (146). Moreover, DAPA mitigated the increased levels of rPRO-C3 and TUM reverting them to the level of controls. Our findings and the positive correlation between these urinary markers and tubulointerstitial fibrosis further prove the antifibrotic property of SGLT2i. We hope our results encourage the validation and widespread clinical use of these novel non-invasive biomarkers of ECM remodeling.

Since RAASi and SGLT2i have different mechanism of action, it is reasonable to apply combination therapy, however to our best knowledge it has not been previously tested in T1DM at all and data in other diseases are also limited. Studies suggest that STZ-induced T1DM is more relevant for investigating DKD, because glucotoxicity could be examined without the frequent comorbidities of T2DM such as insulin resistance, obesity, vascular disease, hypertonia or ageing. Rather surprisingly, in our experiments DAPA alone was as effective as the combination therapy with LOS both concerning *in vivo* and *in vitro* experimental outcomes.

There are some results in clinical as well as experimental T2DM setups, but in each case combination therapy was used when hypertension was present. Combination of DAPA with RAASi resulted in lower albuminuria in T2DM patients, however studies were not designed to assess whether the effect of DAPA on renal variables was independent of glucose or blood pressure control, neither proved the synergistic effect of these two versus other comparators (116). In another study in patients with uncontrolled hypertension by RAASi the value of additional DAPA treatment was assessed on the improvement of blood pressure. This study proved that DAPA reduces blood pressure and body weight in T2DM patients with hypertension and diminishes the need for additional antihypertensive therapy (147). Interestingly enough addition of DAPA resulted in a negative result, since no further albuminuria-lowering effect was detected. In a T2DM rat model 12 weeks of combination therapy of DAPA and irbesartan offered more improvement in renal retention and histological parameters and renal fibrosis than use of either agent separately (148). In Dahl salt-sensitive hypertensive STZ rats combination therapy of luseogliflozin with ACEi afforded greater reduction of blood pressure, hyperfiltration and structural injury. Of note gliflozin therapy did not have any effect on proteinuria, which argues the renoprotective efficacy of the treatment (149). Lastly, variances in experimental setups and protocols could explain the divergences in outcomes and more data and extended investigations are needed to clarify the possible benefits of combination therapy.

The most recent multinational observational cohort study showed that SGLT2 inhibition was associated with a slower rate of kidney function decline and lower risk of clinically meaningful kidney events compared with use of other glucose-lowering drugs in real-world clinical practice databases of T2DM patients (150). One possible explanation for the protective effect of SGLT2i is the induction of multiple processes that have a synergistic beneficial influence on renal and cardiovascular systems e.g. reduction in glucotoxicity, blood pressure and hyperfiltration. The “tubular hypothesis” is based on the fact that hyperglycemia causes increased tubular glucose load leading to SGLT overactivation and consequent enhanced tubular reabsorption of glucose and sodium and downstream activation of TGF. SGLT2i restore TGF resulting in normal GFR (151). According to this SGLT2i have particular effects on glomerular hemodynamics and

improve hard renal end points. However, there is not sufficient knowledge to prove that the renal end points are the result of the associated hemodynamic effects (152).

Various hypotheses exist in the literature regarding how SGLT2i improve renal function and reduce kidney injury in T2DM rodent models. Recent papers discuss that SGLT2i ameliorate DKD via improving glycemic control along with inhibiting inflammation and oxidative stress (153-155). Hyperglycemia-induced renal injury is a complex phenomenon in itself involving various processes in proximal tubules among which increased activation of alternative glucose metabolism pathways and hypoxia have a strong impact and were the focus of our *in vitro* investigations.

O-GlcNAcylation has been shown to have a major role in the regulation of renal transcription factors. Dysfunction of transcription factor Sp1 results from *O*-GlcNAc modifications in diabetes. *O*-GlcNAcylation plays an essential role in high glucose-induced Sp1 transcriptional activity and upregulation of PAI-1 and TGF-β expression contributing to the development of renal fibrosis (67-69). Increased *O*-GlcNAcylation has been reported to enhance fibrogenesis in mesangial cells exposed to high glucose (156, 70). We previously showed that protein *O*-GlcNAcylation (157) and fibrotic processes were induced (146) in diabetic rats as well as in hyperglycemic HK-2 cells. Since DAPA blocks glucose uptake in proximal tubular cells (158) we hypothesized that it can modify protein *O*-GlcNAcylation thus affecting fibrotic processes. DAPA minimized the enhanced protein *O*-GlcNAcylation and reduced OGT levels in HK-2 cells. However, OGA, which is responsible for removing *O*-GlcNAc residues, remained unchanged suggesting that DAPA may inhibit the addition of *O*-GlcNAc rather than facilitate its removal.

When proximal tubular cells are exposed to high glucose due to elevated glucose trafficking through SGLT2, the expression of profibrotic factors is increased, which promotes fibrosis (159). A recent study showed that empagliflozin reduces glucose-induced fibrotic markers in HK-2 cells (160). Therefore, we measured profibrotic growth factors, which were all upregulated in hyperglycemic conditions. Here we found that parallel to *O*-GlcNAcylation, *CTGF* mRNA expression was also considerably less

elevated after DAPA treatment confirming milder injury. Surprisingly *TGFB1* and *PDGFB* were not affected. The antifibrotic effect of DAPA is maybe a consequence of *O*-GlcNAcylation decrement. According to our *in vivo* and *in vitro* results it is tempting to hypothesize that SGLT2i might be particularly useful in ameliorating tubulointerstitial fibrosis in diabetic patients with tubulointerstitial lesions.

In light of these data it is difficult to understand whether these beneficial effects are simply related to the reduction of blood glucose or to synergistic direct protective renal effects. Hence, to investigate whether DAPA is renoprotective independently of its antihyperglycemic effect, an *in vitro* low-grade hypoxia model was applied in HK-2 cells. Recently, tubular hypoxia and altered O_2 handling have received increased attention for their putative roles in the development and progression of DKD (161). Various models and methods throughout the years have confirmed decreased renal tissue O_2 tension in diabetic rats (76, 77). Glomerular hyperfiltration and elevated glucose reabsorption through SGLTs enhances Na^+/K^+-ATPase activity resulting in increased O_2 consumption in hyperglycemia (162). In response to low O_2 levels cells activate adapting mechanisms which are primarily controlled by the master regulator HIF system (163, 78). During hypoxia HIF-α stabilizes and translocates from the cytoplasm to the nucleus, where it dimerizes with HIF-β and the HIF complex binds to hypoxia responsive elements in the promoter sequences of numerous genes involved in cellular O_2 homeostasis (164).

Our experimental setup (1% O_2, 5% CO_2 and 94% N_2) is a widely accepted model of hypoxia (165). As a general hypoxic response *Wang et al.* demonstrated that HIF-1α is activated under 1% O_2 concentration in a large variety of cell types (e.g. mouse Ltk^- fibroblasts, Chinese hamster ovary cells, rat fibroblasts, human Hep3B hepatoblastoma cells or HEK cells) (166). HIF-1α has also been reported to be elevated in 1% O_2 milieu specifically in proximal tubular cells (167-169). Therefore, we used the hypoxic chamber model in which massive HIF-1α elevation was verified by three different methods (qRT-PCR, Western blot, immunocytochemistry). All these data confirmed the severe hypoxic insult and the relevance of HIF-1α as a hypoxia marker. In parallel, nuclear translocation of HIF-1α was investigated. DAPA suspended hypoxia-induced HIF-1α elevation and translocation suggesting its protective effects against hypoxia.

To confirm this phenomenon downstream elements of the general HIF pathway were investigated. After dimerization, the HIF complex binds to hypoxia responsive elements in the promoter sequences of numerous genes involved in maintaining cellular and tissue O_2 homeostasis. EPO is mainly produced by renal fibroblasts; however, tubular epithelial cells, glomerular mesangial cells and interstitial fibroblasts can produce it as well (170). HIF-1α and HIF-2α share many transcriptional targets, EPO appears to be co-regulated, while VEGFA is regulated by HIF-1α. Therefore, we measured the mRNA and protein levels of EPO and VEGFA, which were all induced in response to hypoxia. Parallel to HIF-1α EPO was less elevated in DAPA-treated cells, while VEGFA was not affected. In conclusion, DAPA directly moderates the tubular response to hypoxia as shown by reduced HIF-1α and EPO production. Based on our results one can hypothesize that SGLT2i might be useful in preventing hypoxic injury in kidney diseases of various origins.

Recently, chronic tubulointerstitial hypoxia has been postulated as a final common pathway to ESRD. Chronic hypoxia and subsequent increased HIF expression may be profibrotic and HIF activation may itself induce fibrosis. Hypoxia triggers transformation of tubular cells into myofibroblasts (171). In response to low O_2 tension matrix protein production is upregulated and matrix degradation is suppressed in tubular cells leading to ECM accumulation (82). Hypoxia also induces TGF-β expression, moreover the two can act synergistically in VEGF and EPO regulation (83, 84). HIF activation plays an important role in the direct transcriptional regulation of profibrotic growth factors (85, 172). Thus, we investigated *TGFB1, PDGFB* and *CTGF* mRNA expressions in hypoxic tubular cells, which were all upregulated. Here we showed that DAPA decreased hypoxia-induced *TGFB1* and *PDGFB* production suggesting that its antifibrotic effects might be in direct connection with diminished hypoxia. A detailed clarification of the effect of SGLT2i on hypoxia-induced HIF-mediated complex molecular pathways was beyond the main scope of this study; however, our observations might open a new potential for SGLT2i in hypoxia-associated kidney damage, which should be further examined.

Our results are the first experimental evidence for the antifibrotic properties of non-depressor dose of RAASi offering a possible novel indication for them in the treatment of kidney fibrosis. Our findings have outlined the robust preventive and protective effect of DAPA in experimental T1DM providing a novel therapeutic option to minimize DKD. The antifibrotic effect of DAPA was proved under hyperglycemic and hypoxic conditions that occur simultaneously in the diabetic kidney. These findings provide fresh data supporting the link between glucose toxicity, tubular hypoxia and fibrosis, a vicious trio, which seem to be targeted by DAPA. All these mechanisms are important parts in the puzzle of the complex system behind the organoprotective effect of SGLT2i. Ultimately, our results might support the latest findings that treatment with SGLT2i could be considered for most, if not all, T2DM patients in preventing the onset and progression of DKD.

DOI:10.14753/SE.2020.2400

6 CONCLUSIONS

1. Treatment with non-depressor doses of RAASi in monotherapy is renoprotective and antifibrotic in a rat model of T1DM.

2. SGLT2 inhibitor DAPA treatment is protective in T1DM and subsequent DKD. It substantially ameliorates functional and structural kidney damage.

3. Our *in vivo* and *in vitro* experiments revealed that DAPA has antifibrotic properties. It mitigates the level of novel urinary biomarkers of ECM remodeling, profibrotic growth factors and accumulation of collagen and fibronectin.

4. Hyperglycemia-induced protein *O*-GlcNAcylation in proximal tubules is minimized by DAPA.

5. DAPA directly moderates the tubular response to hypoxia independently of its antihyperglycemic property.

6. DAPA alone is as effective as the combination therapy with non-depressor LOS both concerning *in vivo* and *in vitro* experimental outcomes.

DOI:10.14753/SE.2020.2400

7 SUMMARY

Diabetes and subsequent complication diabetic kidney disease (DKD) lead to a global health crisis and effective therapies are lacking. Current guidelines recommend angiotensin-aldosterone system (RAASi) as the main therapy; however, these merely ameliorate renal impairment, but cannot prevent renal failure. Thus, novel therapies and early intervention directly targeting the diabetic kidney are of paramount importance.

Proximal tubular sodium-glucose cotransporter 2 inhibitors (SGLT2i) are the newest breakthrough antidiabetics. Multicenter clinical trials proved that SGLT2i considerably hinder the progression of DKD. However, this observation has not been confirmed in T1DM yet and the molecular background is not fully understood.

Proximal tubules play a significant role in the early pathogenesis of DKD. Renal fibrosis is the final common pathway of chronic nephropathies. Increased protein *O*-GlcNAcylation enhances profibrotic signaling during hyperglycemia. Elevated tubular O_2 demand leads to hypoxia, which is also a major contributor of fibrogenesis. During my PhD work we aimed to investigate the preventive and antifibrotic effects of RAASi and DAPA in DKD with special focus on protein *O*-GlcNAcylation and tubular hypoxia.

We showed that treatment with non-depressor dose of various RAASi is renoprotective and antifibrotic in a rat model of T1DM offering a possible novel indication in the treatment of kidney damage. Moreover, we demonstrated that DAPA is preventive and protective in experimental T1DM; it ameliorates functional and structural kidney damage. Our *in vivo* and *in vitro* experiments revealed that DAPA has antifibrotic properties in hyperglycemia and hypoxia partly via minimizing *O*-GlcNAcylation and moderating the tubular response to hypoxia. Our results support the link between glucose toxicity, tubular hypoxia and fibrosis, a vicious trio that may be targeted by DAPA.

Ultimately, our results may support the latest findings that treatment with SGLT2i could be considered for most, if not all, T2DM patients for preventing the onset and progression of DKD.

DOI:10.14753/SE.2020.2400

8 ÖSSZEFOGLALÁS

A diabétesz szövődményeként kialakuló diabéteszes vesebetegség (DKD) globális népegészségügyi probléma, amely hatalmas terápiás kihívás. Jelenleg a renin-angiotenzin-aldoszteron rendszer (RAAS) gátlók a gold standard kezelés DKD esetén, melyek javítják a vesefunkciót, de a betegség progresszióját nem állítják meg, ezért új terápiás megoldásokra van szükség.

A legújabb antidiabetikum csoport, a vese proximális tubulusaiban ható Na^+-glükóz kotranszporter 2 gátlók (SGLT2i) áttörést hoztak a diabétesz terápiájában. Klinikai vizsgálatokban kimutatták, hogy az SGLT2i a vércukorszint csökkentése mellett jelentősen gátolják a DKD előrehaladását, azonban a pontos molekuláris mechanizmusok nem egyértelműek.

A proximális tubulus kiemelt szerepet játszik a DKD korai patogenezisében, mely végső soron fibrózishoz vezet. A hiperglikémia következtében megnövekedett fehérje *O*-GlcNAciláció indukálja a profibrotikus útvonalakat. A megnövekedett tubuláris oxigén igény hipoxiához vezet, amely szintén hozzájárul a fibrózishoz. PhD munkám célja a különböző RAAS gátlók és DAPA preventív és antifibrotikus hatásainak vizsgálata, különös tekintettel a fehérje *O*-GlcNAcilációra és a tubuláris hipoxiára.

T1DM patkánymodellben kimutattuk, hogy a különböző RAAS gátlók non-depresszor dózisban renoprotektívek és antifibrotikus hatásúak, mely hozzájárulhat egy új lehetséges indikáció bevezetéséhez vesekárosodás esetén. Bizonyítottuk, hogy a DAPA preventív és protektív hatású, javítja a vesefunkciót és mérsékli a struktúrális károsodást. A DAPA csökkenti a tubuláris *O*-GlcNAcilációt és vércukor csökkentő hatásától függetlenül mérsékli a hipoxiás károsodást tubulus sejtekben, ezáltal hozzájárulhat a fibrózis kivédéséhez.

Eredményeink alátámaszthatják a legújabb megállapításokat, miszerint az SGLT2i kezelést a legtöbb, ha nem az összes T2DM betegnél fontolóra lehet venni a DKD kialakulásának és progressziójának megakadályozása érdekében.

9 REFERENCES

1. Saeedi P, Petersohn I, Salpea P, Malanda B, Karuranga S, Unwin N, Colagiuri S, Guariguata L, Motala AA, Ogurtsova K, Shaw JE, Bright D, Williams R. (2019) TEMPORARY REMOVAL: Global and regional diabetes prevalence estimates for 2019 and projections for 2030 and 2045: results from the International Diabetes Federation Diabetes Atlas, 9(th) edition. Diabetes Res Clin Pract: 107843.
2. Kempler P, Putz Z, Kiss Z, Wittmann I, Abonyi-Tóth Z, Rokszin G, Jermendy G. (2016) A 2-es típusú diabetes előfordulása és költségterheinek alakulása Magyarországon 2001–2014 között – az Országos Egészségbiztosítási Pénztár adatbázis-elemzésének eredményei. Diabetologia Hungarica, 24: 177-188.
3. IDF. (2019) IDF Diabetes Atlas, 9th Edition. 1-168.
4. Karamanou M, Protogerou A, Tsoucalas G, Androutsos G, Poulakou-Rebelakou E. (2016) Milestones in the history of diabetes mellitus: The main contributors. World J Diabetes, 7: 1-7.
5. American Diabetes A. (2019) 2. Classification and Diagnosis of Diabetes: Standards of Medical Care in Diabetes-2019. Diabetes Care, 42: S13-S28.
6. Atkinson MA, Eisenbarth GS, Michels AW. (2014) Type 1 diabetes. Lancet, 383: 69-82.
7. Monaghan M, Helgeson V, Wiebe D. (2015) Type 1 diabetes in young adulthood. Curr Diabetes Rev, 11: 239-250.
8. Kahn SE, Cooper ME, Del Prato S. (2014) Pathophysiology and treatment of type 2 diabetes: perspectives on the past, present, and future. Lancet, 383: 1068-1083.
9. Reinehr T. (2013) Type 2 diabetes mellitus in children and adolescents. World J Diabetes, 4: 270-281.
10. (2014) Diagnostic criteria and classification of hyperglycaemia first detected in pregnancy: a World Health Organization Guideline. Diabetes Res Clin Pract, 103: 341-363.
11. Song C, Lyu Y, Li C, Liu P, Li J, Ma RC, Yang X. (2018) Long-term risk of diabetes in women at varying durations after gestational diabetes: a systematic

review and meta-analysis with more than 2 million women. Obesity Reviews, 19: 421-429.

12. Fetita LS, Sobngwi E, Serradas P, Calvo F, Gautier JF. (2006) Consequences of fetal exposure to maternal diabetes in offspring. J Clin Endocrinol Metab, 91: 3718-3724.
13. Dabelea D, Rewers A, Stafford JM, Standiford DA, Lawrence JM, Saydah S, Imperatore G, D'Agostino RB, Mayer-Davis EJ, Pihoker C, Grp SDYS. (2014) Trends in the Prevalence of Ketoacidosis at Diabetes Diagnosis: The SEARCH for Diabetes in Youth Study. Pediatrics, 133: E938-E945.
14. WHO. (2006) Definition and diagnosis of diabetes mellitus and intermediate hyperglycemia: report of a WHO/IDF consultation.
15. Low Wang CC, Hess CN, Hiatt WR, Goldfine AB. (2016) Clinical Update: Cardiovascular Disease in Diabetes Mellitus: Atherosclerotic Cardiovascular Disease and Heart Failure in Type 2 Diabetes Mellitus - Mechanisms, Management, and Clinical Considerations. Circulation, 133: 2459-2502.
16. Saran R, Robinson B, Abbott KC, Agodoa LYC, Bhave N, Bragg-Gresham J, Balkrishnan R, Dietrich X, Eckard A, Eggers PW, Gaipov A, Gillen D, Gipson D, Hailpern SM, Hall YN, Han Y, He K, Herman W, Heung M, Hirth RA, Hutton D, Jacobsen SJ, Jin Y, Kalantar-Zadeh K, Kapke A, Kovesdy CP, Lavallee D, Leslie J, McCullough K, Modi Z, Molnar MZ, Montez-Rath M, Moradi H, Morgenstern H, Mukhopadhyay P, Nallamothu B, Nguyen DV, Norris KC, O'Hare AM, Obi Y, Park C, Pearson J, Pisoni R, Potukuchi PK, Rao P, Repeck K, Rhee CM, Schrager J, Schaubel DE, Selewski DT, Shaw SF, Shi JM, Shieu M, Sim JJ, Soohoo M, Steffick D, Streja E, Sumida K, Tamura MK, Tilea A, Tong L, Wang D, Wang M, Woodside KJ, Xin X, Yin M, You AS, Zhou H, Shahinian V. (2018) US Renal Data System 2017 Annual Data Report: Epidemiology of Kidney Disease in the United States. Am J Kidney Dis, 71: A7.
17. Wittmann I. (2011) Cukorbetegség okozta vesebetegségek.
18. Reutens AT. (2013) Epidemiology of diabetic kidney disease. Med Clin North Am, 97: 1-18.
19. Tuttle KR, Bakris GL, Bilous RW, Chiang JL, de Boer IH, Goldstein-Fuchs J, Hirsch IB, Kalantar-Zadeh K, Narva AS, Navaneethan SD, Neumiller JJ, Patel

UD, Ratner RE, Whaley-Connell AT, Molitch ME. (2014) Diabetic kidney disease: a report from an ADA Consensus Conference. Diabetes Care, 37: 2864-2883.

20. Li R, Bilik D, Brown MB, Zhang P, Ettner SL, Ackermann RT, Crosson JC, Herman WH. (2013) Medical costs associated with type 2 diabetes complications and comorbidities. Am J Manag Care, 19: 421-430.
21. Costacou T, Ellis D, Fried L, Orchard TJ. (2007) Sequence of progression of albuminuria and decreased GFR in persons with type 1 diabetes: a cohort study. Am J Kidney Dis, 50: 721-732.
22. Molitch ME, Steffes M, Sun W, Rutledge B, Cleary P, de Boer IH, Zinman B, Lachin J, Epidemiology of Diabetes I, Complications Study G. (2010) Development and progression of renal insufficiency with and without albuminuria in adults with type 1 diabetes in the diabetes control and complications trial and the epidemiology of diabetes interventions and complications study. Diabetes Care, 33: 1536-1543.
23. Perkins BA, Ficociello LH, Roshan B, Warram JH, Krolewski AS. (2010) In patients with type 1 diabetes and new-onset microalbuminuria the development of advanced chronic kidney disease may not require progression to proteinuria. Kidney Int, 77: 57-64.
24. Thomas MC, Macisaac RJ, Jerums G, Weekes A, Moran J, Shaw JE, Atkins RC. (2009) Nonalbuminuric renal impairment in type 2 diabetic patients and in the general population (national evaluation of the frequency of renal impairment cO-existing with NIDDM [NEFRON] 11). Diabetes Care, 32: 1497-1502.
25. Tsalamandris C, Allen TJ, Gilbert RE, Sinha A, Panagiotopoulos S, Cooper ME, Jerums G. (1994) Progressive decline in renal function in diabetic patients with and without albuminuria. Diabetes, 43: 649-655.
26. de Boer IH, Rue TC, Cleary PA, Lachin JM, Molitch ME, Steffes MW, Sun WJ, Zinman B, Brunzell JD, Trail DCC. (2011) Long-term Renal Outcomes of Patients With Type 1 Diabetes Mellitus and Microalbuminuria An Analysis of the Diabetes Control and Complications Trial/Epidemiology of Diabetes Interventions and Complications Cohort. Archives of Internal Medicine, 171: 412-420.

27. Perkins BA, Ficociello LH, Silva KH, Finkelstein DM, Warram JH, Krolewski AS. (2003) Regression of microalbuminuria in type 1 diabetes. N Engl J Med, 348: 2285-2293.
28. Tonneijck L, Muskiet MH, Smits MM, van Bommel EJ, Heerspink HJ, van Raalte DH, Joles JA. (2017) Glomerular Hyperfiltration in Diabetes: Mechanisms, Clinical Significance, and Treatment. J Am Soc Nephrol, 28: 1023-1039.
29. Falk RJ, Scheinman JI, Mauer SM, Michael AF. (1983) Polyantigenic expansion of basement membrane constituents in diabetic nephropathy. Diabetes, 32 Suppl 2: 34-39.
30. Kim Y, Kleppel MM, Butkowski R, Mauer SM, Wieslander J, Michael AF. (1991) Differential expression of basement membrane collagen chains in diabetic nephropathy. Am J Pathol, 138: 413-420.
31. White KE, Bilous RW. (2000) Type 2 diabetic patients with nephropathy show structural-functional relationships that are similar to type 1 disease. Journal of the American Society of Nephrology, 11: 1667-1673.
32. Stout LC, Kumar S, Whorton EB. (1993) Focal mesangiolysis and the pathogenesis of the Kimmelstiel-Wilson nodule. Hum Pathol, 24: 77-89.
33. Tervaert TW, Mooyaart AL, Amann K, Cohen AH, Cook HT, Drachenberg CB, Ferrario F, Fogo AB, Haas M, de Heer E, Joh K, Noel LH, Radhakrishnan J, Seshan SV, Bajema IM, Bruijn JA, Renal Pathology S. (2010) Pathologic classification of diabetic nephropathy. J Am Soc Nephrol, 21: 556-563.
34. Brownlee M. (2005) The pathobiology of diabetic complications: a unifying mechanism. Diabetes, 54: 1615-1625.
35. Morrisey K, Steadman R, Williams JD, Phillips AO. (1999) Renal proximal tubular cell fibronectin accumulation in response to glucose is polyol pathway dependent. Kidney International, 55: 160-167.
36. Vallon V, Blantz RC, Thomson S. (2003) Glomerular hyperfiltration and the salt paradox in early type 1 diabetes mellitus: a tubulo-centric view. J Am Soc Nephrol, 14: 530-537.
37. Vallon V, Komers R. (2011) Pathophysiology of the diabetic kidney. Compr Physiol, 1: 1175-1232.

38. Miyazaki M, Takai S. (2006) Tissue angiotensin II generating system by angiotensin-converting enzyme and chymase. J Pharmacol Sci, 100: 391-397.
39. Sparks MA, Crowley SD, Gurley SB, Mirotsou M, Coffman TM. (2014) Classical Renin-Angiotensin system in kidney physiology. Compr Physiol, 4: 1201-1228.
40. Donoghue M, Hsieh F, Baronas E, Godbout K, Gosselin M, Stagliano N, Donovan M, Woolf B, Robison K, Jeyaseelan R, Breitbart RE, Acton S. (2000) A novel angiotensin-converting enzyme-related carboxypeptidase (ACE2) converts angiotensin I to angiotensin 1-9. Circ Res, 87: E1-9.
41. Rice GI, Thomas DA, Grant PJ, Turner AJ, Hooper NM. (2004) Evaluation of angiotensin-converting enzyme (ACE), its homologue ACE2 and neprilysin in angiotensin peptide metabolism. Biochem J, 383: 45-51.
42. Vickers C, Hales P, Kaushik V, Dick L, Gavin J, Tang J, Godbout K, Parsons T, Baronas E, Hsieh F, Acton S, Patane M, Nichols A, Tummino P. (2002) Hydrolysis of biological peptides by human angiotensin-converting enzyme-related carboxypeptidase. J Biol Chem, 277: 14838-14843.
43. Tsutsumi Y, Matsubara H, Masaki H, Kurihara H, Murasawa S, Takai S, Miyazaki M, Nozawa Y, Ozono R, Nakagawa K, Miwa T, Kawada N, Mori Y, Shibasaki Y, Tanaka Y, Fujiyama S, Koyama Y, Fujiyama A, Takahashi H, Iwasaka T. (1999) Angiotensin II type 2 receptor overexpression activates the vascular kinin system and causes vasodilation. J Clin Invest, 104: 925-935.
44. Rohrwasser A, Morgan T, Dillon HF, Zhao L, Callaway CW, Hillas E, Zhang S, Cheng T, Inagami T, Ward K, Terreros DA, Lalouel JM. (1999) Elements of a paracrine tubular renin-angiotensin system along the entire nephron. Hypertension, 34: 1265-1274.
45. Zhang SL, Filep JG, Hohman TC, Tang SS, Ingelfinger JR, Chan JS. (1999) Molecular mechanisms of glucose action on angiotensinogen gene expression in rat proximal tubular cells. Kidney Int, 55: 454-464.
46. Zimpelmann J, Kumar D, Levine DZ, Wehbi G, Imig JD, Navar LG, Burns KD. (2000) Early diabetes mellitus stimulates proximal tubule renin mRNA expression in the rat. Kidney Int, 58: 2320-2330.
47. Braam B, Mitchell KD, Fox J, Navar LG. (1993) Proximal tubular secretion of angiotensin II in rats. Am J Physiol, 264: F891-898.

48. Giacchetti G, Sechi LA, Rilli S, Carey RM. (2005) The renin-angiotensin-aldosterone system, glucose metabolism and diabetes. Trends Endocrinol Metab, 16: 120-126.
49. Siragy HM, Xue C. (2008) Local renal aldosterone production induces inflammation and matrix formation in kidneys of diabetic rats. Exp Physiol, 93: 817-824.
50. Chen JC, Chen JK, Harris RC. (2012) Angiotensin II Induces Epithelial-to-Mesenchymal Transition in Renal Epithelial Cells through Reactive Oxygen Species/Src/Caveolin-Mediated Activation of an Epidermal Growth Factor Receptor-Extracellular Signal-Regulated Kinase Signaling Pathway. Molecular and Cellular Biology, 32: 981-991.
51. Torres CR, Hart GW. (1984) Topography and polypeptide distribution of terminal N-acetylglucosamine residues on the surfaces of intact lymphocytes. Evidence for O-linked GlcNAc. J Biol Chem, 259: 3308-3317.
52. Hart GW, Housley MP, Slawson C. (2007) Cycling of O-linked beta-N-acetylglucosamine on nucleocytoplasmic proteins. Nature, 446: 1017-1022.
53. Hardiville S, Hart GW. (2014) Nutrient regulation of signaling, transcription, and cell physiology by O-GlcNAcylation. Cell Metab, 20: 208-213.
54. Brownlee M. (2001) Biochemistry and molecular cell biology of diabetic complications. Nature, 414: 813-820.
55. Akimoto Y, Miura Y, Toda T, Wolfert MA, Wells L, Boons GJ, Hart GW, Endo T, Kawakami H. (2011) Morphological changes in diabetic kidney are associated with increased O-GlcNAcylation of cytoskeletal proteins including alpha-actinin 4. Clin Proteomics, 8: 15.
56. Buse MG. (2006) Hexosamines, insulin resistance, and the complications of diabetes: current status. Am J Physiol Endocrinol Metab, 290: E1-E8.
57. Clark RJ, McDonough PM, Swanson E, Trost SU, Suzuki M, Fukuda M, Dillmann WH. (2003) Diabetes and the accompanying hyperglycemia impairs cardiomyocyte calcium cycling through increased nuclear O-GlcNAcylation. J Biol Chem, 278: 44230-44237.

58. Walgren JL, Vincent TS, Schey KL, Buse MG. (2003) High glucose and insulin promote O-GlcNAc modification of proteins, including alpha-tubulin. Am J Physiol Endocrinol Metab, 284: E424-434.

59. Hanover JA, Yu S, Lubas WB, Shin SH, Ragano-Caracciola M, Kochran J, Love DC. (2003) Mitochondrial and nucleocytoplasmic isoforms of O-linked GlcNAc transferase encoded by a single mammalian gene. Arch Biochem Biophys, 409: 287-297.

60. Gao Y, Wells L, Comer FI, Parker GJ, Hart GW. (2001) Dynamic O-glycosylation of nuclear and cytosolic proteins: cloning and characterization of a neutral, cytosolic beta-N-acetylglucosaminidase from human brain. J Biol Chem, 276: 9838-9845.

61. Nerlich AG, Sauer U, Kolm-Litty V, Wagner E, Koch M, Schleicher ED. (1998) Expression of glutamine:fructose-6-phosphate amidotransferase in human tissues: evidence for high variability and distinct regulation in diabetes. Diabetes, 47: 170-178.

62. Srinivasan V, Sandhya N, Sampathkumar R, Farooq S, Mohan V, Balasubramanyam M. (2007) Glutamine fructose-6-phosphate amidotransferase (GFAT) gene expression and activity in patients with type 2 diabetes: inter-relationships with hyperglycaemia and oxidative stress. Clin Biochem, 40: 952-957.

63. McClain DA, Lubas WA, Cooksey RC, Hazel M, Parker GJ, Love DC, Hanover JA. (2002) Altered glycan-dependent signaling induces insulin resistance and hyperleptinemia. Proc Natl Acad Sci U S A, 99: 10695-10699.

64. Whelan SA, Dias WB, Thiruneelakantapillai L, Lane MD, Hart GW. (2010) Regulation of Insulin Receptor Substrate 1 (IRS-1)/AKT Kinase-mediated Insulin Signaling by O-Linked beta-N-Acetylglucosamine in 3T3-L1 Adipocytes. Journal of Biological Chemistry, 285: 5204-5211.

65. Akimoto Y, Hart GW, Wells L, Vosseller K, Yamamoto K, Munetomo E, Ohara-Imaizumi M, Nishiwaki C, Nagamatsu S, Hirano H, Kawakami H. (2007) Elevation of the post-translational modification of proteins by O-linked N-acetylglucosamine leads to deterioration of the glucose-stimulated insulin

secretion in the pancreas of diabetic Goto-Kakizaki rats. Glycobiology, 17: 127-140.

66. Liu K, Paterson AJ, Chin E, Kudlow JE. (2000) Glucose stimulates protein modification by O-linked GlcNAc in pancreatic beta cells: linkage of O-linked GlcNAc to beta cell death. Proc Natl Acad Sci U S A, 97: 2820-2825.
67. Goldberg H, Whiteside C, Fantus IG. (2011) O-linked beta-N-acetylglucosamine supports p38 MAPK activation by high glucose in glomerular mesangial cells. Am J Physiol Endocrinol Metab, 301: E713-726.
68. Goldberg HJ, Scholey J, Fantus IG. (2000) Glucosamine activates the plasminogen activator inhibitor 1 gene promoter through Sp1 DNA binding sites in glomerular mesangial cells. Diabetes, 49: 863-871.
69. Goldberg HJ, Whiteside CI, Hart GW, Fantus IG. (2006) Posttranslational, reversible O-glycosylation is stimulated by high glucose and mediates plasminogen activator inhibitor-1 gene expression and Sp1 transcriptional activity in glomerular mesangial cells. Endocrinology, 147: 222-231.
70. Park MJ, Kim DI, Lim SK, Choi JH, Han HJ, Yoon KC, Park SH. (2014) High glucose-induced O-GlcNAcylated carbohydrate response element-binding protein (ChREBP) mediates mesangial cell lipogenesis and fibrosis: the possible role in the development of diabetic nephropathy. J Biol Chem, 289: 13519-13530.
71. James LR, Tang D, Ingram A, Ly H, Thai K, Cai L, Scholey JW. (2002) Flux through the hexosamine pathway is a determinant of nuclear factor kappa B-dependent promoter activation. Diabetes, 51: 1146-1156.
72. Evans RG, Gardiner BS, Smith DW, O'Connor PM. (2008) Intrarenal oxygenation: unique challenges and the biophysical basis of homeostasis. American Journal of Physiology-Renal Physiology, 295: F1259-F1270.
73. Hansell P, Welch WJ, Blantz RC, Palm F. (2013) Determinants of kidney oxygen consumption and their relationship to tissue oxygen tension in diabetes and hypertension. Clinical and Experimental Pharmacology and Physiology, 40: 123-137.
74. Fine LG, Orphanides C, Norman JT. (1998) Progressive renal disease: the chronic hypoxia hypothesis. Kidney Int Suppl, 65: S74-78.

75. Korner A, Eklof AC, Celsi G, Aperia A. (1994) Increased renal metabolism in diabetes. Mechanism and functional implications. Diabetes, 43: 629-633.
76. Palm F, Cederberg J, Hansell P, Liss P, Carlsson PO. (2003) Reactive oxygen species cause diabetes-induced decrease in renal oxygen tension. Diabetologia, 46: 1153-1160.
77. Ries M, Basseau F, Tyndal B, Jones R, Deminiere C, Catargi B, Combe C, Moonen CW, Grenier N. (2003) Renal diffusion and BOLD MRI in experimental diabetic nephropathy. Blood oxygen level-dependent. J Magn Reson Imaging, 17: 104-113.
78. Semenza GL. (1998) Hypoxia-inducible factor 1: master regulator of O2 homeostasis. Curr Opin Genet Dev, 8: 588-594.
79. Eckardt KU, Rosenberger C, Jurgensen JS, Wiesener MS. (2003) Role of hypoxia in the pathogenesis of renal disease. Blood Purif, 21: 253-257.
80. Fine LG, Bandyopadhyay D, Norman JT. (2000) Is there a common mechanism for the progression of different types of renal diseases other than proteinuria? Towards the unifying theme of chronic hypoxia. Kidney International, 57: S22-S26.
81. Kang DH, Kanellis J, Hugo C, Truong L, Anderson S, Kerjaschki D, Schreiner GF, Johnson RJ. (2002) Role of the microvascular endothelium in progressive renal disease. J Am Soc Nephrol, 13: 806-816.
82. Orphanides C, Fine LG, Norman JT. (1997) Hypoxia stimulates proximal tubular cell matrix production via a TGF-beta1-independent mechanism. Kidney Int, 52: 637-647.
83. Sanchez-Elsner T, Botella LM, Velasco B, Corbi A, Attisano L, Bernabeu C. (2001) Synergistic cooperation between hypoxia and transforming growth factor-beta pathways on human vascular endothelial growth factor gene expression. Journal of Biological Chemistry, 276: 38527-38535.
84. Sanchez-Elsner T, Ramirez JR, Rodriguez-Sanz F, Varela E, Bernabeu C, Botella LM. (2004) A cross-talk between hypoxia and TGF-beta orchestrates erythropoietin gene regulation through SP1 and Smads. Journal of Molecular Biology, 336: 9-24.

85. Higgins DF, Biju MP, Akai Y, Wutz A, Johnson RS, Haase VH. (2004) Hypoxic induction of Ctgf is directly mediated by Hif-1. American Journal of Physiology-Renal Physiology, 287: F1223-F1232.
86. Brenner BM, Cooper ME, de Zeeuw D, Keane WF, Mitch WE, Parving HH, Remuzzi G, Snapinn SM, Zhang ZX, Shahinfar S, Investigators RS. (2001) Effects of losartan on renal and cardiovascular outcomes in patients with type 2 diabetes and nephropathy. New England Journal of Medicine, 345: 861-869.
87. Lewis EJ, Hunsicker LG, Bain RP, Rohde RD. (1993) The effect of angiotensin-converting-enzyme inhibition on diabetic nephropathy. The Collaborative Study Group. N Engl J Med, 329: 1456-1462.
88. Lewis EJ, Hunsicker LG, Clarke WR, Berl T, Pohl MA, Lewis JB, Ritz E, Atkins RC, Rohde R, Raz I, Collaborative Study G. (2001) Renoprotective effect of the angiotensin-receptor antagonist irbesartan in patients with nephropathy due to type 2 diabetes. N Engl J Med, 345: 851-860.
89. Investigators HOPES. (2000) Effects of ramipril on cardiovascular and microvascular outcomes in people with diabetes mellitus: results of the HOPE study and MICROHOPE substudy (vol 355, pg 253, 2000). Lancet, 356: 860-860.
90. Fried LF, Emanuele N, Zhang JH, Brophy M, Conner TA, Duckworth W, Leehey DJ, McCullough PA, O'Connor T, Palevsky PM, Reilly RF, Seliger SL, Warren SR, Watnick S, Peduzzi P, Guarino P, Investigators VN-D. (2013) Combined angiotensin inhibition for the treatment of diabetic nephropathy. N Engl J Med, 369: 1892-1903.
91. Mann JFE, Schmieder RE, McQueen M, Dyal L, Schumacher H, Pogue J, Wang XY, Maggioni A, Budaj A, Chaithiraphan S, Dickstein K, Keltai M, Metsarinne K, Oto A, Parkhomenko A, Piegas LS, Svendsen TL, Teo KK, Yusuf S, Investigators O. (2008) Renal outcomes with telmisartan, ramipril, or both, in people at high vascular risk (the ONTARGET study): a multicentre, randomised, double-blind, controlled trial. Lancet, 372: 547-553.
92. Filippatos G, Anker SD, Bohm M, Gheorghiade M, Kober L, Krum H, Maggioni AP, Ponikowski P, Voors AA, Zannad F, Kim SY, Nowack C, Palombo G, Kolkhof P, Kimmeskamp-Kirschbaum N, Pieper A, Pitt B. (2016) A randomized controlled study of finerenone vs. eplerenone in patients with worsening chronic

heart failure and diabetes mellitus and/or chronic kidney disease. Eur Heart J, 37: 2105-2114.

93. Williams B, MacDonald TM, Morant S, Webb DJ, Sever P, McInnes G, Ford I, Cruickshank JK, Caulfield MJ, Salsbury J, Mackenzie I, Padmanabhan S, Brown MJ, British Hypertension Society's PSG. (2015) Spironolactone versus placebo, bisoprolol, and doxazosin to determine the optimal treatment for drug-resistant hypertension (PATHWAY-2): a randomised, double-blind, crossover trial. Lancet, 386: 2059-2068.
94. Barfuss DW, Schafer JA. (1981) Differences in active and passive glucose transport along the proximal nephron. Am J Physiol, 241: F322-332.
95. Wright EM, Loo DD, Hirayama BA. (2011) Biology of human sodium glucose transporters. Physiol Rev, 91: 733-794.
96. Balen D, Ljubojevic M, Breljak D, Brzica H, Zlender V, Koepsell H, Sabolic I. (2008) Revised immunolocalization of the Na+-D-glucose cotransporter SGLT1 in rat organs with an improved antibody. Am J Physiol Cell Physiol, 295: C475-489.
97. Vallon V, Platt KA, Cunard R, Schroth J, Whaley J, Thomson SC, Koepsell H, Rieg T. (2011) SGLT2 mediates glucose reabsorption in the early proximal tubule. J Am Soc Nephrol, 22: 104-112.
98. Vrhovac I, Balen Eror D, Klessen D, Burger C, Breljak D, Kraus O, Radovic N, Jadrijevic S, Aleksic I, Walles T, Sauvant C, Sabolic I, Koepsell H. (2015) Localizations of Na(+)-D-glucose cotransporters SGLT1 and SGLT2 in human kidney and of SGLT1 in human small intestine, liver, lung, and heart. Pflugers Arch, 467: 1881-1898.
99. Rieg T, Masuda T, Gerasimova M, Mayoux E, Platt K, Powell DR, Thomson SC, Koepsell H, Vallon V. (2014) Increase in SGLT1-mediated transport explains renal glucose reabsorption during genetic and pharmacological SGLT2 inhibition in euglycemia. Am J Physiol Renal Physiol, 306: F188-193.
100. Farber SJ, Berger EY, Earle DP. (1951) Effect of diabetes and insulin of the maximum capacity of the renal tubules to reabsorb glucose. J Clin Invest, 30: 125-129.

101. Mogensen CE. (1971) Maximum tubular reabsorption capacity for glucose and renal hemodynamcis during rapid hypertonic glucose infusion in normal and diabetic subjects. Scand J Clin Lab Invest, 28: 101-109.
102. Thomson SC, Deng A, Bao D, Satriano J, Blantz RC, Vallon V. (2001) Ornithine decarboxylase, kidney size, and the tubular hypothesis of glomerular hyperfiltration in experimental diabetes. J Clin Invest, 107: 217-224.
103. Vallon V, Gerasimova M, Rose MA, Masuda T, Satriano J, Mayoux E, Koepsell H, Thomson SC, Rieg T. (2014) SGLT2 inhibitor empagliflozin reduces renal growth and albuminuria in proportion to hyperglycemia and prevents glomerular hyperfiltration in diabetic Akita mice. Am J Physiol Renal Physiol, 306: F194-204.
104. Vallon V, Rose M, Gerasimova M, Satriano J, Platt KA, Koepsell H, Cunard R, Sharma K, Thomson SC, Rieg T. (2013) Knockout of Na-glucose transporter SGLT2 attenuates hyperglycemia and glomerular hyperfiltration but not kidney growth or injury in diabetes mellitus. Am J Physiol Renal Physiol, 304: F156-167.
105. Wright EM. (2001) Renal Na(+)-glucose cotransporters. Am J Physiol Renal Physiol, 280: F10-18.
106. Navale AM, Paranjape AN. (2016) Glucose transporters: physiological and pathological roles. Biophys Rev, 8: 5-9.
107. Santer R, Calado J. (2010) Familial renal glucosuria and SGLT2: from a mendelian trait to a therapeutic target. Clin J Am Soc Nephrol, 5: 133-141.
108. C. P. (1835) Analyse des Phloridzins. Annales Academie Science Francaise: 178.
109. Tsujihara K, Hongu M, Saito K, Kawanishi H, Kuriyama K, Matsumoto M, Oku A, Ueta K, Tsuda M, Saito A. (1999) Na+-glucose cotransporter (SGLT) inhibitors as antidiabetic agents. 4. Synthesis and pharmacological properties of 4 '-dehydroxyphlorizin derivatives substituted on the B ring. Journal of Medicinal Chemistry, 42: 5311-5324.
110. Meng W, Ellsworth BA, Nirschl AA, McCann PJ, Patel M, Girotra RN, Wu G, Sher PM, Morrison EP, Biller SA, Zahler R, Deshpande PP, Pullockaran A, Hagan DL, Morgan N, Taylor JR, Obermeier MT, Humphreys WG, Khanna A, Discenza L, Robertson JG, Wang A, Han S, Wetterau JR, Janovitz EB, Flint OP, Whaley JM, Washburn WN. (2008) Discovery of dapagliflozin: a potent, selective renal

sodium-dependent glucose cotransporter 2 (SGLT2) inhibitor for the treatment of type 2 diabetes. J Med Chem, 51: 1145-1149.

111. Neal B, Perkovic V, Matthews DR. (2017) Canagliflozin and Cardiovascular and Renal Events in Type 2 Diabetes. N Engl J Med, 377: 2099.

112. Wanner C, Inzucchi SE, Zinman B. (2016) Empagliflozin and Progression of Kidney Disease in Type 2 Diabetes. N Engl J Med, 375: 1801-1802.

113. Wiviott SD, Raz I, Bonaca MP, Mosenzon O, Kato ET, Cahn A, Silverman MG, Zelniker TA, Kuder JF, Murphy SA, Bhatt DL, Leiter LA, McGuire DK, Wilding JPH, Ruff CT, Gause-Nilsson IAM, Fredriksson M, Johansson PA, Langkilde AM, Sabatine MS, Investigators D-T. (2019) Dapagliflozin and Cardiovascular Outcomes in Type 2 Diabetes. N Engl J Med, 380: 347-357.

114. Perkovic V, Jardine MJ, Neal B, Bompoint S, Heerspink HJL, Charytan DM, Edwards R, Agarwal R, Bakris G, Bull S, Cannon CP, Capuano G, Chu PL, de Zeeuw D, Greene T, Levin A, Pollock C, Wheeler DC, Yavin Y, Zhang H, Zinman B, Meininger G, Brenner BM, Mahaffey KW, Investigators CT. (2019) Canagliflozin and Renal Outcomes in Type 2 Diabetes and Nephropathy. N Engl J Med, 380: 2295-2306.

115. Zelniker TA, Wiviott SD, Raz I, Im K, Goodrich EL, Furtado RHM, Bonaca MP, Mosenzon O, Kato ET, Cahn A, Bhatt DL, Leiter LA, McGuire DK, Wilding JPH, Sabatine MS. (2019) Comparison of the Effects of Glucagon-Like Peptide Receptor Agonists and Sodium-Glucose Cotransporter 2 Inhibitors for Prevention of Major Adverse Cardiovascular and Renal Outcomes in Type 2 Diabetes Mellitus. Circulation, 139: 2022-2031.

116. Heerspink HJ, Johnsson E, Gause-Nilsson I, Cain VA, Sjostrom CD. (2016) Dapagliflozin reduces albuminuria in patients with diabetes and hypertension receiving renin-angiotensin blockers. Diabetes Obes Metab, 18: 590-597.

117. Dandona P, Mathieu C, Phillip M, Hansen L, Griffen SC, Tschope D, Thoren F, Xu J, Langkilde AM, Investigators D-. (2017) Efficacy and safety of dapagliflozin in patients with inadequately controlled type 1 diabetes (DEPICT-1): 24 week results from a multicentre, double-blind, phase 3, randomised controlled trial. Lancet Diabetes Endocrinol, 5: 864-876.

118. Mathieu C, Dandona P, Gillard P, Senior P, Hasslacher C, Araki E, Lind M, Bain SC, Jabbour S, Arya N, Hansen L, Thoren F, Langkilde AM, Investigators D-. (2018) Efficacy and Safety of Dapagliflozin in Patients With Inadequately Controlled Type 1 Diabetes (the DEPICT-2 Study): 24-Week Results From a Randomized Controlled Trial. Diabetes Care, 41: 1938-1946.
119. Banki NF, Ver A, Wagner LJ, Vannay A, Degrell P, Prokai A, Gellai R, Lenart L, Szakal DN, Kenesei E, Rosta K, Reusz G, Szabo AJ, Tulassay T, Baylis C, Fekete A. (2012) Aldosterone antagonists in monotherapy are protective against streptozotocin-induced diabetic nephropathy in rats. PLoS One, 7: e39938.
120. Failli P, Alfarano C, Franchi-Micheli S, Mannucci E, Cerbai E, Mugelli A, Raimondi L. (2009) Losartan counteracts the hyper-reactivity to angiotensin II and ROCK1 over-activation in aortas isolated from streptozotocin-injected diabetic rats. Cardiovasc Diabetol, 8: 32.
121. Taira M, Toba H, Murakami M, Iga I, Serizawa R, Murata S, Kobara M, Nakata T. (2008) Spironolactone exhibits direct renoprotective effects and inhibits renal renin-angiotensin-aldosterone system in diabetic rats. Eur J Pharmacol, 589: 264-271.
122. Rueden CT, Schindelin J, Hiner MC, DeZonia BE, Walter AE, Arena ET, Eliceiri KW. (2017) ImageJ2: ImageJ for the next generation of scientific image data. BMC Bioinformatics, 18: 529.
123. Genovese F, Boor P, Papasotiriou M, Leeming DJ, Karsdal MA, Floege J. (2016) Turnover of type III collagen reflects disease severity and is associated with progression and microinflammation in patients with IgA nephropathy. Nephrology Dialysis Transplantation, 31: 472-479.
124. Alter ML, Kretschmer A, Von Websky K, Tsuprykov O, Reichetzeder C, Simon A, Stasch JP, Hocher B. (2012) Early urinary and plasma biomarkers for experimental diabetic nephropathy. Clin Lab, 58: 659-671.
125. Nauta FL, Scheven L, Meijer E, van Oeveren W, de Jong PE, Bakker SJ, Gansevoort RT. (2013) Glomerular and tubular damage markers in individuals with progressive albuminuria. Clin J Am Soc Nephrol, 8: 1106-1114.

126. Shweiki D, Itin A, Soffer D, Keshet E. (1992) Vascular Endothelial Growth-Factor Induced by Hypoxia May Mediate Hypoxia-Initiated Angiogenesis. Nature, 359: 843-845.
127. Moranne O, Bakris G, Fafin C, Favre G, Pradier C, Esnault VL. (2013) Determinants and changes associated with aldosterone breakthrough after angiotensin II receptor blockade in patients with type 2 diabetes with overt nephropathy. Clin J Am Soc Nephrol, 8: 1694-1701.
128. Struthers AD. (1995) Aldosterone escape during ACE inhibitor therapy in chronic heart failure. Eur Heart J, 16 Suppl N: 103-106.
129. Bertocchio JP, Warnock DG, Jaisser F. (2011) Mineralocorticoid receptor activation and blockade: an emerging paradigm in chronic kidney disease. Kidney Int, 79: 1051-1060.
130. Han KH, Kang YS, Han SY, Jee YH, Lee MH, Han JY, Kim HK, Kim YS, Cha DR. (2006) Spironolactone ameliorates renal injury and connective tissue growth factor expression in type II diabetic rats. Kidney Int, 70: 111-120.
131. Liao J, Kobayashi M, Kanamuru Y, Nakamura S, Makita Y, Funabiki K, Horikoshi S, Tomino Y. (2003) Effects of candesartan, an angiotensin II type 1 receptor blocker, on diabetic nephropathy in KK/Ta mice. J Nephrol, 16: 841-849.
132. Sun N, Zhai L, Li H, Shi LH, Yao Z, Zhang B. (2016) Angiotensin-Converting Enzyme Inhibitor (ACEI)-Mediated Amelioration in Renal Fibrosis Involves Suppression of Mast Cell Degranulation. Kidney Blood Press Res, 41: 108-118.
133. Neal B, Perkovic V, Mahaffey KW, de Zeeuw D, Fulcher G, Erondu N, Shaw W, Law G, Desai M, Matthews DR, Group CPC. (2017) Canagliflozin and Cardiovascular and Renal Events in Type 2 Diabetes. N Engl J Med, 377: 644-657.
134. Wiviott SD, Raz I, Sabatine MS. (2019) Dapagliflozin and Cardiovascular Outcomes in Type 2 Diabetes. Reply. N Engl J Med, 380: 1881-1882.
135. Zeni L, Norden AGW, Cancarini G, Unwin RJ. (2017) A more tubulocentric view of diabetic kidney disease. J Nephrol, 30: 701-717.
136. Nielsen SE, Schjoedt KJ, Astrup AS, Tarnow L, Lajer M, Hansen PR, Parving HH, Rossing P. (2010) Neutrophil Gelatinase-Associated Lipocalin (NGAL) and

Kidney Injury Molecule 1 (KIM1) in patients with diabetic nephropathy: a cross-sectional study and the effects of lisinopril. Diabet Med, 27: 1144-1150.

137. Oraby MA, El-Yamany MF, Safar MM, Assaf N, Ghoneim HA. (2019) Dapagliflozin attenuates early markers of diabetic nephropathy in fructose-streptozotocin-induced diabetes in rats. Biomed Pharmacother, 109: 910-920.
138. Humphreys BD. (2018) Mechanisms of Renal Fibrosis. Annu Rev Physiol, 80: 309-326.
139. Meng XM, Nikolic-Paterson DJ, Lan HY. (2016) TGF-beta: the master regulator of fibrosis. Nat Rev Nephrol, 12: 325-338.
140. Klinkhammer BM, Floege J, Boor P. (2018) PDGF in organ fibrosis. Mol Aspects Med, 62: 44-62.
141. Lipson KE, Wong C, Teng Y, Spong S. (2012) CTGF is a central mediator of tissue remodeling and fibrosis and its inhibition can reverse the process of fibrosis. Fibrogenesis Tissue Repair, 5: S24.
142. Huang F, Zhao Y, Wang Q, Hillebrands JL, van den Born J, Ji L, An T, Qin G. (2019) Dapagliflozin Attenuates Renal Tubulointerstitial Fibrosis Associated With Type 1 Diabetes by Regulating STAT1/TGFbeta1 Signaling. Front Endocrinol (Lausanne), 10: 441.
143. Heerspink HJL, Perco P, Mulder S, Leierer J, Hansen MK, Heinzel A, Mayer G. (2019) Canagliflozin reduces inflammation and fibrosis biomarkers: a potential mechanism of action for beneficial effects of SGLT2 inhibitors in diabetic kidney disease. Diabetologia, 62: 1154-1166.
144. Farris AB, Colvin RB. (2012) Renal interstitial fibrosis: mechanisms and evaluation. Curr Opin Nephrol Hypertens, 21: 289-300.
145. Genovese F, Manresa AA, Leeming DJ, Karsdal MA, Boor P. (2014) The extracellular matrix in the kidney: a source of novel non-invasive biomarkers of kidney fibrosis? Fibrogenesis Tissue Repair, 7: 4.
146. Koszegi S, Molnar A, Lenart L, Hodrea J, Balogh DB, Lakat T, Szkibinszkij E, Hosszu A, Sparding N, Genovese F, Wagner L, Vannay A, Szabo AJ, Fekete A. (2019) RAAS inhibitors directly reduce diabetes-induced renal fibrosis via growth factor inhibition. J Physiol, 597: 193-209.

147. Weber MA, Mansfield TA, Alessi F, Iqbal N, Parikh S, Ptaszynska A. (2016) Effects of dapagliflozin on blood pressure in hypertensive diabetic patients on renin-angiotensin system blockade. Blood Press, 25: 93-103.
148. Abdel-Wahab AF, Bamagous GA, Al-Harizy RM, ElSawy NA, Shahzad N, Ibrahim IA, Ghamdi SSA. (2018) Renal protective effect of SGLT2 inhibitor dapagliflozin alone and in combination with irbesartan in a rat model of diabetic nephropathy. Biomed Pharmacother, 103: 59-66.
149. Kojima N, Williams JM, Slaughter TN, Kato S, Takahashi T, Miyata N, Roman RJ. (2015) Renoprotective effects of combined SGLT2 and ACE inhibitor therapy in diabetic Dahl S rats. Physiol Rep, 3.
150. Heerspink HJL, Karasik A, Thuresson M, Melzer-Cohen C, Chodick G, Khunti K, Wilding JPH, Rodriguez LAG, Cea-Soriano L, Kohsaka S, Nicolucci A, Lucisano G, Lin FJ, Wang CY, Wittbrodt E, Fenici P, Kosiborod M. (2020) Kidney outcomes associated with use of SGLT2 inhibitors in real-world clinical practice (CVD-REAL 3): a multinational observational cohort study. Lancet Diabetes & Endocrinology, 8: 27-35.
151. Fioretto P, Zambon A, Rossato M, Busetto L, Vettor R. (2016) SGLT2 Inhibitors and the Diabetic Kidney. Diabetes Care, 39 Suppl 2: S165-171.
152. Thomson SC, Vallon V. (2019) Renal Effects of Sodium-Glucose Co-Transporter Inhibitors. Am J Cardiol, 124 Suppl 1: S28-S35.
153. Kojima N, Williams JM, Takahashi T, Miyata N, Roman RJ. (2013) Effects of a new SGLT2 inhibitor, luseogliflozin, on diabetic nephropathy in T2DN rats. J Pharmacol Exp Ther, 345: 464-472.
154. Nagata T, Fukuzawa T, Takeda M, Fukazawa M, Mori T, Nihei T, Honda K, Suzuki Y, Kawabe Y. (2013) Tofogliflozin, a novel sodium-glucose co-transporter 2 inhibitor, improves renal and pancreatic function in db/db mice. Br J Pharmacol, 170: 519-531.
155. Terami N, Ogawa D, Tachibana H, Hatanaka T, Wada J, Nakatsuka A, Eguchi J, Horiguchi CS, Nishii N, Yamada H, Takei K, Makino H. (2014) Long-term treatment with the sodium glucose cotransporter 2 inhibitor, dapagliflozin, ameliorates glucose homeostasis and diabetic nephropathy in db/db mice. PLoS One, 9: e100777.

156. Goldberg H, Whiteside C, Fantus IG. (2011) O-linked beta-N-acetylglucosamine supports p38 MAPK activation by high glucose in glomerular mesangial cells. American Journal of Physiology-Endocrinology and Metabolism, 301: E713-E726.
157. Gellai R, Hodrea J, Lenart L, Hosszu A, Koszegi S, Balogh D, Ver A, Banki NF, Fulop N, Molnar A, Wagner L, Vannay A, Szabo AJ, Fekete A. (2016) Role of O-linked N-acetylglucosamine modification in diabetic nephropathy. Am J Physiol Renal Physiol, 311: F1172-F1181.
158. Lu YT, Ma XL, Xu YH, Hu J, Wang F, Qin WY, Xiong WY. (2019) A Fluorescent Glucose Transport Assay for Screening SGLT2 Inhibitors in Endogenous SGLT2-Expressing HK-2 Cells. Nat Prod Bioprospect, 9: 13-21.
159. Tang SC, Lai KN. (2012) The pathogenic role of the renal proximal tubular cell in diabetic nephropathy. Nephrol Dial Transplant, 27: 3049-3056.
160. Panchapakesan U, Pegg K, Gross S, Komala MG, Mudaliar H, Forbes J, Pollock C, Mather A. (2013) Effects of SGLT2 inhibition in human kidney proximal tubular cells--renoprotection in diabetic nephropathy? PLoS One, 8: e54442.
161. Singh DK, Winocour P, Farrington K. (2008) Mechanisms of disease: the hypoxic tubular hypothesis of diabetic nephropathy. Nat Clin Pract Nephrol, 4: 216-226.
162. Gullans SR, Harris SI, Mandel LJ. (1984) Glucose-dependent respiration in suspensions of rabbit cortical tubules. J Membr Biol, 78: 257-262.
163. Jaakkola P, Mole DR, Tian YM, Wilson MI, Gielbert J, Gaskell SJ, von Kriegsheim A, Hebestreit HF, Mukherji M, Schofield CJ, Maxwell PH, Pugh CW, Ratcliffe PJ. (2001) Targeting of HIF-alpha to the von Hippel-Lindau ubiquitylation complex by O2-regulated prolyl hydroxylation. Science, 292: 468-472.
164. Kallio PJ, Pongratz I, Gradin K, McGuire J, Poellinger L. (1997) Activation of hypoxia-inducible factor 1alpha: posttranscriptional regulation and conformational change by recruitment of the Arnt transcription factor. Proc Natl Acad Sci U S A, 94: 5667-5672.
165. Wu D, Yotnda P. (2011) Induction and testing of hypoxia in cell culture. J Vis Exp.

166. Wang GL, Semenza GL. (1993) General involvement of hypoxia-inducible factor 1 in transcriptional response to hypoxia. Proc Natl Acad Sci U S A, 90: 4304-4308.

167. Fernandez-Martinez AB, Jimenez MI, Hernandez IS, Garcia-Bermejo ML, Manzano VM, Fraile EA, de Lucio-Cazana FJ. (2011) Mutual regulation of hypoxic and retinoic acid related signalling in tubular proximal cells. Int J Biochem Cell Biol, 43: 1198-1207.

168. Leonard MO, Cottell DC, Godson C, Brady HR, Taylor CT. (2003) The role of HIF-1 alpha in transcriptional regulation of the proximal tubular epithelial cell response to hypoxia. J Biol Chem, 278: 40296-40304.

169. Yu WM, Li YP, Wang Z, Liu L, Liu J, Ding FA, Zhang XY, Cheng ZY, Chen PS, Dou J. (2016) Transcriptomic changes in human renal proximal tubular cells revealed under hypoxic conditions by RNA sequencing. International Journal of Molecular Medicine, 38: 894-902.

170. Maxwell PH, Osmond MK, Pugh CW, Heryet A, Nicholls LG, Tan CC, Doe BG, Ferguson DJP, Johnson MH, Ratcliffe PJ. (1993) Identification of the Renal Erythropoietin-Producing Cells Using Transgenic Mice. Kidney International, 44: 1149-1162.

171. Ng YY, Huang TP, Yang WC, Chen ZP, Yang AH, Mu W, Nikolic-Paterson DJ, Atkins RC, Lan HY. (1998) Tubular epithelial-myofibroblast transdifferentiation in progressive tubulointerstitial fibrosis in 5/6 nephrectomized rats. Kidney Int, 54: 864-876.

172. Nangaku M. (2006) Chronic hypoxia and tubulointerstitial injury: a final common pathway to end-stage renal failure. J Am Soc Nephrol, 17: 17-25.

DOI:10.14753/SE.2020.2400

10 BIBLIOGRAPHY OF THE CANDIDATE'S PUBLICATIONS

Publications related to the theme of the PhD thesis

[*]Judit Hodrea, [*]**Dora B Balogh**, Adam Hosszu, Lilla Lenart, Balazs Besztercei, Sandor Koszegi, Nadja Sparding, Federica Genovese, Laszlo J Wagner, Attila J Szabo, Andrea Fekete; Reduced *O*-GlcNAcylation and tubular hypoxia contribute to the antifibrotic effect of SGLT2 inhibitor dapagliflozin in the diabetic kidney. *Am J Physiol Renal Physiol* 2020 **IF=3.323**

Sandor Koszegi, Agnes Molnar, Lilla Lenart, Judit Hodrea, **Dora Bianka Balogh**, Tamas Lakat, Edgar Szkibinszkij, Adam Hosszu, Nadja Sparding, Federica Genovese, Laszlo Wagner, Adam Vannay, Attila J Szabo, Andrea Fekete; RAAS inhibitors directly reduce diabetes-induced renal fibrosis via growth factor inhibition. *J Physiol* 00.0 pp 1-17 2018 **IF=4.984**

Gellai, R, Hodrea, J, Lenart, L, Hosszu, A, Koszegi, S, **Balogh, D**, Ver, A, Banki, NF, Fulop, N, Molnar, A, Wagner, LJ, Vannay, A, Szabo, AJ, Fekete, A.; The role of *O*-linked N-Acetylglucosamine modification in diabetic nephropathy. *Am J Physiol Renal Physiol 311: F1172–F1181*, 2016 **IF=3.390**

Hodrea Judit, **Balogh Dóra Bianka**, Lénárt Lilla, Kőszegi Sándor, Hosszú Ádám, Vannay Ádám, Wagner J László, Reusz György, Szabó J Attila, Fekete Andrea; A nátrium-glükóz-kotranszporterek szerepe a diabeteses nephropathiában. *Hypertonia és nephrologia* 19(4) pp.153-158., 6p. 2015

Other publications

Dora B Balogh, Agnes Molnar, Adam Hosszu, Judit Hodrea, Attila J Szabo, Lilla Lenart, Andrea Fekete; Antidepressant effect in diabetes-associated depression: a novel potential of RAAS inhibition. *Psychoneuroendocrinology* 2020 **IF=4.013**

Lilla Lenart, **Dora B. Balogh**, Nikolett Lenart, Adrienn Barczi, Adam Hosszu, Tamas Farkas, Judit Hodrea, Attila J. Szabo, Krisztian Szigeti, Adam Denes, Andrea Fekete; Novel therapeutic potential of angiotensin receptor 1 blockade in a rat model of diabetes-associated depression parallels altered BDNF signaling. *Diabetologia* 2019 **IF=7.113**

Adam Hosszu, Zsuzsanna Antal, Apor Veres-Szekely, Lilla Lenart, **Dora Bianka Balogh**, Edgar Szkibinszkij, Lilla Illesy, Judit Hodrea, Nora F. Banki, Laszlo Wagner, Adam Vannay, Attila J. Szabo, Andrea Fekete; The role of Sigma-1 receptor in sex-specific heat shock response in an experimental rat model of renal ischaemia/reperfusion injury. *Transplant International* 2018 **IF=3.526**

Adam Hosszu, Zsuzsanna Antal, Judit Hodrea, Sandor Koszegi, Lilla Lenart, **Dora B Balogh**, Nora F Banki, Laszlo Wagner, Adam Denes, Peter Hamar, Adam Vannay, Peter Degrell, Attila J Szabo, Andrea Fekete; σ1-Receptor Agonism Protects against Renal Ischemia-Reperfusion Injury. *J Am Soc Nephrol 27* 2017 **IF=8.655**

Lenart, Lilla; Hodrea, Judit; Hosszu, Adam; Koszegi, Sandor; Zelena, Dora; **Balogh, Dora**; Szkibinszkij, Edgar; Veres-Szekely, Apor; Wagner, Laszlo; Vannay, Adam; Szabo, Attila; Fekete, Andrea; The role of sigma-1 receptor and brain-derived neurotrophic factor in the development of diabetes and comorbid depression in streptozotocin-induced diabetic rats. *Psychopharmacology* 2016 **IF=3.308**

DOI:10.14753/SE.2020.2400

11 ACKNOWLEDGEMENTS

Firstly, I would like to express my deep sense of gratitude and profound respect to my supervisor Andrea Fekete for the continuous support of my PhD study and related research. Her tireless dedication, immense knowledge and motivation have given me power and spirit through the years. She is my mentor and the best advisor beyond the imagination.

I wish to sincerely thank Professor Attila Szabo for his support and help in completing my PhD work successfully in the Research Laboratory of the 1st Department of Pediatrics, Semmelweis University.

I express my gratitude and gratefulness to the postdocs of our group, Judit Hodrea, Adam Hosszu and Lilla Lenart for giving me encouragement and sharing insightful suggestions. Without their precious support it would not have been possible to conduct this research. Judit Hodrea and Lilla Lenart have played a major role in polishing my research skills. Special thanks to Adam Hosszu for the improvement in my writing skills. Their endless guidance is hard to forget throughout my life.

I would like to thank all my colleagues at the lab for the stimulating discussions, the enthusiasm when we were working together before deadlines and for all the fun we had in the last five years. Special thanks to Tamas Lakat for his invaluable help in molecular measurements and figure design, to Sandor Koszegi for preparing the histological evaluation and to Laszlo Wagner for his clinically relevant comments. I could not be more thankful to Maria Bernath for her constant help with *in vitro* experiments and laboratory work, not to mention the delicious birthday cakes. I am privileged of having the fellow labmates as well: Nora Beres, Apor Veres-Szekely, Edgar Szkibinszkij, Agnes Molnar and Csenge Mezei, thanks to you for helping me to survive these years.

Last but not the least, all special thanks to my husband and to my whole family for helping me throughout my PhD studies and writing this thesis. Without their constant support and love this work could not have been completed.

12 FIGURES AND TABLES

Figures

Tables